DIMETHYLSULFONIOPROPIONATE ASSIMILATION BY MARINE BACTERIA

by

CHRISTOPHER R. REISCH

(Under the Direction of William B. Whitman)

ABSTRACT

Dimethylsulfoniopropionate (DMSP) is ubiquitous in marine surface waters where it is produced by marine phytoplankton for use as an osmolyte amongst other functions. Some marine bacteria, including the model organism *Ruegeria pomeroyi* DSS-3, maintain two competing pathways for the degradation of DMSP. Only recently have the genes and biochemical pathways that degrade DMSP been investigated and identified. The DMSP-dependent demethylase, designated DmdA, was the first enzyme identified to directly catalyze a reaction involving DMSP. Upon purification and characterization of the enzyme it was confirmed that methylmercaptopropionate (MMPA) and 5-methyl-tetrahydrofolate were the reaction products. Interestingly, the enzyme possessed a low affinity for DMSP and the host bacterium was shown to accumulate DMSP to high intracellular concentrations, promoting maximal enzyme activity. The complete biochemical pathway for the catabolism of methylmercaptopropionate (MMPA), the product of DMSP demethylation, was also elucidated. This pathway was composed of four enzymes, three of which catalyzed novel reactions that had never been previously observed. The genes that encoded for these novel enzymes were identified by purification from crude cell extracts. Phylogenetic analysis showed that these genes were remarkably widespread in bacteria from marine and non-marine origin. Lastly, the

biochemical pathway for assimilation of acrylate, the three carbon intermediate of the DMSP

cleavage reaction, was also elucidated. This pathway was also composed of several CoA-

mediated reactions that led to the production of propionyl-CoA. Two of the three novel enzymes

that composed this pathway were identified. A ^{13}C tracer was used to investigate the

assimilation of DMSP carbon and support the physiological significance of the proposed

pathways for MMPA and acrylate assimilation. This work has tremendously advanced the

understanding of microbial DMSP metabolism on both the molecular and biochemical levels.

INDEX WORDS: Dimethylsulfoniopropionate; DMSP; Methylmercaptopropionate; MMPA;

Methanethiol; Dimethylsulfide; DMS; Acrylate; 3-Hydroxypropionate;

Roseobacters; Sulfur; Metabolism; *Ruegeria pomeroyi; Candidatus*

Pelagibacter ubique.

DIMETHYLSULFONIOPROPIONATE ASSIMILATION BY MARINE BACTERIA

by

CHRISTOPHER R. REISCH

B.S., Clemson University, 2005

A Dissertation Submitted to the Graduate Faculty of The University of Georgia in Partial

Fulfillment of the Requirements for the Degree

DOCTOR OF PHILOSOPHY

ATHENS, GEORGIA

2011

DIMETHYLSULFONIOPROPIONATE ASSIMILATION BY MARINE BACTERIA

by

CHRISTOPHER RONALD REISCH

Major Professor:	William B. Whitman
Committee:	Mary Ann Moran
	James T. Hollibaugh
	William Lanzilotta
	Mark Schell

Electronic Version Approved:

Maureen Grasso
Dean of the Graduate School
The University of Georgia
August 2011

TABLE OF CONTENTS

CHAPTER

CHAPTER 1

INTRODUCTION AND LITERATURE REVIEW

The purpose the investigations described in this dissertation were to better understand the bacterial catabolism of the algal metabolite dimethylsulfoniopropionate (DMSP). Prior to these studies, the pathways for assimilation of DMSP in the model organism *Ruegeria pomeroyi* DSS-3 were mostly unknown. These pathways are important because their distribution and activity in marine surface waters control the flux of sulfur to the atmosphee on a global scale.

DMSP is found in marine surface waters worldwide, ranging in concentration from less than 1 nM in the open oceans to several micromolar in blooms of phytoplankton which produce DMSP (20). The primary sources of DMSP in marine surface waters are micro and macro-algae (24), although some halophytic plants also produce DMSP (13). Pytoplankton release DMSP upon cellular lysis caused by zooplankton grazing (22), senescence (16), and viral infection (6). DMSP is produced by marine phytoplankton where it has been shown to possess a variety of functions, although its osmotic potential to regulate cell volume is the most widely recognized (10). In some organisms it may function as an antioxidant (17), predator deterrent (22), and cryoprotectant (8). These functions are common properties of other well studied organic osmolytes (23), thus DMSP may have different roles in different organisms. Consistent with its function as an organic osmolyte, DMSP accumulates to very high and osmotically significant concentrations in some marine phytoplankton, ranging from 0.1 to 1 M (Reviewed in (15, 24).

DMSP's importance on global scale lies not only in its availability as a source of reduced sulfur and carbon for marine microbes, but also because DMSP is the precursor for the

climatically active gas dimethylsulfide (DMS) (12). DMS is the primary natural source of sulfur

to the atmosphere, where it is oxidized to sulfate, sulfur dioxide, methanesulfonic acid and other

products that act as cloud condensation nuclei (5). The total flux of DMS into the atmosphere is

less than half of anthropogenic sulfur dioxide emissions; however, longer residence time of DMS

oxidation products in the atmosphere and the global distribution of DMS release result in a

greater contribution of DMS to the atmospheric sulfur burden (3). The relationship between

solar radiation and DMS concentration isformerly known as the CLAW hypothesis, an acronym

from the first letter of the author's surnames (2), which states that increased solar radiation and

the resulting higher temperatures should encourage growth of DMSP-producing marine

phytoplankton and increase total DMSP production. The concomitant increase in the amount of

DMS released into the atmosphere then causes an increase in the abundance of cloud

condensation nuclei, which then causes a decrease in solar radiation, slower growth of marine

phytoplankton, and decreased DMSP production. The coupling of these processes form a

negative feed-back loop which would essentially regulate global climate. Alternatively, James

Lovelock, an author on the original CLAW hypothesis, later proposed the "anti-CLAW"

hypothesis, which described a positive feedback between global temperature and DMS

production. Increasing global temperatures and resulting surface water temperatures may cause

increased stratification of the oceans. Stratification would stifle nutrient transport from deeper

water to the surface, possibily resulting in decreased phytoplankton growth, thereby decreasing

DMSP and DMS production (11).

The CLAW hypothesis is supported by data that shows strong correlations between DMS

concentration and the dose of solar radiation have been reported (19). However, the factors

governing the production and atmospheric release of DMS are complicated. Marine bacteria

were only identified as the primary mediators of DMSP catabolism after the publication of the CLAW hypothesis. It was also discovered that marine bacteria consume DMSP through an alternative pathway that does not produce DMS. Instead, it produces the more highly reactive volatile sulfur species methanethiol (MeSH) that contributes little to the atmopheric sulfur flux (9, 18). This phenomenon led to the proposal of a "bacterial switch", in which marine bacteria shift between producing more or less DMS and MeSH (14). The gene responsible for the initial demethylation of DMSP leading to MeSH production, whose expression and activity contribute to control for the bacterial switch, was identified in 2006 (7). This was first of several genes identified that encode enzymes that directly consume DMSP, the details of which are discussed below. Many of these studies were performed in cultured representatives of the well-studied roseobacters, a phylogenetically coherent clade of clade of *Alphaproteobacteria* that are mostly marine in origin (1, 21). This includes the aforementioned model organism *R. pomeroyi*, a roseobacter that was isolated in a salt-marsh on the coast of Georgia (4).

References

1.   **Buchan, A., J. M. Gonzalez, and M. A. Moran.** 2005. Overview of the marine Roseobacter lineage. Appl Environ Microbiol **71:**5665-5677.

2.   **Charlson, R. J., J. E. Lovelock, M. O. Andreae, and S. G. Warren.** 1987. Oceanic phytoplankton, atmospheric sulfur, cloud albedo and climate. Nature **326:**655-661.

3.   **Chin, M., and D. J. Jacob.** 1996. Anthropogenic and natural contributions to tropospheric sulfate: A global model analysis. J Geophys Res-Atmos **101:**18691-18699.

4.   **Gonzalez, J. M., J. S. Covert, W. B. Whitman, J. R. Henriksen, F. Mayer, B. Scharf, R. Schmitt, A. Buchan, J. A. Fuhrman, R. P. Kiene, and M. A. Moran.** 2003. *Silicibacter pomeroyi* sp nov and *Roseovarius nubinhibens* sp nov., dimethylsulfoniopropionate-demethylating bacteria from marine environments. Int. J. Syst. Evol. Micr. **53:**1261-1269.

5.   **Hatakeyama, S., M. Okuda, and H. Akimoto.** 1982. Formation of sulfur-dioxide and methanesulfonic-acid in the photo-oxidation of dimethyl sulfide in the air. Geophys Res Lett **9:**583-586.

6.   **Hill, R. W., B. A. White, M. T. Cottrell, and J. W. H. Dacey.** 1998. Virus-mediated total release of dimethylsulfoniopropionate from marine phytoplankton: a potential climate process. Aquat Mirob Ecol **14:**1-6.

7.   **Howard, E. C., J. R. Henriksen, A. Buchan, C. R. Reisch, H. Burgmann, R. Welsh, W. Ye, J. M. Gonzalez, K. Mace, S. B. Joye, R. P. Kiene, W. B. Whitman, and M. A. Moran.** 2006. Bacterial taxa that limit sulfur flux from the ocean. Science **314:**649-652.

8.   **Karsten, U., K. Kuck, C. Vogt, and G. O. Kirst.** 1996. Dimethylsulphoniopropionate production in phototrophic organisms and its physiological function as a cryoprotectant., p. 143-153. *In* R. P. Kiene, P. T. Visscher, M. D. Keller, and G. O. Kirst (ed.), Biological and Environmental Chemistry of DMSP and Related Sulfonium Compounds. Plenum Press, New York.

9.   **Kiene, R. P., and B. F. Taylor.** 1988. Demethylation of dimethylsulfoniopropionate and production of thiols in anoxic marine sediments. Appl Environ Microbiol **54:**2208-2212.

10.   **Kirst, G. O.** 1990. Salinity tolerance of eukaryotic marine algae. Annu Rev Plant Phys **41:**21-53.

11.   **Lovelock, J.** 2006. The revenge of Gaia : earth's climate in crisis and the fate of humanity. Basic Books, New York.

12.   **Lovelock, J. E., R. J. Maggs, and R. A. Rasmussen.** 1972. Atmospheric dimethyl sulfide and natural sulfur cycle. Nature **237:**452-453.

13.   **Otte, M. L., G. Wilson, J. T. Morris, and B. M. Moran.** 2004. Dimethylsulphoniopropionate (DMSP) and related compounds in higher plants. J Exp Bot **55:**1919-1925.

14.   **Simo, R.** 2001. Production of atmospheric sulfur by oceanic plankton: biogeochemical, ecological and evolutionary links. Trends Ecol Evol **16:**287-294.

15.   **Stefels, J.** 2000. Physiological aspects of the production and conversion of DMSP in marine algae and higher plants. J Sea Res **43:**183-197.

16.   **Stefels, J., and W. Van Boeckel.** 1993. Production of DMS from dissolved DMSP in axenic cultures of the marine phytoplankton species *Phaeocystis* sp. MAR ECOL-PROG SER **97:**11-18.

17.   **Sunda, W., D. J. Kieber, R. P. Kiene, and S. Huntsman.** 2002. An antioxidant function for DMSP and DMS in marine algae. Nature **418:**317-320.

18.   **Taylor, B. F., and D. C. Gilchrist.** 1991. New routes for aerobic biodegradation of dimethylsulfoniopropionate. Appl Environ Microbiol **57:**3581-3584.

19.   **Vallina, S. M., and R. Simo.** 2007. Strong relationship between DMS and the solar radiation dose over the global surface ocean. Science **315:**506-508.

20.   **van Duyl, F. C., W. W. C. Gieskes, A. J. Kop, and W. E. Lewis.** 1998. Biological control of short-term variations in the concentration of DMSP and DMS during a *Phaeocystis* spring bloom. J Sea Res **40:**221-231.

21.   **Wagner-Dobler, I., and H. Biebl.** 2006. Environmental biology of the marine Roseobacter lineage. Annu Rev Microbiol **60:**255-280.

22.   **Wolfe, G. V., and M. Steinke.** 1997. Grazing-activated chemical defence in a unicellular marine alga. Nature **387:**894-897.

23.   **Yancey, P. H.** 2005. Organic osmolytes as compatible, metabolic and counteracting cytoprotectants in high osmolarity and other stresses. J Exp Biol **208:**2819-2830.

24.   **Yoch, D. C.** 2002. Dimethylsulfoniopropionate: its sources, role in the marine food web, and biological degradation to dimethylsulfide. Appl Environ Microbiol **68:**5804-5815.

CHAPTER 2

BACTERIAL CATABOLISM OF DIMETHYLSULFONIOPROPIONATE

Abstract

Dimethylsulfoniopropionate (DMSP) is a metabolite produced primarily by marine phytoplankton and the main precursor to the climatically important gas dimethylsulfide (DMS). DMS is released upon bacterial catabolism of DMSP, but it is not the only possible fate of DMSP sulfur. An alternative demethylation/demethiolation pathway results in the eventual release of methanethiol (MeSH), a highly reactive volatile sulfur compound that contributes little to the atmospheric sulfur flux. The activity of these pathways control the natural flux of sulfur released to the atmosphere. Although these biochemical pathways and the factors that regulate them are of great interest, they are poorly understood. Only recently have some of the genes and pathways responsible for DMSP catabolism been elucidated. Thus far, six different enzymes have been identified that catalyze the cleavage of DMSP, resulting in the release of DMS. In addition, five of these enzymes appear to produce acrylate, while one produces 3-hydroxypropionate. In contrast, only one enzyme, designated DmdA, has been identified that catalyzes the demethylation reaction producing methylmercaptopropionate (MMPA). The metabolism of MMPA is performed by a series of three coenzyme-A mediated reactions catalyzed by DmdB, DmdC, and DmdD. Interestingly, *Candidatus* Pelagibacter ubique, a member of the SAR11 clade of *Alphaproteobacteria* that is highly abundant in marine surface waters, possessed functional DmdA, DmdB, and DmdC enzymes. Microbially mediated transformations of both DMS and methanethiol are also possible, although many of the biochemical and molecular genetic details are still unknown. This review will focus on the recent discoveries in the biochemical pathways that mineralize and assimilate DMSP carbon and sulfur, as well as the areas for which a comprehensive understanding is still lacking.

Introduction

Dimethylsulfoniopropionate (DMSP) is ubiquitous in marine surface waters, ranging in concentration from less than 1 nM in the open oceans to several micromolar in phytoplankton blooms (84). The primary sources of DMSP in marine surface waters are micro and macro-algae (95), although some halophytic plants also produce DMSP (55). DMSP is released from phytoplankton upon cellular lysis caused by zooplankton grazing (92), senescence (64), and viral infection (31). DMSP is produced by marine phytoplankton where it has been shown to possess a variety of functions, although its osmotic potential to regulate cell volume is the most widely recognized (44). In some organisms it may function as an antioxidant (67), predator deterrent (92), and cryoprotectant (35). These functions are common properties of other well studied organic osmolytes (94), thus DMSP may have different roles in different organisms. Consistent with its function as an organic osmolyte, DMSP accumulates to very high and osmotically significant concentrations in some marine phytoplankton, ranging from 0.1 to 1 M (Reviewed in (63, 95).

The importance of DMSP lies not only in its availability as a source of reduced sulfur and carbon for marine microbes, but also because DMSP is the precursor for the climatically active gas dimethylsulfide (DMS) (47). DMS is the primary natural source of sulfur to the atmosphere, where it is oxidized to sulfate, sulfur dioxide, methanesulfonic acid and other products that act as cloud condensation nuclei (28). Although the total flux of DMS is less than half that of anthropogenic sulfur dioxide emissions, the longer residence time of DMS oxidation products in the atmosphere and the global distribution of DMS release result in a greater contribution of DMS to the atmospheric sulfur burden (10). The relationship between solar radiation and DMS concentration is known as the CLAW hypothesis, an acronym from the first letter of the author's

surnames (9), which states that increased levels of solar radiation and the resulting higher

temperatures encourage growth of DMSP-producing marine phytoplankton and increased total

DMSP production. The resulting increase in the amount of DMS released into the atmosphere

then causes an increase in the abundance of cloud condensation nuclei, which then causes a

decrease in solar radiation, slower growth of marine phytoplankton, and decreased DMSP

production. These coupled processes then form a negative feed-back loop. James Lovelock, an

author on the original CLAW hypothesis, later proposed the "anti-CLAW" hypothesis, which

described a positive feedback between global temperature and DMS production. Increasing

global temperatures and resulting surface water temperatures may cause increased stratification

of the oceans. Stratification would then decrease the flux of nutrients from deeper waters to the

surface, resulting in decreased phytoplankton growth, thereby decreasing DMSP and DMS

production (46).

In support of the CLAW hypothesis, strong correlations between DMS concentration and

the dose of solar radiation have been reported (81). However, the factors governing the

production and atmospheric release of DMS are complicated. Marine bacteria were only

identified as the primary mediators of DMSP catabolism after the publication of the CLAW

hypothesis. It was also discovered that marine bacteria consume DMSP through an alternative

pathway that does not produce DMS. Instead, it produces the more highly reactive volatile

sulfur species methanethiol (MeSH) that contributes little to the global sulfur flux (41, 69). This

phenomenon led to the proposal of a "bacterial switch", in which marine bacteria shift between

producing DMS and MeSH (62). The gene responsible for the initial demethylation of DMSP

leading to MeSH production, whose expression and activity contribute to control for the bacterial

switch, was identified in 2006 (32). This was first of several genes identified that encode

enzymes that directly consume DMSP, the details of which are discussed below. Many of these studies were performed in cultured representatives of the well-studied roseobacters, a phylogenetically coherent clade of clade of *Alphaproteobacteria* that are mostly marine in origin (8, 90).

Background

Studies involving the enzymatic reactions of important sulfur transformations have been ongoing for years. Despite this, there are large gaps in our understanding of the specific transformations of DMSP and its degradation products. While a number of enzymes were previously purified and characterized as discussed below, the genes were not identified at the time. The lack of identified genes was unfortunate as the explosion in metagenomic and metatranscriptomic data provided an opportunity to further our understanding of their distribution and expression in the environment. However, in the last few years the identification of gene products responsible for the direct transformations of DMSP through the cleavage or demethylation pathways, as well as down-stream metabolic pathways, have made such studies possible (33, 56, 58, 86, 88).

DMSP Synthesis

Three pathways have been described for the biosynthesis of DMSP: in the beach sunflower (*Wollastonia biflora* (L.) DC) (59), the smooth chordgrass (*Spartina alterniflora Loisel)* (45), and sea lettuce (*Ulva lactuca* Linnaeus) (24). However, the genes that encode most of the enzymes are not known. Each of these pathways share methionine as the starting compound but differ in the subsequent steps. Thus, the sulfur from DMSP and methionine share the same origin. Most evidence suggests that this sulfur is assimilated from sulfate using the adenosine 5'-phosphosulfate / 3'-phosphoadenosine 5'-phosphosulfate (APS/PAPS) system that

produces sulfite (63). Sulfite is then reduced to sulfide in a reaction catalyzed by sulfite reductase and requiring six electrons. Sulfide is incorporated into cysteine, the precursor of methionine biosynthesis.

Environmental Fate of DMSP

There are three separate fates of DMSP sulfur: 1) production of volatile species and evolution to the atmosphere, 2) assimilation by marine microorganisms, 3) oxidation followed by release or re-assimilation. These three fates were demonstrated in a study using a ^{35}S DMSP tracer to track the partitioning of DMSP sulfur to various products in oceanic and coastal seawater (38). About 15% of added DMSP was taken up by bacterial cells but not further metabolized even after 24 hours of incubation, suggesting an intracellular accumulation of DMSP. This phenomenon was also observed in studies of chemostat-grown *Ruegeria pomeroyi,* a model organism for the roseobacter clade of marine *Alphaproteobacterium* (57). In the Kiene and Linn study most of the DMSP was incorporated into protein or transformed to dissolved non-volatile products (DNVS). The DNVS was probably formed by oxidation to DMSO and sulfate. There was also a large difference in the amount of DMSP routed through the demethylation pathway and partitioned as protein or DNVS between coastal and open ocean waters. In coastal samples, 60% of DMSP was assimilated. In ocean samples, only 16% was assimilated, and the remainder was found as DNVS. The reason for this difference is thought to be related to the sulfur demand of the cells from different marine environments. Cells within the coastal samples are likely to have higher growth rates and therefore an increased sulfur demand, causing more sulfur to be assimilated and less oxidized. In both coastal and oceanic samples, only a small portion of the total DMSP, an average of 10%, was routed through the DMSP cleavage pathway and DMS production.

Phytoplankton Cleavage

Marine phytoplankton are the primary synthesizers of DMSP, while marine bacteria are the primary degraders. However, field studies have suggested that dinoflagellates may contribute significantly to the release of DMS in phytoplankton blooms (65), and some marine phytoplankton also have the capacity to degrade DMSP through the cleavage pathway. Four out of five cultured strains of the dinoflagellate *Symbiodinium microadriaticum* possessed DMSP lyase activity, although the rates varied significantly between strains (96). In addition, while DMSP production in coccolithophores is ubiquitous, DMSP lyase activity is not. A study of ten strains of coccolithophores found that only those closely related to *Emiliania huxleyi* (Lohm.) Hay or Mohler and *Gephyrocapsa oceanica* Kamptner were capable of DMS production (22). *E. huxleyi* is a well studied model organism that is highly abundant in marine surface waters where it is often, but not always, numerically dominant. The distribution of DMSP lyase activity across the phylogenetic range of the coccolithophores is not yet known, complicating our understanding of the coccolithophore contribution to DMS production (22). Studies of *E. huxleyi* showed that significant amounts of DMS are only produced upon cell damage. This evidence suggests that the DMSP lyase is physically separated from the cell's cytoplasm, where intracellular DMSP is stored and may act as a signaling molecule (93).

DMSP lyase enzymes have been purified from the green macroalga (*Ulva curvata* (Kützing) De Toni) (15) and the red macroalga (*Polysiphonia paniculata* Montagne) (52). The identities of genes encoding these enzymes remain unknown, and it is not known whether or not the two enzymes are related.

While marine bacteria are the primary mediators of DMSP degradation, there is evidence that phytoplankton may be responsible for a large part of the DMSP-cleavage reaction and DMS

release in the ocean. A number of modeling studies have recently attributed increased

importance to the phytoplankton contribution to DMS production (77-79). One study found that

the solar radiation-induced release of DMS from phytoplankton cells was necessary to produce

realistic DMS predictions and reproduce the summer DMS accumulation found in surface waters

(82). Models that omit DMS release from phytoplankton underestimate the surface-to-air flux

by 25%, indicating a significant phytoplankton contribution to the DMSP cleavage pathway (83).

Bacterial Cleavage

DMSP in marine waters undergoes a non-enzymatic hydrolysis that releases DMS and

acrylate. In the absence of biotic processes, the half-life of DMSP in seawater is about 8 years, a

rate of hydrolysis that is far too low to account for the observed turnover of DMSP in natural

waters (13). This realization and the identification of DMS-producing bacteria suggested that

bacteria were the primary mediators of DMSP degradation. A bacterial DMSP lyase (E.C.

4.4.1.3) was first purified and characterized in 1995 from a marine isolate, *Alcaligenes faecalis*

M3A (16). The enzyme had a K_m for DMSP of 1.41 mM and a V_{max} of 402 μmol min^{-1} mg of

protein^{-1}. However, the protein-encoding gene was not identified until about 15 years later.

DMSP-cleavage enzyme DddY

A recent re-examination of *A. facecalis* M3A identified the gene responsible for

encoding the DMSP lyase (11). This protein, designated DddY, possessed no known functional

domains, and unlike the other DMSP cleavage enzymes identified was located in the bacterial

periplasmic space, as originally found in 1995 (16). The *dddY* gene was located on the

chromosome near genes that conferred the ability to metabolize acrylate, much like the pathway

discussed below from *Halomonas* HTNK1 (Figure 3). Interestingly, this gene was not present in

the global ocean survey (GOS) marine metagenomic database (60), which suggests that it does

not play a major role in DMSP processing in marine surface waters. However, it may be abundant in anoxic areas of marine sediment, where it may have some ecological significance (11).

DMSP-cleavage enzyme DddD

Most early predictions regarding the pathways of DMSP catabolism assumed that the DMSP-cleavage pathway would split DMSP into DMS and acrylate. Identification of genes catalyzing the cleavage reaction have mostly proven these early hypotheses correct, with the exception of the first cleavage enzyme identified, DddD. This enzyme turned out to produce 3-hydroxypropionate instead of acrylate (74, 76). The gene was identified in a bacterial isolate cultured from the rhizosphere of the salt marsh grass *Spartina anglica* C.E.Hubb. Based upon 16S rRNA gene sequencing, the bacterium was closely related to the *Gammaproteobacteria Marinomonas* and was designated strain MWYL1. A *dddD* mutation in this organism completely abolished DMS production. However, in *R. pomeroyi*, *dddD* does not appear to encode a major pathway of DMSP cleavage. Inactivation of the *dddD* gene in *R. pomeroyi* had no effect on DMSP metabolism under the conditions tested, but this organism contains three additional DMSP-cleavage enzymes, as discussed below (73). The *dddD* gene possessed similarity to acyl-CoA transferases, which was unexpected for a lyase. Because of this annotation, the enzyme was originally hypothesized to catalyze the formation of a DMSP-coenzyme-A-thioester, which would spontaneously hydrolyze to DMS and 3-hydroxypropionyl-CoA. Although the DddD enzyme has not been purified and characterized biochemically, the activity of the recombinant *dddD* from *Halomonas* HTNK1 was investigated (74). When *dddD* alone was expressed and the culture was provided with [^{13}C-1] or [^{14}C-1] DMSP, only 3-hydroxypropionate was detected after overnight incubation. The authors conclude that 3-

hydroxypropionate, not a DMSP-CoA thioester as initially proposed, was the product of the DddD catalyzed reaction. However, these experiments used mM concentrations of DMSP, and it is unlikely that an equimolar buildup of a coenzyme-A thioester would occur. Thus, the actual product of DddD may be a coenzyme-A thioester, such as acryloyl-CoA or 3-hydroxypropionyl-CoA, which *E. coli* then metabolizes releasing 3-hydroxypropionate. The authors note that, for unknown reasons, cell extracts with DddD possess no activity, thus precluding in vitro biochemical characterization.

DMSP-cleavage enzyme DddL

Identification of the first gene encoding an authentic DMSP lyase was reported in 2008 and designated *dddL* (12). The gene was identified by expression of a cosmid library of the *Sulfitobacter* sp. EE-36 genome in the *Rhizobium leguminosarum* strain J391. This strain was used for expression because it was an *Alphaproteobacterium*, like *Sulfitobacter* sp. EE-36, making expression of recombinant proteins more likely. The clone that possessed *dddL* was able produce low levels of DMS and consequently a *dddL* deletion mutant in *Sulfitobacter* EE-36 was unable to produce DMS from DMSP. The amino acid sequence of DddL lacked similarity to any proteins of known function, and homologous genes in both the cultured and metagenomic databases were rare. However, two strains of *Rhodobacter sphaeroides,* a well-studied organism not previously known to consume DMSP, possessed *dddL*, while a third strain did not. Accordingly, the two strains with *dddL* produced DMS from DMSP but not the third. Although DddL was not purified and characterized in vitro, recombinant *E. coli* expressing DddL released large amounts of acrylate into the medium when provided DMSP, suggesting that DddL was a DMSP lyase.

DMSP-cleavage enzyme DddP

In 2009 a third enzyme, designated DddP, was identified using a cosmid library from *Roseovarius nubinhibens* ISM (72). Mutation of the *dddP* gene in both *R. nubinhibens* and *R. pomeroyi* significantly decreased but did not abolish the production of DMS from DMSP, suggesting that these organisms possessed a second DMSP-cleaving enzyme (72, 73). Upon purification and characterization of the enzyme, ^{13}C and ^{14}C-DMSP isotope studies showed that the enzyme was a true DMSP lyase, releasing DMS and acrylate (43). The gene was originally annotated as an M24 metallopeptidase, but the subsequent characterization showed that the DddP was neither a metalloenzyme nor a peptidase. This observation was unusual, but not unprecedented. Creatinase from *Paracoccus* sp. WB1 was also annotated as a metallopeptidase but also did not contain metals (91). The enzyme had a K_m of 13.8 mM and V_{max} of 0.3 μmol min^{-1} mg of protein^{-1} with DMSP as the substrate. Compared to the kinetic values described above for DddY, both the affinity and maximum rate of catalysis are low. Low affinities for DMSP were previously reported for a DMSP-cleavage enzyme (16) and the DMSP demethylase discussed below. Unfortunately, substrate specificity of the enzyme was not examined, and given the low V_{max} it is possible that DMSP is not the only physiological substrate. Thus, the enzyme may have a broad substrate specificity and catalyze multiple reactions in the cell. While the enzymes specificity may have physiological implications, it would nonetheless catalyze the DMSP-cleavage reaction. Close homologs to the *dddP* gene were found in several roseobacters and, surprisingly, in a few fungal species. It was confirmed that fungal species with the *dddP* gene produced DMS, while those without the gene were not, suggesting that horizontal gene transfer was responsible for this unusual gene distribution (72).

DMSP-cleavage enzyme DddQ

The fourth enzyme identified was encoded by a gene designated *dddQ* (73). As stated above, the *dddP* gene knockout in *Roseovarius nubinhibens* did not abolish the production of DMS. Therefore, the cosmid library was searched for a second gene capable of conferring DMSP-cleavage activity. Two adjacent genes in the middle of a ten gene cluster were identified. When cloned and expressed in *E. coli*, each gene conferred the ability to produce DMS from DMSP, and they were designated *dddQ*. Assays with cell extracts from the recombinant *E. coli* with [^{13}C-1] and [^{14}C-1] DMSP showed that the three carbon moiety produced in the reaction was acrylate. A few roseobacters possessed *dddQ* homologs, including *Ruegeria pomeroyi*. Unlike *R. nubinhibens,* which has two adjacent copies, *R. pomeroyi* possesses only one copy. *R. pomeroyi* with a mutation in the *dddQ* gene was still capable of DMS production, though the rate was diminished by 95%, which is consistent with the presence of additional DMSP-cleavage enzymes.

DMSP-cleavage enzyme DddW

The sixth enzyme identified that catalyzes DMSP cleavage was encoded by a gene designated *dddW*. This gene was identified in *R. pomeroyi*, where microarray experiments showed that the gene was significantly induced in the presence of DMSP. Cloning and expressing the gene in *E. coli* conferred the ability to form DMS from DMSP. Cell-free extracts possessed activity that cleaved DMSP into acrylate and DMS. This gene possessed no sequence similarity to genes with known function, but the polypeptide sequence possessed a predicted cupin-binding fold, like that of DddP and DddQ.

Distribution of DMSP-cleavage enzymes

The distribution and abundance of the DMSP-catabolizing genes in the metagenomic database have recently been reported (33, 50, 56). While numbers alone are unlikely to fully decipher the ecological role or significance of DMSP catabolism in the environment, they do reveal which genes are likely to be important on a global scale. As discussed below, the DMSP demethylase gene, *dmdA*, is the most abundant gene found in the GOS that acts directly on DMSP. Of the DMSP-cleavage enzymes identified thus far, *dddP* is by far the most abundant, found in 6% of bacteria examined in the GOS (50). This abundance is due to the genes presence in many roseobacters, as well as *Candidatus* Puniceispirillum marinum, the cultured representative of the SAR116 clade of *Alphaproteobacteria*. The abundance is consistent with the ribotype abundance identified in the GOS, where the SAR116 cluster represented 2.7% and the roseobacters 2.6% of sequences (5). In contrast, the SAR11 clade of the *Alphaproteobacteria* constitutes 31% of sequenced ribotypes in the GOS (5), which is consistent with the *dmdA* abundance of 27% (50).

The diversity of the DMSP-cleavage enzymes identified thus far is surprising. While there are numerous examples of non-homologous isofunctional enzymes (54), six examples in closely related bacteria is unusual. This diversity suggests that there may be more, yet-unidentified enzymes catalyzing the cleavage reaction. For example, *dddW*, the most recently identified DMSP lyase gene, has only one highly similar homolog in the entire genomic database (75). This gene was identified in the well-studied bacterium *R. pomeroyi*, and it is likely that if other bacteria were screened with similar depth, by either whole-genome transcriptional analysis or whole-genome cloning, more cleavage enzymes would be found. The contribution of these low-abundance DMSP cleavage enzymes to the flux of DMSP in the environment is probably

minimal on an individual basis. But if there are in fact more of these novel DMSP lyases

harbored by less understood bacteria, they may contribute significantly to the total flux.

DMSP Demethylation

The gene catalyzing the initial demethylation of DMSP was identified in 2006 in *R.*

pomeroyi using a transposon mutant library. The gene, designated *dmdA*, was originally

annotated as a glycine cleavage T-protein (GcvT), one of four proteins in the glycine degradation

system (53). Like GcvT, DmdA requires tetrahydrofolate (THF) to accept the methyl group

from DMSP. DmdA from both *Candidatus* Pelagibacter ubique and *R. pomeroyi* were purified

and characterized, and both possessed similar kinetic properties (57). The enzymes had low

affinities for DMSP, with K_ms of 13.2 and 5.4 mM for the enzymes from *Candidatus* P. ubique

and *R. pomeroyi*, respectively. During growth on DMSP, *R. pomeroyi* cultures maintained an

intracellular concentration of DMSP of ~70 mM, which would allow for near maximal activity

of DmdA in vivo. Such a high concentration of DMSP is osmotically significant and suggests

that *R. pomeroyi* accumulates DMSP as an organic osmolyte. It is notable that the enzyme had a

strict substrate specificity, indicating that the enzyme evolved to function with DMSP and was

not a promiscuous enzyme that catalyzed multiple reactions.

Subsequent analysis of *dmdA* in marine metagenomic data showed that this gene is

particularly abundant in ocean surface waters, with estimates placing the number of cells that

possess this gene ranged at 27% (50). One reason for this high abundance was confirmed

recently. In laboratory experiments the SAR11 clade bacterium *Candidatus* P. ubique required

an exogenous source of reduced sulfur, such as DMSP or methionine, to reach high cell density

in culture (80). Despite very high concentrations of sulfate in most of the surface ocean,

Candidatus P. ubique is incapable of utilizing this potential sulfur source as it does not possess

the genes required for assimilatory sulfate reduction (80). Instead, the bacterium uses only reduced sources of sulfur, and they are even selective in their use of reduced species. For instance, cysteine did not increase growth yields to the same extent as DMSP and methionine. Presumably, the inability to assimilate oxidized sulfur compounds results from the energetic costs associated with sulfate reduction. For these extreme oligotrophs, electron donors may be very scarce.

First Demethylation Carbon

There are two products of the DMSP demethylation reaction catalyzed by DmdA, MMPA and 5-methyl-THF, which carries the methyl group removed from DMSP (Fig. 1). The fate of 5-methyl-THF has not been directly studied, but the possibilities are numerous as it is a major donor of single carbon units in bacterial cells (Fig. 3). Many organisms oxidize 5-methyl-THF to 5,10-methylene-THF by 5,10-methylene-THF reductase (MetF, 1.5.1.20) and subsequently to 5-formyl-THF by methylene-THF dehydrogenase (FolD, 1.5.1.5). 5-methyl-THF is also the methyl donor for methionine and S-adenosyl-methionine synthesis, while 5-formyl-THF is the source of two carbon atoms in purine nucleoside biosynthesis. 5,10-methylene-THF serves as a carbon donor for the conversion of glycine to serine, a reaction that is also part of the serine assimilation pathway for C-1 assimilation.

MMPA Demethiolation

Most MMPA produced during DMSP degradation is further processed through a demethiolation pathway that releases the volatile sulfur compound MeSH (Fig. 2). This transformation was long thought be the result of a cleavage or a reductive cleavage reaction, producing the three carbon intermediate propionate or acrylate (41, 69). However, an alternative hypothesis suggested that MMPA may be catabolized in a fatty acid β-oxidation-like pathway (4,

70). Recently, it was confirmed that the latter pathway is present in *R. pomeroyi* and required for

MeSH production (58). In this pathway, a series of three coenzyme-A-mediated reactions

catalyze the demethiolation of MMPA. First, a MMPA-CoA thioester is formed in an ATP-

dependent reaction catalyzed by an enzyme designated as DmdB, encoded by a gene originally

annotated as a medium chain fatty-acid-CoA ligase. Next, the MMPA moiety of MMPA-CoA is

dehydrogenated between its α and β carbons, creating a double bond, transferring two electrons

to FAD, and forming methylthioacryloyl-CoA (MTA-CoA). The third step, which mediates the

actual demethiolation, is a unique reaction catalyzed by a crotonase-type enzyme. Hydration of

MTA-CoA leads to its decomposition into MeSH, acetaldehyde, CO_2, and free CoA. Like

dmdA, the genes that encode *dmdB* and *dmdC* are abundant in the marine metagenomic database.

In contrast, *dmdD* is rare, although an organism that did not possess *dmdD* was also capable of

the DmdD-catalyzed reaction, suggesting a non-orthologous gene had replaced *dmdD* in at least

some bacteria. Unlike *dmdA* though, the MMPA-CoA pathway was shown to be present in a

wide variety of bacteria, including many that are not associated with DMSP catabolism.

Methionine as a Source of MMPA

The distribution of the key genes (*dmdB* and *dmdC*) is much broader than that of *dmdA*.

Moreover, recombinant proteins from many terrestrial bacteria possess these activities and whole

cells of several distantly related bacteria release MeSH from MMPA. Conservation of this

pathway amongst such a diverse group of bacteria suggests physiological importance but raises

the question of how cells that are incapable of demethylating DMSP obtain MMPA.

A possible source of MMPA may be the methionine salvage pathway, which is found in

many types of organisms and has a primary function of recycling the reduced thiomethyl moiety

from methionine (reviewed in (2). The condensation of methionine and ATP results in

21

production of the one-carbon donor S-adenosyl-methionine (SAM). In polyamine synthesis, the aminopropyl group of decarboxylated SAM is transferred to putrescine, yielding spermine and methylthioadenosine (MTA). MTA, which contains the methylthio moiety of methionine, is the start of the methionine salvage pathway. After several steps there is a branch point where an aci-reductone dioxygenase can catalyze one of two reactions, depending upon the presence of either Fe^{2+} or Ni^{2+}. When bound to Fe^{2+}, the enzyme catalyzes the production of formate and 4-methylthio-2-oxobutyrate, which can be aminated to methionine in a single step (29). However, when bound to Ni^{2+}, the enzyme produces MMPA, carbon monoxide, and formate in an "off-pathway" reaction (14). The physiological significance of this off-pathway transformation is unknown and it has not been demonstrated that it is an alternative source of MMPA.

MeSH Assimilation

The product of MMPA degradation, MeSH, is a source of cellular sulfur for marine bacteria. A report in 1999 examined the fate of DMSP sulfur in pure cultures of several marine *Alphaproteobacteria* (26). Using ^{35}S-labeled DMSP, this work showed that nearly all the sulfur from DMSP was converted into TCA-insoluble material, most of which was protein. Interestingly, the percentage of ^{35}S that was found in TCA-insoluble material decreased significantly as the concentration of DMSP increased. The authors hypothesized that once the bacterial sulfur demand was fulfilled; most DMSP was routed through the cleavage pathway and released as DMS. A more extensive study describing the fate of the sulfur and methyl carbons of DMSP was performed using both pure cultures and natural populations in marine surface waters (39). These experiments also showed that much of the DMSP-derived sulfur was found in TCA-insoluble material. Pure cultures of an organism incapable of producing MeSH from DMSP were nonetheless capable of assimilating sulfur from ^{35}S-MeSH, which is consistent with the

widespread distribution of the MMPA-CoA pathway. Furthermore, with [^{3}H-methyl] MeSH, the methyl group was incorporated into the methyl group of methionine. Similar trends and rates of assimilation were observed when using ^{35}S- and ^{3}H-MeSH, suggesting that both the S and methyl groups are directly incorporated into methionine, possibly by the enzyme cystathionine γ-synthetase (34, 39). This hypothesis is supported by the observation that two inhibitors of the enzyme, vinylglycine and propargylglycine, caused a significant decrease in the incorporation of ^{35}S into TCA-insoluble material.

While the direct incorporation of MeSH into sulfur-containing amino acids is likely, it is also possible that the sulfur and methyl moieties are incorporated independently. The initial demethylation of DMSP transfers one methyl group to tetrahydrofolate, producing 5-methyl-tetrahydrofolate (57). The traditional route of methionine biosynthesis through methionine synthase transfers a methyl group from 5-methyl-THF to homocysteine. Therefore, organisms rapidly consuming DMSP will likely have an abundance of 5-methyl-THF that can be used in methylating reactions, including methionine synthesis. It is also likely that different organisms possess different metabolic capabilities, leaving open the possibility that both the direct incorporation of MeSH and the separate incorporation of C and S are possible in different organisms. Biochemical confirmation of these hypothesized pathways and elucidation of the genes catalyzing these reactions will allow for further investigation of the cellular assimilation of MeSH.

MeSH Oxidation

While one major fate of MeSH in marine surface waters is the incorporation into sulfur-containing amino acids, much of the MeSH is completely oxidized (Fig. 4). This MeSH oxidation pathway is expected to be initiated by a MeSH-oxidase (E.C. 1.8.3.4), which produces

formaldehyde, hydrogen sulfide, and hydrogen peroxide. This enzyme has been purified from

Thiobacillus thioparus (27), *Hyphomicrobium* EG (68), and *Rhodococcus rhodochrous* (42), but

the gene encoding this enzyme has not been reported. None of the enzymes require exogenous

cofactors, but the reported molecular weights are different, making it unclear as to whether these

enzymes are related. Given the high turnover reported for MeSH in marine surface waters (36,

39) and for cultured marine bacteria (26), identification of this enzyme would be a significant

step in understanding of the fate of MeSH in marine systems.

DMS Consumption

The fate of DMS in marine surface waters is of great interest due to its contribution to

cloud condensation nuclei in the atmosphere. Due to biotic and abiotic consumption of DMS in

the ocean mixed layer, only 2- 10% of the DMS produced is released to the atmosphere (3, 37,

97). The biological degradation of DMS in seawater has long been recognized, but these

transformations are still poorly understood. Unlike MeSH, very little sulfur from DMS is

assimilated into cells in natural populations, suggesting that only specialized methylotrophs are

capable of its assimilation (87). Nonetheless, numerous bacteria have been isolated by their

ability to grow on DMS, although many were not isolated from marine sources (reviewed in

(61). The biological fates of DMS are oxidation to DMSO, sulfate, thiosulfate, and tetrathionate

(7, 17, 18, 87) (Fig 1 and 4).   In marine surface waters, the primary fates are likely DMSO and

sulfate, as these compounds persist at the highest concentrations, although it is possible that

much of the flux is routed through thiosulfate or tetrathionate, which are then rapidly consumed

to produce sulfate.

A dimethylsulfide dehydrogenase that catalyzes the oxidation of DMS to DMSO was

identified in *Rhodovulum sulfidophilum*, a purple non-sulfur member of the *Alphaproteobacteria*

(49). The protein belonged to the DMSO reductase family of molybdoproteins, and showed high

similarity to nitrate reductase. Few highly similar homologs are found in the genomic or

metagenomic databases, thus the ecological significance of this reaction is unclear. However,

the biological production of DMSO from DMS in marine surface has been demonstrated, so

other DMSO dehydrogenase reactions must occur (18).

A DMS monooxygenase, which oxidizes DMS to MeSH and formaldehyde, was

characterized from *Hyphomicrobium sulfonivorans*, an *Alphaproteobacterium* belonging to the

order *Rhizobiales* that was originally isolated from garden soil (6). Homologs to the gene

encoding the monooxygenase gene were abundant in the genomic database, but the organisms

harboring the genes were mostly terrestrial in origin. Only one member of the roseobacters

possessed close homologs, *Citreicella sp.* SE45. Likewise, GOS metagenomic database

contained only a few homologs. Thus, it is unlikely that this DMS monooxygenase plays a

significant role in marine surface waters. Nevertheless it is possible that an unrelated enzyme

catalyzes a similar reaction in the marine systems.

A member of the *Gammaproteobacteria, Methylophaga thiooxidans* sp. nov. possessed a

novel pathway of DMS oxidation that produced tetrathionate with thiosulfate as an intermediate

(7). In the environment, tetrathionate would probably be rapidly oxidized because it is rich in

electrons. The genes involved in the production of tetrathionate through this pathway and,

therefore, its distribution and abundance in the environment are unknown. Similarly,

Methylophaga sulfidovorans was able to transform DMS into thiosulfate (17). Again,

biochemical and molecular specifics of this conversion were not reported, and it is unclear if this

is a common fate of DMS in marine systems.

Sulfur Oxidation

A major fate of DMSP-derived sulfur in environmental studies is the complete oxidation

to sulfate (38), but there is remarkably little information on the enzymes and pathways utilized

by bacteria that inhabit marine surface waters. Overall, there is a large diversity of bacterial

sulfur oxidation systems (reviewed in (25), but the distribution of these systems in marine

surface waters is unclear. It is assumed that most, if not all, of the sulfur transformed into sulfate

is routed through the demethylation/demethiolation pathway. Since the sulfur moiety from the

demethiolation pathway is in the form MeSH, complete oxidation of the sulfur and carbon would

yield 14 electrons. If methanethiol oxidase initiates the oxidation of MeSH in marine bacteria,

the sulfur moiety is transformed to sulfide. In the *Alphaproteobacteria*, it is likely that sulfide

oxidation proceeds through the well studied Kelly–Friedrich pathway (23, 48). The Kelly-

Friedrich pathway is widely distributed in the marine roseobacters, as 23 of the 32 sequenced

genomes have the SOX genes that encode for this pathway (51). This system completely

oxidizes sulfide to sulfate without the formation of sulfite. Those roseobacters that possess the

Kelly-Friedrich pathway are able to gain energy from the oxidation of sulfide derived from

MeSH or possibly DMS degradation. However, a number of roseobacters that possess DMSP

degradation genes do not possess the SOX system, making the fate of reduced sulfur in these

bacteria unclear. Thus, it is possible that some of these roseobacters that have been cultured and

sequenced, but not physiologically characterized, may possess an alternative and as yet

unidentified system to oxidize sulfur.

Double Demethylation of DMSP

One possible fate of DMSP that has remained largely unstudied involves a second

demethylation of DMSP and the conversion of MMPA to mercaptopropionate (MPA). The

production of MPA from DMSP was first reported in 1988 in anoxic surface sediments (40), but the importance of MPA in aerobic surface waters remains unclear. An aerobic bacterium showed a stoichiometric production of MPA from DMSP or MMPA (89), suggesting it may be a dead-end product of limited physiological significance. Other reports have indicated that pure cultures of anaerobic bacteria metabolized MPA to H_2S and acrylate (70). Methane production from MMPA has also been demonstrated in a limited number of strains of the strictly anaerobic methanogens of the genus *Methanosarcina*, where it was hypothesized that a transmethylation of coenzyme-M from MMPA was the likely mechanism (85). The biological implications of this reaction may be significant in anoxic areas, but most evidence suggests that double demethylation is not a major fate of DMSP in marine surface waters. However, until progress is made in understanding the biochemical reactions and gene products catalyzing these reactions, the possibility of a major role cannot be ruled out.

Acrylate and 3-hydroxypropionate Assimilation

In addition to the uncertainty in the initial steps of DMSP metabolism, the fate of the three carbon moiety of DMSP is not well understood. As detailed above, five of the DMSP cleavage enzymes identified thus far likely result in the production of acrylate, while the other results in 3-hydroxypropionate (Fig. 3). In *Halomonas* HTNK1, acrylate is believed to be metabolized to 3-hydroxypropionate, indicating that DMSP and acrylate degradation share a common intermediate (74). 3-hydroxypropionate is further metabolized by an alcohol dehydrogenase, encoded by *dddA,* which produces an intermediate hypothesized to be malonate semialdehyde (Figure 3). The gene product of *dddC,* which encodes for an enzyme annotated as a methylmalonate-semialdehyde dehydrogenase, may transform malonate-semialdehyde to acetyl-CoA (66, 74). In *E. coli* expressing *dddC* and provided [^{14}C-1] DMSP, the ^{14}C is released

as carbon dioxide, presumably by decarboxylation of malonate-semialdehyde. The distribution of this first pathway identified for bacterial DMSP cleavage and its ecological significance remain unclear, as homologs for *dddA* and *dddC* in the metagenomic databases are rare.

Another possibility is that acrylate is assimilated as a three carbon moiety in a pathway similar to that of propionate. In the methylmalonyl-CoA pathway, propionyl-CoA is carboxylated to the four carbon intermediate methylmalonyl-CoA, which is then re-arranged to the TCA cycle intermediate succinyl-CoA (21). The genes for this pathway are widespread throughout members of roseobacter clade. The transformation of acrylate to propionyl-CoA could occur through at least two different mechanisms. One possibility is the direct reduction of acrylate or acryl-CoA to propionate or propionyl-CoA, respectively. The CoA-dependent reduction of acrylate to propionate was observed in the Crenarchaeota and in *Clostridium propionicum* (30, 71). Given the distant taxonomic relationship between these prokaryotes and Proteobacteria, it is difficult to identify an ortholog in the roseobacter genomes solely on sequence similarity. An alternative route for forming propionyl-CoA would involve an initial hydration of acrylate or acryloyl-CoA to 3-hydroxypropionate or 3-hydroxypropionyl-CoA, as discussed above for *Halomonas* HTNK1. A reduction to propionate or propionyl-CoA is then possible. A trifunctional enzyme that catalyzes the complete conversion of 3-hydroxypropionate to propionyl-CoA was identified in *Chloroflexus atlanticus* (1). Again, the distant taxonomic relationship between *Chloroflexus* and Proteobacteria make it difficult to identify this enzyme in bacteria in marine surface waters.

Acetate Assimilation

As described above, DMSP catabolism frequently yields acetate. The simplest form of acetate assimilation, the glyoxylate shunt, is absent from most roseobacters but present in the

cultured representatives of the SAR11 clade. The glyoxylate shunt requires only two enzymes, isocitrate lyase (E.C. 4.1.3.1) and malate synthase (E.C. 2.3.3.9) in addition to the enzymes of the TCA cycle. The glyoxylate shunt bypasses the two decarboxylation steps of the TCA cyle, resulting in the net assimilation of acetate. The pathway for acetate assimilation in isocitrate lyase-negative organisms has been the subject of investigation for decades, but recently a complete pathway was described and designated the ethylmalonyl-CoA pathway (19). All of the enzymes in the pathway were subsequently identified (20), and homologous genes for most of the proteins in this pathway are present in *R. pomeroyi* and other roseobacters. However, further investigations are needed to confirm the physiological significance of this pathway for the assimilation of DMSP.

Conclusions

Several major discoveries regarding the molecular biology and enzymology of DMSP metabolism have occurred during the last several years. These discoveries have enabled the use of molecular approaches to dissect DMSP biogeochemistry and interrogate the environmental significance of DMSP transformations. While these breakthroughs have significantly enhanced our understanding of DMSP and sulfur transformation in the environment, many of the microbial sulfur transformations remain "black boxes". Elucidation of the carbon and sulfur transformations within these black boxes on both the molecular and biochemical level is critical to our understanding of the marine microbial food web and global sulfur cycle.
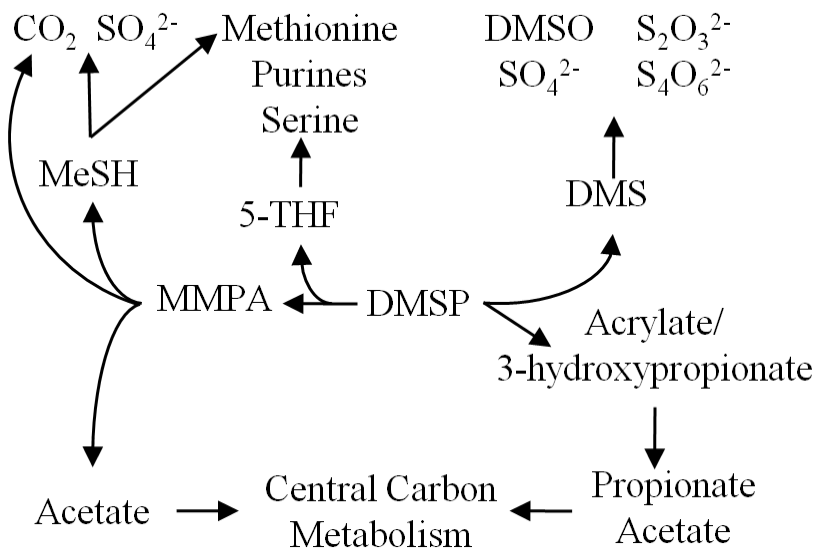
Figure 1-1.

Overview of DMSP catabolic pathways in marine bacteria with the fates of carbon and sulfur.
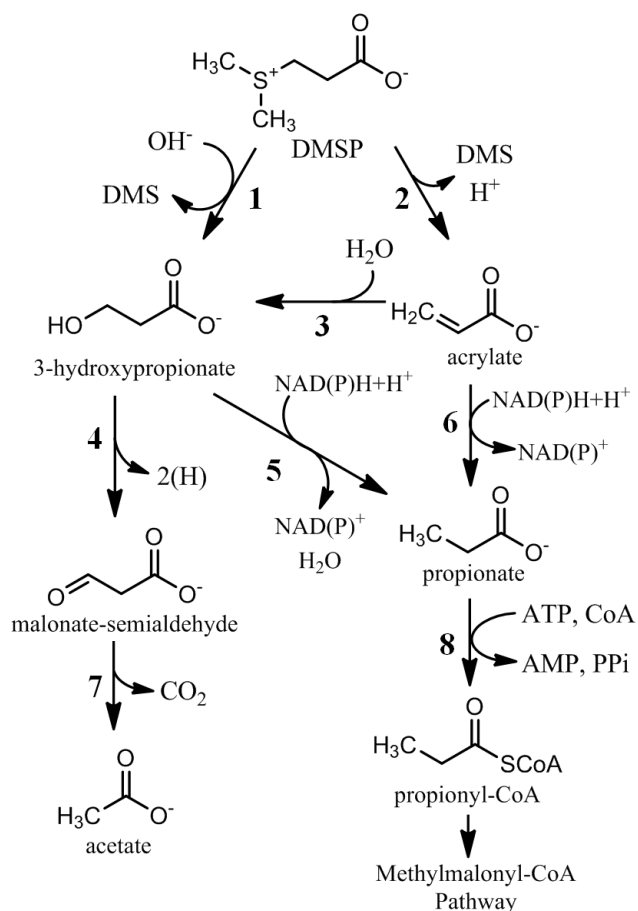
Figure 1-2.
DMSP cleavage pathways leading to central carbon metabolism. Reactions 5 and 6 may be coenzyme-A mediated and would therefore bypass reaction 8. 1, DMSP cleavage enzyme (DddD); 2, DMSP lyase (DddL, DddP, DddQ, DddY, DddW, E.C. 4.4.1.3); 3, acrylate hydratase; 4, 3-hydroxypropionate dehydrogenase; 5, 3-hydroxypropionate reductase; 6, acrylate reductase (1.3.99.3); 7, malonate semialdehyde dehydrogenase/decarboxylase (E.C. 1.2.1.18); 8, propionate-CoA ligase (PrpE, E.C. 6.2.1.17).
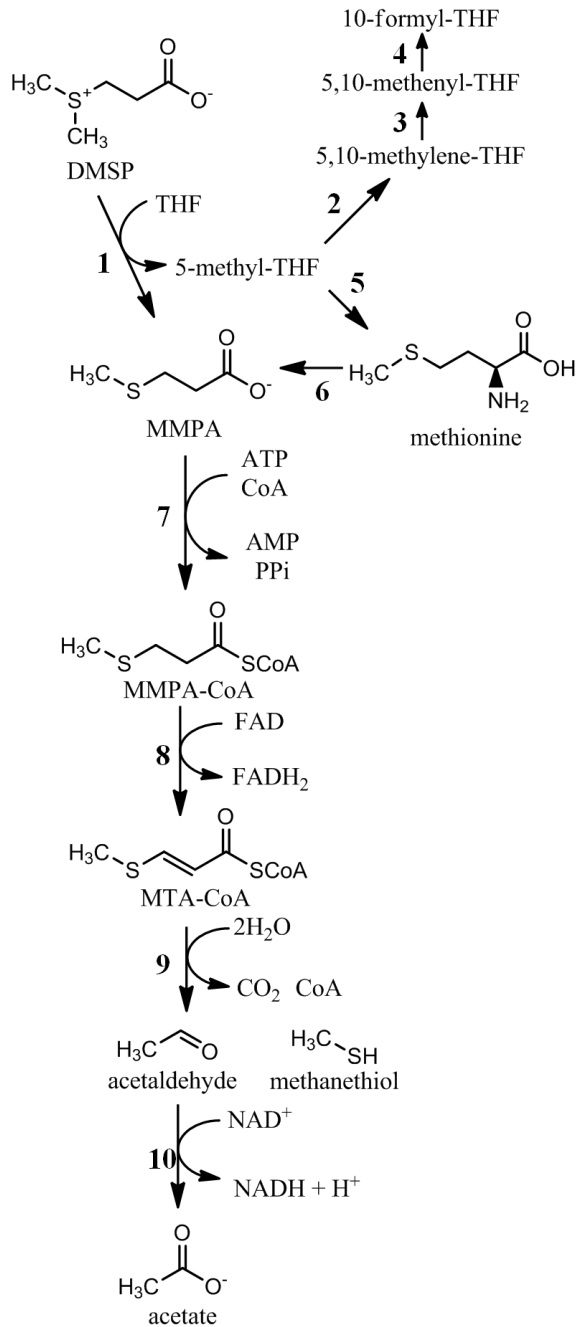
Figure 1-3. Biochemical pathways of DMSP demethylation. 1, DMSP demethylase (DmdA); 2, 5,10-methylene-THF reductase (MetF, E.C. 1.5.1.20); 3,4; methylene-THF dehydrogenase (FolD, E.C. 1.5.1.5) 5, methionine synthase (MetH, E.C. 2.1.1.13); 6, methionine salvage pathway (multiple enzymes); 7, MMPA-CoA ligase (DmdB); 8, MMPA-CoA dehydrogenase (DmdC); 9, Methylthioacryloyl-CoA hydratase (DmdD); 10, acetaldehyde dehydrogenase (E.C. 1.2.1.10).
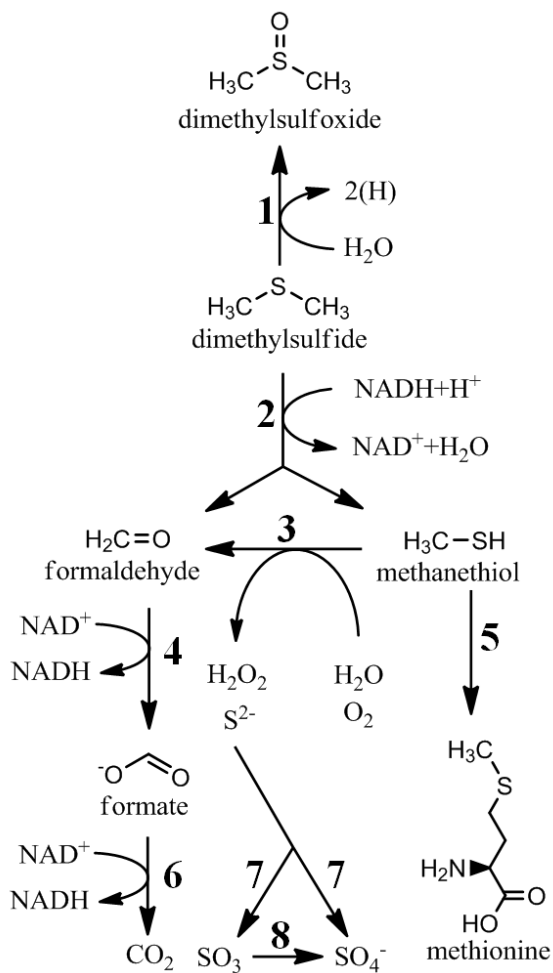
Figure 1-4.

Bioconversions of dimethylsulfide and methanethiol. 1, DMS dehydrogenase; 2, DMS monooxygenase; 3, methanethiol oxidase (E.C. 1.8.3.4); 4, formaldehyde oxidation (various enzymes); 5, cystathionine γ-synthetase; 6, formate dehydrogenase; 7, sulfide oxidation (many enzymes), 8, sulfite dehydrogenase (E.C. 1.8.2.1).

References

1. **Alber, B. E., and G. Fuchs.** 2002. Propionyl-coenzyme A synthase from *Chloroflexus aurantiacus*, a key enzyme of the 3-hydroxypropionate cycle for autotrophic CO_2 fixation. J Biol Chem **277:**12137-12143.

2. **Albers, E.** 2009. Metabolic characteristics and importance of the universal methionine salvage pathway recycling methionine from 5 '-methylthioadenosine. Iubmb Life **61:**1132-1142.

3. **Archer, S. D., F. J. Gilbert, P. D. Nightingale, M. V. Zubkov, A. H. Taylor, G. C. Smith, and P. H. Burkill.** 2002. Transformation of dimethylsulphoniopropionate to dimethyl sulphide during summer in the North Sea with an examination of key processes via a modelling approach. Deep-Sea Res Pt Ii **49:**3067-3101.

4. **Bentley, R., and T. G. Chasteen.** 2004. Environmental VOSCs--formation and degradation of dimethyl sulfide, methanethiol and related materials. Chemosphere **55:**291-317.

5. **Biers, E. J., S. L. Sun, and E. C. Howard.** 2009. Prokaryotic genomes and diversity in surface ocean waters: interrogating the global ocean sampling metagenome. Appl Environ Microbiol **75:**2221-2229.

6. **Boden, R., E. Borodina, A. P. Wood, D. P. Kelly, J. C. Murrell, and H. Schafer.** 2011. Purification and characterization of dimethylsulfide monooxygenase from *Hyphomicrobium sulfonivorans*. J Bacteriol**:**JB.00977-00910.

7. **Boden, R., D. P. Kelly, J. C. Murrell, and H. Schafer.** 2010. Oxidation of dimethylsulfide to tetrathionate by *Methylophaga thiooxidans* sp. nov.: a new link in the sulfur cycle. Environ Microbiol **12:**2688-2699.

8. **Buchan, A., J. M. Gonzalez, and M. A. Moran.** 2005. Overview of the marine Roseobacter lineage. Appl Environ Microbiol **71:**5665-5677.

9. **Charlson, R. J., J. E. Lovelock, M. O. Andreae, and S. G. Warren.** 1987. Oceanic phytoplankton, atmospheric sulfur, cloud albedo and climate. Nature **326:**655-661.

10. **Chin, M., and D. J. Jacob.** 1996. Anthropogenic and natural contributions to tropospheric sulfate: A global model analysis. J Geophys Res-Atmos **101:**18691-18699.

11. **Curson, A. R., M. J. Sullivan, J. D. Todd, and A. W. Johnston.** 2011. DddY, a periplasmic dimethylsulfoniopropionate lyase found in taxonomically diverse species of Proteobacteria. ISME J.

12. **Curson, A. R. J., R. Rogers, J. D. Todd, C. A. Brearley, and A. W. B. Johnston.** 2008. Molecular genetic analysis of a dimethylsulfoniopropionate lyase that liberates the

climate-changing gas dimethylsulfide in several marine alpha-proteobacteria and *Rhodobacter sphaeroides*. Environ Microbiol **10:**1099-1099.

13. **Dacey, J. W. H., and N. V. Blough.** 1987. Hydroxide decomposition of dimethylsulfoniopropionate to form dimethylsulfide. Geophys Res Lett **14:**1246-1249.

14. **Dai, Y., P. C. Wensink, and R. H. Abeles.** 1999. One protein, two enzymes. J Biol Chem **274:**1193-1195.

15. **de Souza, M. P., and D. C. Yoch.** 1995. Comparative physiology of dimethyl sulfide production by dimethylsulfoniopropionate lyase in *Pseudomonas doudoroffii* and *Alcaligenes* sp. strain M3A. Appl Environ Microbiol **61:**3986-3991.

16. **de Souza, M. P., and D. C. Yoch.** 1995. Purification and characterization of dimethylsulfoniopropionate lyase from an *Alcaligenes*-like dimethyl sulfide-producing marine isolate. Appl Environ Microbiol **61:**21-26.

17. **De Zwart, J., J. Sluis, and J. G. Kuenen.** 1997. Competition for dimethyl sulfide and hydrogen sulfide by *Methylophaga sulfidovorans* and *Thiobacillus thioparus* T5 in continuous cultures. Appl Environ Microbiol **63:**3318-3322.

18. **del Valle, D. A., D. J. Kieber, and R. P. Kiene.** 2007. Depth-dependent fate of biologically-consumed dimethylsulfide in the Sargasso Sea. Mar Chem **103:**197-208.

19. **Erb, T. J., I. A. Berg, V. Brecht, M. Muller, G. Fuchs, and B. E. Alber.** 2007. Synthesis Of C-5-dicarboxylic acids from C-2-units involving crotonyl-CoA carboxylase/reductase: The ethylmalonyl-CoA pathway. P Natl Acad Sci USA **104:**10631-10636.

20. **Erb, T. J., G. Fuchs, and B. E. Alber.** 2009. (2S)-Methylsuccinyl-CoA dehydrogenase closes the ethylmalonyl-CoA pathway for acetyl-CoA assimilation. Mol Microbiol **73:**992-1008.

21. **Flavin, M., and S. Ochoa.** 1957. Metabolism of propionic acid in animal tissues. 1. Enzymatic conversion of propionate to succinate. J Biol Chem **229:**965-979.

22. **Franklin, D. J., M. Steinke, J. Young, I. Probert, and G. Malin.** 2010. Dimethylsulphoniopropionate (DMSP), DMSP-lyase activity (DLA) and dimethylsulphide (DMS) in 10 species of coccolithophore. MAR ECOL-PROG SER **410:**13-23.

23. **Friedrich, C. G., D. Rother, F. Bardischewsky, A. Quentmeier, and J. Fischer.** 2001. Oxidation of reduced inorganic sulfur compounds by bacteria: Emergence of a common mechanism? Appl Environ Microbiol **67:**2873-2882.

24.   **Gage, D. A., and D. Rhodes.** 1997. A new route for synthesis of dimethylsulphoniopropionate in marine algae. Nature **387:**891.

25.   **Ghosh, W., and B. Dam.** 2009. Biochemistry and molecular biology of lithotrophic sulfur oxidation by taxonomically and ecologically diverse bacteria and archaea. Fems Microbiol Rev **33:**999-1043.

26.   **Gonzalez, J. M., R. P. Kiene, and M. A. Moran.** 1999. Transformation of sulfur compounds by an abundant lineage of marine bacteria in the alpha-subclass of the class Proteobacteria. Appl Environ Microbiol **65:**3810-3819.

27.   **Gould, W. D., and T. Kanagawa.** 1992. Purification and properties of methyl mercaptan oxidase from *Thiobacillus thioparus* TK-m. J Gen Microbiol **138:**217-221.

28.   **Hatakeyama, S., M. Okuda, and H. Akimoto.** 1982. Formation of sulfur-dioxide and methanesulfonic-acid in the photo-oxidation of dimethyl sulfide in the air. Geophys Res Lett **9:**583-586.

29.   **Heilbronn, J., J. Wilson, and B. J. Berger.** 1999. Tyrosine aminotransferase catalyzes the final step of methionine recycling in *Klebsiella pneumoniae*. J Bacteriol **181:**1739-1747.

30.   **Hetzel, M., M. Brock, T. Selmer, A. J. Pierik, B. T. Golding, and W. Buckel.** 2003. Acryloyl-CoA reductase from *Clostridium propionicum*. An enzyme complex of propionyl-CoA dehydrogenase and electron-transferring flavoprotein. Eur J Biochem **270:**902-910.

31.   **Hill, R. W., B. A. White, M. T. Cottrell, and J. W. H. Dacey.** 1998. Virus-mediated total release of dimethylsulfoniopropionate from marine phytoplankton: a potential climate process. Aquat Mirob Ecol **14:**1-6.

32.   **Howard, E. C., J. R. Henriksen, A. Buchan, C. R. Reisch, H. Burgmann, R. Welsh, W. Ye, J. M. Gonzalez, K. Mace, S. B. Joye, R. P. Kiene, W. B. Whitman, and M. A. Moran.** 2006. Bacterial taxa that limit sulfur flux from the ocean. Science **314:**649-652.

33.   **Howard, E. C., S. L. Sun, E. J. Biers, and M. A. Moran.** 2008. Abundant and diverse bacteria involved in DMSP degradation in marine surface waters. Environ Microbiol **10:**2397-2410.

34.   **Kanzaki, H., M. Kobayashi, T. Nagasawa, and H. Yamada.** 1987. Purification and characterization of cystathionine gamma-synthase type-II from *Bacillus sphaericus*. Eur J Biochem **163:**105-112.

35.   **Karsten, U., K. Kuck, C. Vogt, and G. O. Kirst.** 1996. Dimethylsulphoniopropionate production in phototrophic organisms and its physiological function as a cryoprotectant., p. 143-153. *In* R. P. Kiene, P. T. Visscher, M. D. Keller, and G. O. Kirst (ed.), Biological

and Environmental Chemistry of DMSP and Related Sulfonium Compounds. Plenum Press, New York.

36. **Kiene, R. P.** 1996. Production of methanethiol from dimethylsulfoniopropionate in marine surface waters. Mar Chem **54:**69-83.

37. **Kiene, R. P., and T. S. Bates.** 1990. Biological removal of dimethyl sulfide from seawater. Nature **345:**702-705.

38. **Kiene, R. P., and L. J. Linn.** 2000. The fate of dissolved dimethylsulfoniopropionate (DMSP) in seawater: Tracer studies using S-35-DMSP. Geochim Cosmochim Ac **64:**2797-2810.

39. **Kiene, R. P., L. J. Linn, J. Gonzalez, M. A. Moran, and J. A. Bruton.** 1999. Dimethylsulfoniopropionate and methanethiol are important precursors of methionine and protein-sulfur in marine bacterioplankton. Appl Environ Microbiol **65:**4549-4558.

40. **Kiene, R. P., and B. F. Taylor.** 1988. Biotransformations of organosulfur compounds in sediments via 3-mercaptopropionate. Nature **332:**148-150.

41. **Kiene, R. P., and B. F. Taylor.** 1988. Demethylation of dimethylsulfoniopropionate and production of thiols in anoxic marine sediments. Appl Environ Microbiol **54:**2208-2212.

42. **Kim, S. J., H. J. Shin, Y. C. Kim, D. S. Lee, and J. W. Yang.** 2000. Isolation and purification of methyl mercaptan oxidase from *Rhodococcus rhodochrous* for mercaptan detection. Biotechnol Bioloproc E **5:**465-468.

43. **Kirkwood, M., N. E. Le Brun, J. D. Todd, and A. W. B. Johnston.** 2010. The dddP gene of *Roseovarius nubinhibens* encodes a novel lyase that cleaves dimethylsulfoniopropionate into acrylate plus dimethyl sulfide. Microbiol-Sgm **156:**1900-1906.

44. **Kirst, G. O.** 1990. Salinity tolerance of eukaryotic marine algae. Annu Rev Plant Phys **41:**21-53.

45. **Kocsis, M. G., and A. D. Hanson.** 2000. Biochemical evidence for two novel enzymes in the biosynthesis of 3-dimethylsulfoniopropionate in *Spartina alterniflora*. Plant Physiol **123:**1153-1161.

46. **Lovelock, J.** 2006. The revenge of Gaia : earth's climate in crisis and the fate of humanity. Basic Books, New York.

47. **Lovelock, J. E., R. J. Maggs, and R. A. Rasmussen.** 1972. Atmospheric dimethyl sulfide and natural sulfur cycle. Nature **237:**452-453.

48. **Lu, W. P., B. E. P. Swoboda, and D. P. Kelly.** 1985. Properties of the thiosulfate-oxidizing multi-enzyme system from *Thiobacillus versutus*. Biochim Biophys Acta **828:**116-122.

49. **McDevitt, C. A., P. Hugenholtz, G. R. Hanson, and A. G. McEwan.** 2002. Molecular analysis of dimethyl sulphide dehydrogenase from *Rhodovulum sulfidophilum*: its place in the dimethyl sulphoxide reductase family of microbial molybdopterin-containing enzymes. Mol Microbiol **44:**1575-1587.

50. **Moran, M. A., C. R. Reisch, R. P. Kiene, and W. B. Whitman.** 2012. Genomic Insights into Bacterial DMSP Transformations. Annu Rev Mar Sci **4**.

51. **Newton, R. J., L. E. Griffin, K. M. Bowles, C. Meile, S. Gifford, C. E. Givens, E. C. Howard, E. King, C. A. Oakley, C. R. Reisch, J. M. Rinta-Kanto, S. Sharma, S. L. Sun, V. Varaljay, M. Vila-Costa, J. R. Westrich, and M. A. Moran.** 2010. Genome characteristics of a generalist marine bacterial lineage. ISME J **4:**784-798.

52. **Nishiguchi, M. K., and L. J. Goff.** 1995. Isolation, purification, and characterization of DMSP lyase (dimethylpropiothetin dethiomethylase (4.4.1.3)) from the red alga *Polysiphonia paniculata*. J PHYCOL **31:**567-574.

53. **Okamuraikeda, K., K. Fujiwara, and Y. Motokawa.** 1982. Purification and characterization of chicken liver T-protein, a component of the glycine cleavage system. J Biol Chem **257:**135-139.

54. **Omelchenko, M. V., M. Y. Galperin, Y. I. Wolf, and E. V. Koonin.** 2010. Non-homologous isofunctional enzymes: A systematic analysis of alternative solutions in enzyme evolution. Biol Direct **5:**-.

55. **Otte, M. L., G. Wilson, J. T. Morris, and B. M. Moran.** 2004. Dimethylsulphoniopropionate (DMSP) and related compounds in higher plants. J Exp Bot **55:**1919-1925.

56. **Raina, J. B., E. A. Dinsdale, B. L. Willis, and D. G. Bourne.** 2010. Do the organic sulfur compounds DMSP and DMS drive coral microbial associations? Trends Microbiol **18:**101-108.

57. **Reisch, C. R., M. A. Moran, and W. B. Whitman.** 2008. Dimethylsulfoniopropionate-dependent demethylase (DmdA) from *Pelagibacter ubique* and *Silicibacter pomeroyi*. J Bacteriol **190:**8018-8024.

58. **Reisch, C. R., M. J. Stoudemayer, V. A. Varaljay, I. J. Amster, M. A. Moran, and W. B. Whitman.** 2011. Novel pathway for assimilation of dimethylsulphoniopropionate widespread in marine bacteria. Nature **473:**208-211.

59. **Rhodes, D., D. A. Gage, A. Cooper, and A. D. Hanson.** 1997. S-Methylmethionine conversion to dimethylsulfoniopropionate: evidence for an unusual transamination reaction. Plant Physiol **115:**1541-1548.

60. **Rusch, D. B., A. L. Halpern, G. Sutton, K. B. Heidelberg, S. Williamson, S. Yooseph, D. Y. Wu, J. A. Eisen, J. M. Hoffman, K. Remington, K. Beeson, B. Tran, H. Smith, H. Baden-Tillson, C. Stewart, J. Thorpe, J. Freeman, C. Andrews-Pfannkoch, J. E. Venter, K. Li, S. Kravitz, J. F. Heidelberg, T. Utterback, Y. H. Rogers, L. I. Falcon, V. Souza, G. Bonilla-Rosso, L. E. Eguiarte, D. M. Karl, S. Sathyendranath, T. Platt, E. Bermingham, V. Gallardo, G. Tamayo-Castillo, M. R. Ferrari, R. L. Strausberg, K. Nealson, R. Friedman, M. Frazier, and J. C. Venter.** 2007. The Sorcerer II Global Ocean Sampling expedition: Northwest Atlantic through Eastern Tropical Pacific. Plos Biol **5:**398-431.

61. **Schafer, H., N. Myronova, and R. Boden.** 2010. Microbial degradation of dimethylsulphide and related C-1-sulphur compounds: organisms and pathways controlling fluxes of sulphur in the biosphere. J Exp Bot **61:**315-334.

62. **Simo, R.** 2001. Production of atmospheric sulfur by oceanic plankton: biogeochemical, ecological and evolutionary links. Trends Ecol Evol **16:**287-294.

63. **Stefels, J.** 2000. Physiological aspects of the production and conversion of DMSP in marine algae and higher plants. J Sea Res **43:**183-197.

64. **Stefels, J., and W. Van Boeckel.** 1993. Production of DMS from dissolved DMSP in axenic cultures of the marine phytoplankton species *Phaeocystis* sp. MAR ECOL-PROG SER **97:**11-18.

65. **Steinke, M., G. Malin, S. D. Archer, P. H. Burkill, and P. S. Liss.** 2002. DMS production in a coccolithophorid bloom: evidence for the importance of dinoflagellate DMSP lyases. Aquat Microb Ecol **26:**259-270.

66. **Stines-Chaumeil, C., F. Talfournier, and G. Branlant.** 2006. Mechanistic characterization of the MSDH (methylmalonate semialdehyde dehydrogenase) from *Bacillus subtilis*. Biochem J **395:**107-115.

67. **Sunda, W., D. J. Kieber, R. P. Kiene, and S. Huntsman.** 2002. An antioxidant function for DMSP and DMS in marine algae. Nature **418:**317-320.

68. **Suylen, G. M. H., P. J. Large, J. P. Vandijken, and J. G. Kuenen.** 1987. Methyl mercaptan oxidase, a key enzyme in the metabolism of methylated sulfur-compounds by *Hyphomicrobium* EG. J Gen Microbiol **133:**2989-2997.

69. **Taylor, B. F., and D. C. Gilchrist.** 1991. New routes for aerobic biodegradation of dimethylsulfoniopropionate. Appl Environ Microbiol **57:**3581-3584.

70.   **Taylor, B. F., and P. T. Visscher.** 1996. Metabolic pathways involved in DMSP degradation, p. 265-276. *In* R. P. Kiene, P. T. Visscher, M. D. Keller, and G. O. Kirst (ed.), Biological and Environmental Chemistry of DMSP and Related Sulfonium Compounds. Plenum Press, New York.

71.   **Teufel, R., J. W. Kung, D. Kockelkorn, B. E. Alber, and G. Fuchs.** 2009. 3-hydroxypropionyl-coenzyme A dehydratase and acryloyl-coenzyme A reductase, enzymes of the autotrophic 3-hydroxypropionate/4-hydroxybutyrate cycle in the Sulfolobales. J Bacteriol **191:**4572-4581.

72.   **Todd, J. D., A. R. Curson, C. L. Dupont, P. Nicholson, and A. W. Johnston.** 2009. The *dddP* gene, encoding a novel enzyme that converts dimethylsulfoniopropionate into dimethyl sulfide, is widespread in ocean metagenomes and marine bacteria and also occurs in some *Ascomycete* fungi. Environ Microbiol **11:**1376-1385.

73.   **Todd, J. D., A. R. Curson, M. Kirkwood, M. J. Sullivan, R. T. Green, and A. W. Johnston.** 2010. DddQ, a novel, cupin-containing, dimethylsulfoniopropionate lyase in marine roseobacters and in uncultured marine bacteria. Environ Microbiol.

74.   **Todd, J. D., A. R. Curson, N. Nikolaidou-Katsaraidou, C. A. Brearley, N. J. Watmough, Y. Chan, P. C. Page, L. Sun, and A. W. Johnston.** 2009. Molecular dissection of bacterial acrylate catabolism - unexpected links with dimethylsulfoniopropionate catabolism and dimethyl sulfide production. Environ Microbiol.

75.   **Todd, J. D., M. Kirkwood, S. Newton-Payne, and A. W. Johnston.** 2011. DddW, a third DMSP lyase in a model Roseobacter marine bacterium, *Ruegeria pomeroyi* DSS-3. ISME J.

76.   **Todd, J. D., R. Rogers, Y. G. Li, M. Wexler, P. L. Bond, L. Sun, A. R. Curson, G. Malin, M. Steinke, and A. W. Johnston.** 2007. Structural and regulatory genes required to make the gas dimethyl sulfide in bacteria. Science **315:**666-669.

77.   **Toole, D. A., and D. A. Siegel.** 2004. Light-driven cycling of dimethylsulfide (DMS) in the Sargasso Sea: Closing the loop. Geophys. Res. Lett. **31:**-.

78.   **Toole, D. A., D. A. Siegel, and S. C. Doney.** 2008. A light-driven, one-dimensional dimethylsulfide biogeochemical cycling model for the Sargasso Sea. J Geophys Res-Biogeo **113:**-.

79.   **Toole, D. A., D. Slezak, R. P. Kiene, D. J. Kieber, and D. A. Siegel.** 2006. Effects of solar radiation on dimethylsulfide cycling in the western Atlantic Ocean. Deep-Sea Res Pt I **53:**136-153.

80. **Tripp, H. J., J. B. Kitner, M. S. Schwalbach, J. W. H. Dacey, L. J. Wilhelm, and S. J. Giovannoni.** 2008. SAR11 marine bacteria require exogenous reduced sulphur for growth. Nature **452:**741-744.

81. **Vallina, S. M., and R. Simo.** 2007. Strong relationship between DMS and the solar radiation dose over the global surface ocean. Science **315:**506-508.

82. **Vallina, S. M., R. Simo, T. R. Anderson, A. Gabric, R. Cropp, and J. M. Pacheco.** 2008. A dynamic model of oceanic sulfur (DMOS) applied to the Sargasso Sea: Simulating the dimethylsulfide (DMS) summer paradox. J Geophys Res-Biogeo **113:**-.

83. **van den Berg, A. J., S. M. Turner, F. C. vanDuyl, and P. Ruardij.** 1996. Model structure and analysis of dimethylsulphide (DMS) production in the southern North Sea, considering phytoplankton dimethylsulphoniopropionate- (DMSP) lyase and eutrophication effects. MAR ECOL-PROG SER **145:**233-244.

84. **van Duyl, F. C., W. W. C. Gieskes, A. J. Kop, and W. E. Lewis.** 1998. Biological control of short-term variations in the concentration of DMSP and DMS during a *Phaeocystis* spring bloom. J Sea Res **40:**221-231.

85. **Vandermaarel, M. J. E. C., M. Jansen, and T. A. Hansen.** 1995. Methanogenic conversion of 3-S-methylmercaptopropionate to 3-mercaptopropionate. Appl Environ Microbiol **61:**48-51.

86. **Varaljay, V. A., E. C. Howard, S. Sun, and M. A. Moran.** 2010. Deep sequencing of a dimethylsulfoniopropionate-degrading gene (*dmdA*) by using PCR primer pairs designed on the basis of marine metagenomic data. Appl Environ Microbiol **76:**609-617.

87. **Vila-Costa, M., D. A. del Valle, J. M. Gonzalez, D. Slezak, R. P. Kiene, O. Sanchez, and R. Simo.** 2006. Phylogenetic identification and metabolism of marine dimethylsulfide-consuming bacteria. Environ Microbiol **8:**2189-2200.

88. **Vila-Costa, M., J. M. Rinta-Kanto, S. Sun, S. Sharma, R. Poretsky, and M. A. Moran.** 2010. Transcriptomic analysis of a marine bacterial community enriched with dimethylsulfoniopropionate. ISME J **4:**1410-1420.

89. **Visscher, P. T., and B. F. Taylor.** 1994. Demethylation of dimethylsulfoniopropionate to 3-mercaptopropionate by an aerobic marine bacterium. Appl Environ Microbiol **60:**4617-4619.

90. **Wagner-Dobler, I., and H. Biebl.** 2006. Environmental biology of the marine Roseobacter lineage. Annu Rev Microbiol **60:**255-280.

91. **Wang, Y. Y., X. H. Ma, W. F. Zhao, X. M. Jia, L. Kai, and X. H. Xu.** 2006. Study on the creatinase from *Paracoccus* sp strain WB1. Process Biochem **41:**2072-2077.

92.   **Wolfe, G. V., and M. Steinke.** 1997. Grazing-activated chemical defence in a unicellular marine alga. Nature **387:**894-897.

93.   **Wolfe, G. V., and M. Steinke.** 1996. Grazing-activated production of dimethyl sulfide (DMS) by two clones of *Emiliania huxleyi*. Limnol Oceanogr **41:**1151-1160.

94.   **Yancey, P. H.** 2005. Organic osmolytes as compatible, metabolic and counteracting cytoprotectants in high osmolarity and other stresses. J Exp Biol **208:**2819-2830.

95.   **Yoch, D. C.** 2002. Dimethylsulfoniopropionate: its sources, role in the marine food web, and biological degradation to dimethylsulfide. Appl Environ Microbiol **68:**5804-5815.

96.   **Yost, D. M., and C. L. Mitchelmore.** 2009. Dimethylsulfoniopropionate (DMSP) lyase activity in different strains of the symbiotic alga *Symbiodinium microadriaticum*. MAR ECOL-PROG SER **386:**61-70.

97.   **Zubkov, M. V., B. M. Fuchs, S. D. Archer, R. P. Kiene, R. Amann, and P. H. Burkill.** 2002. Rapid turnover of dissolved DMS and DMSP by defined bacterioplankton communities in the stratified euphotic zone of the North Sea. Deep-Sea Res Pt II **49:**3017-3038.

CHAPTER 3

DMSP DEPENDENT DEMETHYLASE (DMDA) FROM *PELAGIBACTER UBIQUE* AND

SILICIBACTER POMEROYI[2]

Abstract

The ubiquitous algal metabolite dimethylsulfoniopropionate (DMSP) is a major source of carbon and reduced sulfur for marine bacteria. Recently, the enzyme responsible for the demethylation of DMSP, designated DmdA, was identified and homologs were found to be common in marine bacterioplankton cells. The recombinant DmdAs from the cultured marine bacteria *Pelagibacter ubique* HTCC1062 and *Silicibacter pomeroyi* DSS-3 were purified with a three step procedure using anion exchange, hydrophobic interaction, and hydroxyapatite chromatography. The *P. ubique* enzyme possessed a M_r on SDS-PAGE of 38,500. Under non-denaturing conditions, the M_r was 68,000, suggesting that the enzyme was likely to be a dimer. The purified enzyme exhibited strict substrate specificity for DMSP, as DmdA from both *S. pomeroyi P. ubique* possessed no detectible demethylase activity with glycine betaine, dimethyl glycine, methylmercaptopropionate, methionine, or dimethylsulfonioacetate. Less than 1% activity was found with dimethylsulfoniobutanoate and dimethylsulfoniopentanoate. The apparent K_ms for DMSP were 13.2 ±2.0 and 5.4 ±2.3 mM for the *P. ubique* and *S. pomeroyi* enzymes, respectively. In cell extracts of *S. pomeroyi* DSS-3, the apparent K_m for DMSP was 8.6 ±1.2 mM, similar to that of purified recombinant DmdA. The intracellular concentration of DMSP in chemostat-grown *S. pomeroyi* DSS-3 was 70 mM. These results suggest that marine bacterioplankton may actively accumulate DMSP to osmotically-significant concentrations that favor near maximal rates of DMSP demethylation activity.

Introduction

Dimethylsulfoniopropionate (DMSP) is synthesized by marine phytoplankton primarily for use as an intracellular osmolyte, although the compound has also been recognized as an antioxidant and predator deterrent (26, 39, 46). DMSP production by phytoplankton may account for 10% of the total carbon fixation in parts of the ocean (3, 37). Once released from phytoplankton cells, the carbon and sulfur in DMSP are both rapidly transformed in the marine microbial food web. While some phytoplankton are capable of degrading DMSP to dimethylsulfide (DMS), marine bacteria are considered the primary mediators of DMSP transformation in seawater (36). DMSP consumption by marine bacteria satisfies 1-15% of their carbon demand and most, if not all, of the bacterial sulfur demand (20, 37).

Bacterial degradation of DMSP occurs through two competing pathways, known as the cleavage and the demethylation pathways. The cleavage pathway results in the formation of DMS, the major natural source of sulfur to the atmosphere (2, 36). In the atmosphere, oxidation of DMS produces aerosols that can influence global climate by causing solar radiation backscatter and acting as cloud condensation nuclei (5, 29). A majority of DMSP, however, is degraded through the demethylation pathway (19). The initial step of the demethylation pathway is removal of a methyl group from DMSP to form methylmercaptopropionate (MMPA). Subsequently, MMPA can be demethylated to form mercaptopropionate or demethiolated to form methanethiol (MeSH) and acrylate or another 3-carbon compound (19, 43). MeSH is rapidly taken up by marine bacteria and incorporated into proteins (19).

The initial demethylation of DMSP is critical to oceanic sulfur flux because it precludes the possibility of DMS emission (15). Recently, the enzyme responsible for the demethylation of DMSP, designated DmdA, was discovered in two marine isolates from the Roseobacter and

45

SAR11 taxa, *Silicibacter pomeroyi* DSS-3 and *Pelagibacter ubique* HTCC1062, respectively.
These taxa are among the most abundant bacterial groups found in ocean surface waters (13, 31).
Based on metagenomic sequence data in the Sorcerer II Global Ocean Sampling Expedition, it
has been estimated that 58% of marine bacteria possess the gene encoding for DmdA (16).

Phylogenetic analyses of all identified DmdA sequences reveal a diverse set of proteins
that form five evolutionarily distinct clades, known as clades A, B, C, D, and E (16). However,
the bacterioplankton that harbor these DmdA orthologs remain largely unknown. At present,
clades B and C lack genes from any cultured organisms. Having no taxonomic anchors, it is not
possible to make comparisons of DmdA phylogeny to organismal phylogeny or determine if the
clades of DmdA are a result of organismal evolution or ecological adaptation. To examine this
question and gain insights into biological controls on DMSP degradation, the recombinant
DmdA from *S. pomeroyi* and *P. ubique,* representatives of clades A and D, respectively, were
purified and characterized.

Methods and Materials

Plasmid Construction and Expression of Recombinant Proteins

The *dmdA* homologs in the *Pelagibacter ubique* genome (11), SAR11_0246, and
Silicibacter pomeroyi DSS-3 genome (30), SPO_1913, were synthesized commercially with *E. coli* codon usage (GenScript Corporation). The synthesized genes were inserted into the
expression vector pCYB1 (New England Biolabs) to generate pABX101 and pCRX1,
respectively, which were transformed into *E. coli* Top10F' and BL21(DE3), respectively.
Plasmid-bearing cells were grown in Luria-Bertani broth at $37^{o}C$ until cultures reached an OD_{600}
of 0.6, at which time the cultures were induced with 25 μM or 200 μM IPTG for pABX101 and
pCRX1, respectively, and transferred to $25^{o}C$ for overnight incubation. Cells were harvested by

centrifugation at 10,000 x g for 10 min. Pellets were resuspended in 50 mM Tris-HCl, pH 8.0, with 1 mM EDTA and placed on ice. Cells were then lysed by sonication, using three 30 second bursts. Lysed cells were centrifuged at 30,000 x g for 30 min to remove cell debris from the supernatant.

Preparation of *Silicibacter pomeroyi* DSS-3 Extract

Silicibacter pomeroyi DSS-3 was grown in batch or continuous culture using an artificial seawater medium consisting of 0.08 M HEPES (pH 6.9), 0.29 mM KH_2PO_4, 7.1 mM NH_4Cl, 0.068 mM FeEDTA, 2% (w/v) sea salts (Sigma), and 0.1% (v/v) vitamin solution (12) . Cell extract was prepared after two days of growth on DMSP as the sole carbon source in batch culture. Cells were harvested by centrifugation at 10,000 x g for 10 min and washed once in growth medium without DMSP. The pellet was resuspended in 400 mM HEPES, pH 7.5, with 1 mM EDTA and placed on ice. Cells were then lysed by sonication, and centrifuged as described above.

Purification of DmdA

The recombinant DmdA from *P. ubique* was purified from 8 mL of *E. coli* soluble extract after induction of the plasmid borne-gene. The extract was loaded onto a Q-Sepharose HP (GE Healthcare) column (1.6 x 10.0 cm) equilibrated with 50 mM Tris-HCl, pH 8.0, and 1 mM EDTA with a flow rate of 1 mL/min. The column was washed with the buffer at a flow rate of 1 mL/min. All enzyme activity was retained in 8 mL of flow through. Active fractions were pooled and brought to 1.7 M $(NH_4)_2SO_4$ with the addition of the finely ground solid $(NH_4)_2SO_4$. The sample was applied to a Phenyl Superose (GE Healthcare) column (1.0 x 10 cm) equilibrated with 50 mM Tris-HCl, pH 8.0, containing 1.7 M $(NH_4)_2SO_4$ and 1 mM EDTA. Proteins were eluted with a linear gradient from 1.7-0 mM $(NH_4)_2SO_4$ in a total volume of 80

mL. Activity eluted at about 0.8 M NH_4SO_4. Fractions containing activity were pooled and concentrated using a Centricon Ultracel YM-10 filter. Concentrated protein was diluted eight times with 10 mM Na_2HPO_4, pH 7.0, and applied to a CHT Ceramic Hydroxyapatite Type 1 (BioRad) column (1.0 x 9 cm) at a flow rate of 0.5 mL/min. The column was washed with 10 mL of 10 mM Na_2HPO_4, pH 7.0, and proteins were eluted with linear gradient of 10-500 mM Na_2HPO_4, pH 7.0, in a total volume of 50 mL. Activity eluted at about 200 mM Na_2HPO_4. The active fractions were concentrated to 8 mg/mL using a Centricon Ultracel YM-10 filter.

The recombinant DmdA from *S. pomeroyi* was purified similarly to the *P. ubique* enzyme except for the following modifications. A linear gradient from 1.1-0 M $(NH_4)_2SO_4$ was used to elute proteins from the Phenyl Superose column. Activity eluted at about 0.7 M $(NH_4)_2SO_4$. Fractions containing activity were pooled and concentrated to about 0.1 mL using a Centricon Ultracel YM-10 filter. Concentrated protein was then diluted to 2 mL in 5 mM Na_2HPO_4, pH 6.8, and again concentrated. Concentrated protein was diluted eight times with 5 mM Na_2HPO_4, pH 6.8, and 0.03mM $CaCl_2$ and applied to a CHT Ceramic Hydroxyapatite Type 1 (BioRad) column (1.0 x 9 cm) equilibrated with the same buffer at a flow rate of 0.5 mL/min. The column was then washed with 10 mL of 5 mM Na_2HPO_4, pH 6.8, and 0.03mM $CaCl_2$ at a flow rate of 0.5mL/min. Enzyme activity eluted in the flow through. The active fraction was concentrated to 0.3 mg/mL using a Centricon Ultracel YM-10 filter.

Protein Concentration

The concentration of purified DmdA from *P. ubique* was determined by the Biuret method using bovine serum albumin as a standard (14). The mass extinction coefficient at 280 nm was determined to be 10.72 $g^{-1}L\ cm^{-1}$. Protein concentration was then routinely determined

using the mass extinction coefficient. Concentrations of other proteins were determined using BioRad Bradford reagent with bovine serum albumin as the standard.

Enzyme Assays

To minimize the effect of DMSP on reaction pH, a stock of buffered DMSP was prepared. A 600 mM solution of DMSP in 10 mL of 400 mM HEPES with 1 mM EDTA was brought to pH 6.5 with the dropwise addition of about 2 mL of 0.5 M NaOH with constant stirring. The final volume was then brought to 20 mL with 400 mM HEPES, 1 mM EDTA, pH 7.5. HPLC analysis of the buffered DMSP stock showed the presence of about 1 mM acrylate, indicating that only a small portion of DMSP was hydrolyzed during the neutralization procedure.

Unless specified differently, assays were performed using 400 mM HEPES, pH 7.5, 1 mM EDTA, 2 mM DTT, in 0.1 mL by combining 20 µL of 300 mM buffered DMSP stock solution and 0.685 mM tetrahydrofolate (THF). Due to the sensitivity of THF to O_2, assays were performed in an anaerobic chamber under a N_2/H_2 (95:5% v/v) atmosphere. Reactions were initiated with the addition of enzyme, incubated for 10 minutes, quenched by addition of 20 µL of 50% H_3PO_4, and briefly centrifuged to remove denatured proteins. Formation of either 5-methyl-THF or MMPA was determined by HPLC.

To determine the pH optimum, 400 mM of the following buffers were used at the indicated pH values: sodium 1,3-bis(tris(hydroxymethyl)methylamino)propane (BisTris propane; 6.5, 7.0, 7.5, 8.0, 8.5, 9.0, 9.5), sodium 2-(*N*-morpholino)ethanesulfonic acid (MES; 5.5, 6.0, 6.5), sodium 3-(N-morpholino)propanesulfonic acid (MOPS; 6.5, 7.0, 7.5), sodium HEPES (7.0, 7.5, 8.0) and Tris-HCl (7.5, 8.0, 8.5, 9.0). Activity was determined with 10 mM DMSP.

Assays to determine substrate specificity were performed using either 4 mM or 10 mM of analog. Reactions contained 2 µg of DmdA and were performed for three hours.

Kinetic analyses were performed as described above except that the DMSP concentrations were 2.5, 5.0, 10, 20, 40, and 60 mM and the THF concentrations were 0.042, 0.085, 0.17, 0.34, and 0.68 mM. Assays with *S. pomeroyi* DSS-3 extract were incubated for 35 minutes before quenching. Inhibition kinetics were determined using 5, 20, and 60 mM DMSP with 0, 1, 5, 10, and 20 mM inhibitor. Kinetic data was analyzed using SigmaPlot 10.0 with the Enzyme Kinetics module (Systat Software Inc.).

HPLC analysis was performed using Waters Alliance 4600 with a reverse phase SB-AQ column (2.6 x 250 mm, Agilent). The running buffer consisted of 6 % (v/v) acetonitrile, 25 mM NaH_2PO_4, and 0.8% (v/v) H_3PO_4 with a flow rate of 0.75 ml/min. MMPA and acrylate were detected by UV absorption at 214 nm, and 5-methyl-THF was detected at 280 nm.

To confirm the reaction products, 2 µg of *P. ubique* DmdA was incubated with 60 mM DMSP and 0.17 mM THF for 2 hours, at which time most THF was consumed, as determined by HPLC analysis. The reaction was diluted 1:20 in 100 mM phosphate buffer, pH 7.0, and a UV spectrum of the reaction mixture was taken.

Determination of native molecular weight by gel filtration

Purified DmdA from *P. ubique* was applied to a Sephacryl S200 HR (GE Healthcare) column (1.6 x 32 cm) equilibrated with 50 mM Tris-HCl pH 8.0, 1 mM EDTA, and 200 mM NaCl at a flow rate of 0.5 mL/min. Under the same conditions the following molecular weight standards were chromatographed: carbonic anhydrase (29 kDa), albumin from chicken egg white (46 kDa), bovine serum albumin monomer (66 kDa) and dimer (132 kDa).

PAGE

SDS-PAGE was performed using the NEXT-GEL system (AMRESCO) with 12.5% polyacrylamide mini-gels. Gels were stained with 0.1% Coomassie Blue in 50% methanol/10% acetic acid.

Substrate Synthesis

MMPA was synthesized by alkaline hydrolysis of its methyl ester, methyl-3-(methylthio)propionate (44). Dimethylsulfonioacetate and dimethylsulfoniopropionate were synthesized from bromoacetic acid and DMS or acrylic acid and DMS as described previously (4, 38). Dimethylsulfoniobutanoate and dimethylsulfoniopentanoate were synthesized by mixing 2 g of bromobutyric acid or bromovaleric acid, respectively, with 10 mL of DMS in a round bottom flask and heating the flask briefly in warm water to initiate the reaction. Vessels were covered and allowed to incubate at room temperature for 5 days. The remaining DMS was then evaporated, the product was dissolved in 5 mL of dH_2O, and an equal volume of diethyl ether was added. The solution was mixed thoroughly for several minutes, and the aqueous layer containing the product was removed and evaporated. The last step was repeated, and the products were confirmed using ^{1}H NMR.

To determine if the analogs were contaminated with DMSP, small amounts of DMSP were added to the analogs. The ^{1}H NMR peaks for DMSP were then compared to the background in the analog spectrum to determine the sensitivity for small amounts of contamination.

Intracellular DMSP

S. pomeroyi DSS-3 was grown at 30^oC in a carbon-limited chemostat using 1 mM DMSP at a flow rate of 0.1 mL/min and a dilution rate of 0.0416 per hour. After five volumetric

exchanges, the chemostat outflow was collected on ice for 5 minutes, and 0.4 mL of outflow was immediately centrifuged for 1 minute to pellet cells. The cells were then washed in 1 mL of medium without DMSP, and the supernatant was transferred into a 9.8 mL vial. Finally, the cells were resuspended in medium without DMSP and transferred to a 9.8 mL vial. The vials were sealed with Teflon-coated stoppers, and 1 mL of 5 M NaOH was added with a syringe. Alkaline hydrolysis of DMSP yields equimolar concentrations of DMS and acrylate. The vials were vortexed briefly and incubated for 15 minutes at 30°C. The headspace was then analyzed for DMS by gas chromatography on a SRI 8610-C GC with a Chromosil 330 column with nitrogen carrier gas a flow rate of 60 mL min^{-1}, oven temperature of 60°C and a flame photometric detector (8). Cell volume was calculated by first converting absorbance at 660 nm to dry weight using the equation: dry weight (μg mL^{-1}) $= 364.74A_{660} + 6.7A_{660}$ (27). Dry weight was converted to wet weight by assuming that 30% of the cell's total weight was dry weight and then subtracting dry weight (32). The volume was then calculated by using the density of water to convert from the water weight to volume. To measure the amount of DMSP remaining in spent medium, 1.5 mL of culture was collected on ice and immediately centrifuged for 1 min. The supernatant was decanted and placed into a 9.8 mL vial. The medium was then purged with N_2 for 5 min to remove dissolved DMS. The vial was then sealed and analyzed for DMSP as described above.

Phylogenetic Analysis

DmdA homologs were found using BLASTp searches against selected genomes. Sequences were aligned, edited, and analyzed using MEGA version 4.0 (40). Sequences were manually trimmed to 261 amino acids. A phylogenetic tree was constructed using the minimum evolution method, including 1000 bootstrap replicates. The GenBank accession number for all

sequences used in the phylogenetic analysis are as follows; *Homo* (P48728), *Pisum* (P49364), *Escherichia* (P27248), *Saccharomyces* (P48015), *Silicibacter* V (AAV97197), *Bacillus* (P54378), *Desulfovibrio* (ABB38793), *Pelagibacter* IV (AAZ21486), *Pyrococcus* (O58888), *Silicibacter* I (AAV95190), *Pelagibacter* I (AAZ21068), Clade B (ECV34452), Clade C (EDI11852), Clade E (EAW42451), *Rattus* I (Q64380), *Rattus* II (Q63342), *Haloarcula* (AAV45054), *Rhizobium* II (AAQ87218), *Silicibacter* VI (AAV96623), *Roseovarius* (EAP75561), *Burkholderia* (EDT09370), *Silicibacter* III (AAV94849), *Mycobacterium* (ABP47600), *Silicibacter* IV (AAV94866), *Rhizobium* (EDR75388), *Pelagibacter* III (AAZ22069), *Marinobacter* (EDM49742), *Pelagibacter* II (EAS84178), and *Silicibacter* II (AAV94935).

Results

Purification of DmdA

Recombinant DmdA from *P. ubique* was purified to electrophoretic homogeneity using a three step chromatographic purification as shown in Figure 2-1A. SDS-PAGE of the purified protein failed to detect contaminating proteins and comparison to a standard indicated a purity of >92%. Initial purifications yielded a labile enzyme which lost activity in a matter of days. Addition of EDTA to buffers greatly improved enzyme stability. In 50 mM Tris-HCl, pH 8.0, with 1 mM EDTA, the enzyme was stable for more than six months when stored at either -20° or 4°C. The enzyme did not bind to anion or cation exchange resins within ranges of pH 6-9. This inability to bind anion exchange resin was also observed in the recombinant glycine cleavage T-protein, which is homologous to DmdA (33). Nevertheless, substantial purification was obtained by passing the extracts through either anion or cation exchange resin.

Similarly, the recombinant DmdA from *S. pomeroyi* did not bind anion exchange resin at pH 8.0. Moreover, the enzyme also failed to bind CHT Ceramic Hydroxyapatite Type 1, even at very low salt concentrations. Thus, it was not possible to purify this protein to electrophoretic homogeneity by these methods. Integration of the bands identified on SDS-PAGE, as shown in Figure 2-1B, indicated a purity of 70%.

Properties of DmdA

Upon SDS-PAGE, the M_r of the denatured enzymes were 38,500-39,500, which was consistent with the predicted molecular mass based on the amino acid sequence of 39.5-41.5 kDa. The native molecular mass of the DmdA from *P. ubique* was investigated by gel filtration. In duplicate experiments, DmdA eluted as a single peak with a M_r of 66,000-69,000, indicating that the enzyme may exist as a dimer. Because the enzyme did not enter native PAGE gels, it was not possible to confirm the native molecular mass by this method. The inability of DmdA to bind to ion exchange resins or migrate into native PAGE gels suggests that the recombinant enzyme was neutral in charge. However, the predicted isoelectric points were 6.5 and 5.3 for Dmda from *P.ubique* and *S. pomeroyi*, respectively. Therefore, the absence of observed charge with ion exchange and native PAGE suggests that the charge on DmdA was hidden.

The activity of DmdA in several buffers was examined to find the optimum reaction conditions. BisTris propane, which has a wide buffering range, was inhibitory at pHs above 7.5 and was not used further. The DmdA from *P. ubique* was consistently more active in HEPES buffer, as compared to MOPS or Tris-HCl buffers at the same pH. Similarly, the DmdA from *S. pomeroyi* was more active in HEPES than MOPS buffer, but the activity in HEPES and Tris-HCl buffers are the same. These differences in activities are not due to differences in the counterions or ionic strengths of the buffers. For instance, 400 mM of $(NH_4)_2SO_4$, K_2HPO_4, $MgSO_4$, Na-

acetate, NaCl, and KCl had no effect on the enzyme activity. In contrast, 100 mM and 400 mM

$MgCl_2$ inhibited activity by 20 and 80%, respectively. Therefore, the different activities

observed in the buffers were due to direct interaction of DmdA with the buffers and not the

counterions.

The optimum pHs for the DmdA from *P. ubique* and *S. pomeroyi* were similar.

Maximum activity was observed at pH 7.0-8.0 for both enzymes. The *P. ubique* DmdA

possessed about 50% activity at pH's of 6.5 and 8.3. The DmdA from *S. pomeroyi* possessed

50% activity at pH's 6.0 and 8.8. Thus, all subsequent assays were carried out at pH 7.5 using

400 mM sodium HEPES buffer.

Product Confirmation

To confirm that the reaction transfers a methyl group from DMSP to THF, the products

of the enzyme reaction were examined by UV absorption spectroscopy and chromatographic

analysis. An enzyme reaction was run to completion so that most of the THF was consumed as

determined by UV spectra of the products. The product possessed an absorption maximum at

290 and minimum at 245 nm, identical to that of authentic 5-methyl-THF in the same buffer

(18). The formation of 5-methyl-THF was further confirmed because the product co-eluted with

the authentic 5-methyl-THF on HPLC (data not shown). The production of MMPA was also

confirmed by comparison of the elution time of the reaction product with the authentic

compound upon HPLC (data not shown).

Substrate specificity

The methyl donor specificity of DmdA from both *P. ubique* and *S. pomeroyi* was

investigated using a number of substrate analogs (Table 2-1). No activity was observed with

dimethylsulfonioacetate or the nitrogen-containing compounds tested. Very low rates of methyl-

THF formation were observed from the DMSP analogs dimethylsulfoniobutanoate and dimethylsulfoniopentanoate. This activity could be due to either the low activities of DmdA for these substrates or contamination of the analogs by DMSP. Examination of the ^{1}H NMR spectra indicated that the analogs contained less than 1% DMSP. Next, enzyme assays were performed with low concentrations of the analogs. Under these conditions, >3% of the substrates were consumed. Since the amount of substrate demethylated was greater than the maximum amount of DMSP contamination, the activity could not be attributed solely to DMSP contamination.

Inhibition

Inhibition of DMSP demethylation by the purified DmdA from *P. ubique* was studied using the substrate analogs and the product of DMSP demethylation, MMPA. DMSP demethylation was strongly inhibited by MMPA, where Lineweaver-Burke plots showed a series of non-parallel lines intersecting to the left of the origin, indicative of non-competitive inhibition (Figure 2-4). The data fit best to a non-competitive partial model of inhibition with a K_i of 2.1 ±0.4 mM. The substrate analogs dimethylsulfoniobutanoate and dimethylsulfoniopentanoate were weak inhibitors of DMSP demethylation. Kinetic analysis of dimethylsulfoniobutanoate and dimethylsulfoniopentanoate inhibition yielded a best fit to the mixed partial model, with K_i's of 47 and 19 mM, respectively.

Kinetics

The Michaelis-Menten constants for purified DmdA from *P. ubique* and *S. pomeroyi* were determined. Lineweaver-Burke plots showed a series of intersecting lines (Figure 2-2), indicative of a sequential mechanism in which both DMSP and THF must bind to the enzyme before catalysis. A random bi-bi mechanism, where the order of substrate binding and product release occurs randomly, yielded the best fit to each data set (Table 2-2). The high K_m values of

the purified enzyme for DMSP suggested that the recombinant enzymes might not be in their physiological conformation. To test this hypothesis, the kinetic constants for the native enzyme in cell extracts of *S. pomeroyi* were determined (Table 2-2 and Figure 2-2). The agreement of the K_m values for the recombinant and native activities confirmed that the recombinant enzymes were in their physiologically active forms.

Intracellular DMSP

The high K_m values observed and low concentration of DMSP typically found in the environment (nM range) suggested that cells might be accumulating DMSP intracellularly. To test this hypothesis, the intracellular concentration of DMSP in *S. pomeroyi* DSS-3 was measured by growing cells in a chemostat with DMSP as the limiting nutrient. The initial concentration of DMSP in the medium was 1 mM. The spent medium contained 2 μM, indicating that the cells consumed 99.8% of the available DMSP. In contrast, the intracellular DMSP was determined to be 152 and 157 μmols (g dry wt of cells)$^{-1}$ in duplicate measurements, implying that the intracellular DMSP concentration was about 70 mM. DMSP was not detected in the supernatant of the single wash step, indicating that the intracellular measurement was not affected by DMSP carryover and that cells did not readily lose significant amounts of DMSP during the washing. Thus, chemostat-grown *S. pomeroyi* cells accumulated very high levels of DMSP despite the very low concentrations in the culture medium.

Phylogenetic Analyses

DmdA is a member of a diverse enzyme family that includes the glycine cleavage T-protein and domains of dimethylglycine oxidase and sarcosine dehydrogenase (Figure 2-3). Phylogenetic analyses showed that proteins confirmed as glycine cleavage T-proteins from prokaryotes, eukaryotes, and Archaea clustered together, distinct from proteins with DMSP

demethylase activity. The carboxy termini of the dimethylglycine oxidase (E.C. 1.5.3.10) and sarcosine dehydrogenase (E.C. 1.5.99.1) are homologous to the T-protein (28). The sarcosine dehydrogenase and dimethylglycine oxidase enzymes from *Rattus* and several ORFs from proteobacteria also form an independent cluster. Several ORFs with unknown function but annotated as aminomethyl transferase proteins from both Bacteria and Archaea form additional clusters. Presumably, these represent novel enzymes within this family.

Discussion

The properties of the purified DmdAs from *S. pomeroyi* and *P. ubique* are consistent with their role in the THF-dependent demethylation of DMSP as previously hypothesized (15). The protein sequence of DmdA places the enzyme in the aminomethyl transferase family (E.C. 2.1.2.10), which includes the well characterized T-protein of the glycine cleavage system. The glycine cleavage system is comprised of four proteins which catalyze the conversion of glycine to 5,10-methylene-THF, CO_2, and NH_3. First, the P-protein catalyzes the decarboxylation of glycine and transfers the remaining aminomethylene group to the lipoic acid arm of the H-protein. Next, the T-protein liberates ammonia and transfers the methylene group to THF. Finally, the L-protein oxidizes the lipoic acid moiety of the H-protein (25). This complicated multiprotein system contrasts with the demethylation of DMSP, which is catalyzed by a single enzyme. Even though the glycine cleavage T-proteins and DmdA form separate groups within a diverse enzyme family, they possess similar K_ms for THF, 0.17 mM for T-protein (34) and 0.21-0.29 mM for DmdA. In the glycine cleavage system, the carbon donor is covalently bound to the H-protein, so it is not possible to compare these kinetic constants.

A THF-dependent DMSP demethylating enzyme was previously purified from a sulfate-reducing bacterium, but the identity of the gene encoding this protein was not reported (17).

This enzyme possessed a M_r upon SDS-PAGE of 35,000 but was extremely labile and O_2 sensitive. Despite the similarity in molecular weight to DmdA, the difference in O_2 sensitivity suggests that these enzymes are not closely related. In addition, phylogenetic analyses of DmdA against all sequenced δ-proteobacteria, which includes the sulfate-reducing bacteria, did not identify a potential ortholog of DmdA.

The K_m of DmdA for DMSP is higher than observed for bacterial DMSP-cleavage enzymes that mediate the competing pathway to DMS. DMSP lyase purified from a facultatively anaerobic *Alcaligenes* species had a K_m for DMSP of 1.4 mM (8), while the K_m of a purified DMSP lyase from *Desulfovibrio acrylicus* was 0.45 mM (9). These values are close to those expected for enzymes active with common intracellular metabolites, but are an order of magnitude lower than the values for DmdA. Whether or not similarly low K_ms for DMSP cleavage enzymes will be found in planktonic marine bacteria is not yet known, but the answer may shed light on the routing of DMSP to the demethylation vs. cleavage pathways in situ. If the intracellular concentrations of DMSP in *S. pomeroyi* and *P. ubique* are in the range typical for many other metabolites, DmdA would have only low activity in vivo. Instead, the kinetic constants for DmdA are consistent with the accumulation of DMSP to the high levels typical of osmoprotectants. For example, the common osmolyte glycine betaine is accumulated to intracellular concentrations of 130-170 mM by some bacteria (1, 35). Similarly, DMSP is a known osmoprotectant in marine and other bacteria (6, 10, 45). Natural populations of marine microorganisms taking up ^{35}S-labeled DMSP can retain most of the compound untransformed for 30 hours, suggesting intracellular accumulation (21, 22). The assimilation of both glycine betaine and DMSP in the marine environment may rely on the same high affinity transport system capable of taking up the compounds at low nM levels typical of seawater (24). The fact

that *S. pomeroyi* accumulates DMSP to 70 mM from a medium concentration of 2 µM suggests it may rely on DMSP as an osmolyte while metabolizing only that which is supplied in excess of the cells' requirement for osmoprotection.

Although measurements of intracellular DMSP concentration in *P. ubique* were not performed because of the challenges of maintaining cultures of this oligotrophic marine bacterium in the laboratory, the enzyme kinetics suggest this microorganism must also accumulate high levels of DMSP for demethylation to occur. Recently, it was shown that growth of *P. ubique* is dependent on an exogenous source of reduced sulfur, such as methionine or DMSP (42). In radiotracer experiments using ^{35}S-labeled DMSP, *P. ubique* took up 70% and incorporated 50% of DMSP-sulfur into protein (42). For DMSP sulfur to be incorporated into cellular protein, DMSP must first be demethylated by DmdA (23). Therefore, the assimilation of DMSP sulfur suggests that *P. ubique* also accumulates DMSP intracellularly to high levels.

To investigate whether the phylogenetic diversity of DmdA has functional significance, the properties of DmdA from *S. pomeroyi* and *P. ubique*, which represent phylogenetic clades A and D, were compared. The enzymes exhibited similar pH optimum and kinetics properties, and both had strict substrate specificities. While the K_ms for THF were very similar, the K_ms for DMSP were somewhat different, 5.4 mM and 13.2 mM for *S. pomeroyi* and *P. ubique*, respectively. Likewise, the calculated turnover numbers were also different, 2.4 s^{-1} for *S. pomeroyi* and 8.1 s^{-1} for *P. ubique*. Despite these differences, the catalytic efficiencies (k_{cat}/K_m) were very similar. Whether or not these small differences in K_m and V_{max} reflect physiological adaptations of DmdA harbored by *S. pomeroyi* and *P. ubique* is of ecological interest. Although both organisms probably use DMSP as an osmoprotectant, *P. ubique* requires DMSP or another exogenous source of reduced sulfur for growth (42), while *S. pomeroyi* is capable assimilating

sulfate. *S. pomeroyi* is also able to degrade DMSP through the cleavage pathway. While the ability of *P. ubique* to cleave DMSP has yet to be determined, homologs of recently identified genes involved in DMSP cleavage are absent in *P. ubique* (7, 41). Thus, it is possible that *P. ubique* lacks the cleavage pathway. These potential physiological differences may be reflected in the differing K_ms for DMSP, which may be part of the strategies for controlling DmdA activity in situ. The characterization of additional DmdAs, particularly from clades B, C, and E, is needed to further examine the kinetic diversity of DmdA. Nevertheless, the properties of DmdA reported here greatly expand our knowledge of the conditions under which DMSP demethylation can occur.

Acknowledgments

References

1. **Abee, T., R. Palmen, K. J. Hellingwerf, and W. N. Konings.** 1990. Osmoregulation in *Rhodobacter sphaeroides*. J Bacteriol **172:**149-54.

2. **Andreae, M. O., and H. Raemdonck.** 1983. Dimethyl sulfide in the surface ocean and the marine atmosphere: a global view. Science **221:**744-747.

3. **Archer, S. D., C. E. Widdicombe, G. A. Tarran, A. P. Rees, and P. H. Burkill.** 2001. Production and turnover of particulate dimethylsulphoniopropionate during a coccolithophore bloom in the northern North Sea. Aquatic Microbial Ecology **24:**225-241.

4.   **Chambers, S. T., C. M. Kunin, D. Miller, and A. Hamada.** 1987. Dimethylthetin can substitute for glycine betaine as an osmoprotectant molecule for *Escherichia coli*. J Bacteriol **169:**4845-7.

5.   **Charlson, R. J., J. E. Lovelock, M. O. Andreae, and S. G. Warren.** 1987. Oceanic phytoplankton, atmospheric sulfur, cloud albedo and climate. Nature **326:**655-661.

6.   **Cosquer, A., V. Pichereau, J. A. Pocard, J. Minet, M. Cormier, and T. Bernard.** 1999. Nanomolar levels of dimethylsulfoniopropionate, dimethylsulfonioacetate, and glycine betaine are sufficient to confer osmoprotection to *Escherichia coli*. Appl Environ Microbiol **65:**3304-11.

7.   **Curson, A. R., R. Rogers, J. D. Todd, C. A. Brearley, and A. W. Johnston.** 2008. Molecular genetic analysis of a dimethylsulfoniopropionate lyase that liberates the climate-changing gas dimethylsulfide in several marine alpha-proteobacteria and Rhodobacter sphaeroides. Environ Microbiol **10:**757-67.

8.   **de Souza, M. P., and D. C. Yoch.** 1995. Purification and characterization of dimethylsulfoniopropionate lyase from an *Alcaligenes*-like dimethyl sulfide-producing marine isolate. Appl Environ Microbiol **61:**21-26.

9.   **der Maarel, M. J. E. C., W. Aukema, and T. A. Hansen.** 1996. Purification and characterization of a dimethylsulfoniopropionate cleaving enzyme from *Desulfovibrio acrylicus*. FEMS Microbiology Letters **143:**241-245.

10.   **Diaz, M. R., P. T. Visscher, and B. F. Taylor.** 1992. Metabolism of dimethylsulfoniopropionate and glycine betaine by a marine bacterium. FEMS Microbiology Letters **96:**61-65.

11.   **Giovannoni, S. J., H. J. Tripp, S. Givan, M. Podar, K. L. Vergin, D. Baptista, L. Bibbs, J. Eads, T. H. Richardson, M. Noordewier, M. S. Rappe, J. M. Short, J. C. Carrington, and E. J. Mathur.** 2005. Genome streamlining in a cosmopolitan oceanic bacterium. Science **309:**1242-5.

12.   **Gonzalez, J. M., F. Mayer, M. A. Moran, R. E. Hodson, and W. B. Whitman.** 1997. *Microbulbifer hydrolyticus* gen. nov., sp. nov., and *Marinobacterium georgiense* gen. nov., sp. nov., two marine bacteria from a lignin-rich pulp mill waste enrichment community. Int J Syst Bacteriol **47:**369-76.

13.   **Gonzalez, J. M., and M. A. Moran.** 1997. Numerical dominance of a group of marine bacteria in the alpha-subclass of the class Proteobacteria in coastal seawater. Appl Environ Microbiol **63:**4237-42.

14.   **Gornall, A. G., C. J. Bardawill, and M. M. David.** 1949. Determination of serum proteins by means of the biuret reaction. J Biol Chem **177:**751-66.

15. **Howard, E. C., J. R. Henriksen, A. Buchan, C. R. Reisch, H. Burgmann, R. Welsh, W. Ye, J. M. Gonzalez, K. Mace, S. B. Joye, R. P. Kiene, W. B. Whitman, and M. A. Moran.** 2006. Bacterial taxa that limit sulfur flux from the ocean. Science **314:**649-52.

16. **Howard, E. C., S. Sun, E. J. Biers, and M. A. Moran.** 2008. Abundant and diverse bacteria involved in DMSP degradation in marine surface waters. Environ Microbiol **10:**2397-2410.

17. **Jansen, M., and T. A. Hansen.** 2000. DMSP: tetrahydrofolate methyltransferase from the marine sulfate-reducing bacterium strain WN. Journal of Sea Research **43:**225-231.

18. **Kaufman, B. T., K. O. Donaldson, and J. C. Keresztesy.** 1963. Chromatographic separation of the diastereoisomers of dl, L-5, 10-methylenetetrahydrofolate. J Biol Chem **238:**1498-500.

19. **Kiene, R. P.** 1996. Production of methanethiol from dimethylsulfoniopropionate in marine surface waters. Marine Chemistry **54:**69-83.

20. **Kiene, R. P., and L. J. Linn.** 2000. Distribution and turnover of dissolved DMSP and its relationship with bacterial production and dimethylsulfide in the Gulf of Mexico. Limnology and Oceanography **45:**849-861.

21. **Kiene, R. P., and L. J. Linn.** 2000. The fate of dissolved dimethylsulfoniopropionate (DMSP) in seawater: tracer studies using ^{35}S-DMSP. Geochimica et Cosmochimica Acta **64:**2797-2810.

22. **Kiene, R. P., L. J. Linn, and J. A. Bruton.** 2000. New and important roles for DMSP in marine microbial communities. Journal of Sea Research **43:**209-224.

23. **Kiene, R. P., L. J. Linn, J. Gonzalez, M. A. Moran, and J. A. Bruton.** 1999. Dimethylsulfoniopropionate and methanethiol are important precursors of methionine and protein-sulfur in marine bacterioplankton. Appl Environ Microbiol **65:**4549-58.

24. **Kiene, R. P., L. P. H. Williams, and J. E. Walker.** 1998. Seawater microorganisms have a high affinity glycine betaine uptake system which also recognizes dimethylsulfoniopropionate. Aquatic Microbial Ecology **15:**39-51.

25. **Kikuchi, G.** 1973. The glycine cleavage system: composition, reaction mechanism, and physiological significance. Mol Cell Biochem **1:**169-87.

26. **Kirst, G. O.** 1996. Osmotic adjustment in phytoplankton and macroalgae: the use of dimethylsulfoniopropionate (DMSP), p. 121-129. *In* R. P. Kiene, P. T. Visscher, M. D. Keller, and G. O. Kirst (ed.), Biological and environmental chemistry of DMSP and related sulfonium compounds. Plenum Press, New York, NY.

27.   **Koch, A. L.** 1994. Growth Measurement, p. 248-277. *In* P. Gerhardt, R. G. E. Murray, W. A. Wood, and N. R. Krieg (ed.), Methods for general and molecular bacteriology. American Society for Microbiology, Washington, D.C.

28.   **Leys, D., J. Basran, and N. S. Scrutton.** 2003. Channelling and formation of 'active' formaldehyde in dimethylglycine oxidase. EMBO J **22:**4038-48.

29.   **Lovelock, J. E., R. J. Maggs, and R. A. Rasmussen.** 1972. Atmospheric dimethyl sulphide and the natural sulphur cycle. Nature **237:**452-453.

30.   **Moran, M. A., A. Buchan, J. M. Gonzalez, J. F. Heidelberg, W. B. Whitman, R. P. Kiene, J. R. Henriksen, G. M. King, R. Belas, C. Fuqua, L. Brinkac, M. Lewis, S. Johri, B. Weaver, G. Pai, J. A. Eisen, E. Rahe, W. M. Sheldon, W. Ye, T. R. Miller, J. Carlton, D. A. Rasko, I. T. Paulsen, Q. Ren, S. C. Daugherty, R. T. Deboy, R. J. Dodson, A. S. Durkin, R. Madupu, W. C. Nelson, S. A. Sullivan, M. J. Rosovitz, D. H. Haft, J. Selengut, and N. Ward.** 2004. Genome sequence of Silicibacter pomeroyi reveals adaptations to the marine environment. Nature **432:**910-3.

31.   **Morris, R. M., M. S. Rappe, S. A. Connon, K. L. Vergin, W. A. Siebold, C. A. Carlson, and S. J. Giovannoni.** 2002. SAR11 clade dominates ocean surface bacterioplankton communities. Nature **420:**806-10.

32.   **Neidhardt, F. C., J. L. Ingraham, and M. Schaechter.** 1990. Physiology of the bacterial cell: a molecular approach. Sinauer Associates, Sunderland, Mass.

33.   **Okamura-Ikeda, K., K. Fujiwara, and Y. Motokawa.** 1992. Molecular cloning of a cDNA encoding chicken T-protein of the glycine cleavage system and expression of the functional protein in *Escherichia coli*. Effect of mRNA secondary structure in the translational initiation region on expression. J Biol Chem **267:**18284-90.

34.
       Okamura-Ikeda, K., K. Fujiwara, and Y. Motokawa. 1982. Purification and characterization of chicken liver T-protein, a component of the glycine cleavage system. J Biol Chem **257:**135-9.

35.   **Perroud, B., and D. Le Rudulier.** 1985. Glycine betaine transport in *Escherichia coli*: osmotic modulation. J Bacteriol **161:**393-401.

36.   **Simo, R.** 2001. Production of atmospheric sulfur by oceanic plankton: biogeochemical, ecological and evolutionary links. Trends Ecol Evol **16:**287-294.

37.   **Simo, R., S. D. Archer, C. Pedros-Alio, L. Gilpin, and C. E. Stelfox-Widdicombe.** 2002. Coupled dynamics of dimethylsulfoniopropionate and dimethylsulfide cycling and the microbial food web in surface waters of the North Atlantic. Limnology and Oceanography **47:**53-61.

38.   **Slow, S., M. Vasudevamurthy, R. Fraser, C. McEntyre, M. Lever, S. Chambers, and P. George.** 2007. Dimethylthetin treatment causes diffuse alveolar lung damage: a pilot study in a sheep model of Continuous Ambulatory Peritoneal Dialysis (CAPD). Exp Toxicol Pathol **58:**285-90.

39.   **Sunda, W., D. J. Kieber, R. P. Kiene, and S. Huntsman.** 2002. An antioxidant function for DMSP and DMS in marine algae. Nature **418:**317-20.

40.   **Tamura, K., J. Dudley, M. Nei, and S. Kumar.** 2007. MEGA4: Molecular Evolutionary Genetics Analysis (MEGA) software version 4.0. Mol Biol Evol **24:**1596-9.

41.   **Todd, J. D., R. Rogers, Y. G. Li, M. Wexler, P. L. Bond, L. Sun, A. R. Curson, G. Malin, M. Steinke, and A. W. Johnston.** 2007. Structural and regulatory genes required to make the gas dimethyl sulfide in bacteria. Science **315:**666-9.

42.   **Tripp, H. J., J. B. Kitner, M. S. Schwalbach, J. W. Dacey, L. J. Wilhelm, and S. J. Giovannoni.** 2008. SAR11 marine bacteria require exogenous reduced sulphur for growth. Nature **452:**741-4.

43.   **Visscher, P. T., M. R. Diaz, and B. F. Taylor.** 1992. Enumeration of bacteria which cleave or demethylate dimethylsulfoniopropionate in the Caribbean Sea. Marine Ecology-Progress Series **89:**293-296.

44.   **Wackett, L. P., J. F. Honek, T. P. Begley, V. Wallace, W. H. Orme-Johnson, and C. T. Walsh.** 1987. Substrate analogues as mechanistic probes of methyl-S-coenzyme M reductase. Biochemistry **26:**6012-8.

45.   **Wolfe, G. V.** 1996. Accumulation of dissolved DMSP by marine bacteria and its degradation via bacterivory, p. 277-291. *In* R. P. Kiene, P. T. Visscher, M. D. Keller, and G. O. Kirst (ed.), Biological and environmental chemistry of DMSP and related sulfonium compounds. Plenum Press, New York, NY.

46.   **Wolfe, G. V., and M. Steinke.** 1997. Grazing-activated chemical defence in a unicellular marine alga. Nature **387:**894-897.

Table 2-1. Rates of demethylation for DMSP and analogs.

Substrate	Sp act for recombinant DmdA from:[a]	
	P. ubique	*S. pomeroyi*
Dimethyl Glycine	<0.6	<0.6
Glycine Betaine	<0.6	<0.6
Methionine	<0.6	<0.6
Dimethylsulfonioacetate	<0.6	<0.6
Dimethylsulfoniopropionate	2490	649
Dimethylsulfoniobutanoate	7	2
Dimethylsulfoniopentanoate	11	8

[a] Values are averages of duplicate experiments expressed in nmols min^{-1} mg^{-1} using 4 mM substrate.

Table 2-2. Kinetic constants of DmdA.

Enzyme	R^2 (Random Bi-Bi)	K_m [mM THF]	K_m [mM DMSP]	V_{max} (μmols min^{-1} mg^{-1})	k_{cat} (s^{-1})	k_{cat}/K_m (M^{-1} s^{-1})
P. ubique	0.994	0.29 ±0.03	13.2 ±2.0	11.7	8.1	618
S. pomeroyi	0.976	0.21 ±0.04	5.4 ±2.3	3.7[a]	2.4	450
S. pomeroyi crude extract	0.997	0.26 ±0.02	8.6 ±1.2	0.0105	n.a.[b]	n.a.[b]

[a] Vmax for the recombinant *S. pomeroyi* enzyme was corrected for a protein purity of 70%.
[b] n.a. – not applicable
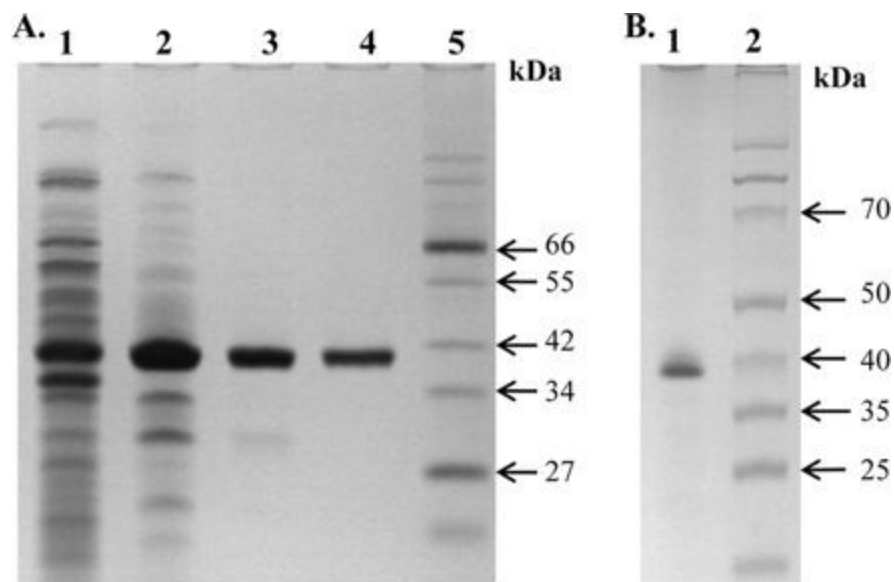
Fig 2-1. SDS-PAGE of purified recombinant *P. ubique* DmdA (A) and *S. pomeroyi* DmdA (B). The proteins from various purification steps were separated by SDS-PAGE on 12.5% polyacrylamide and stained with Coomassie Blue. (A) Crude soluble cell extract of recombinant *E. coli* (lane 1), Q-Sepharose flow through (lane 2), phenyl Superose eluate (lane 3), hydroxyapatite eluate (lane 4), and Broad Range protein marker (New England Biolabs, lane 5). (B) Hydroxyapatite flow through (lane 1), Broad Range Protein Marker (Fermentas, lane 2).
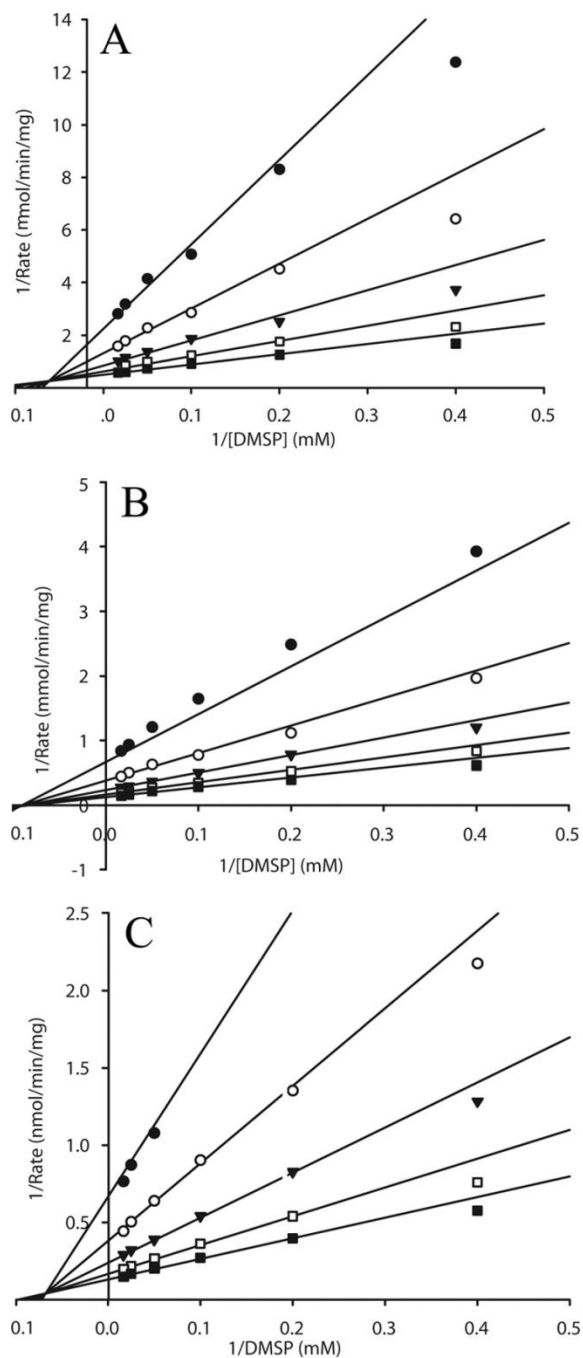
Fig 2-2. Lineweaver-Burke plots of DMSP demethylation. A, DmdA from *S. pomeroyi*. B, DmdA from *P. ubique*. C, crude cell extract from *S. pomeroyi* DSS-3. Lines are best fit to the overall data set of each graph using the random bi-bi model. Each plot indicates a different concentration of THF, as follows; 0.042 mM ●, 0.085 mM ○, 0.17 mM ▼, 0.34 mM □, and 0.68 mM ■.
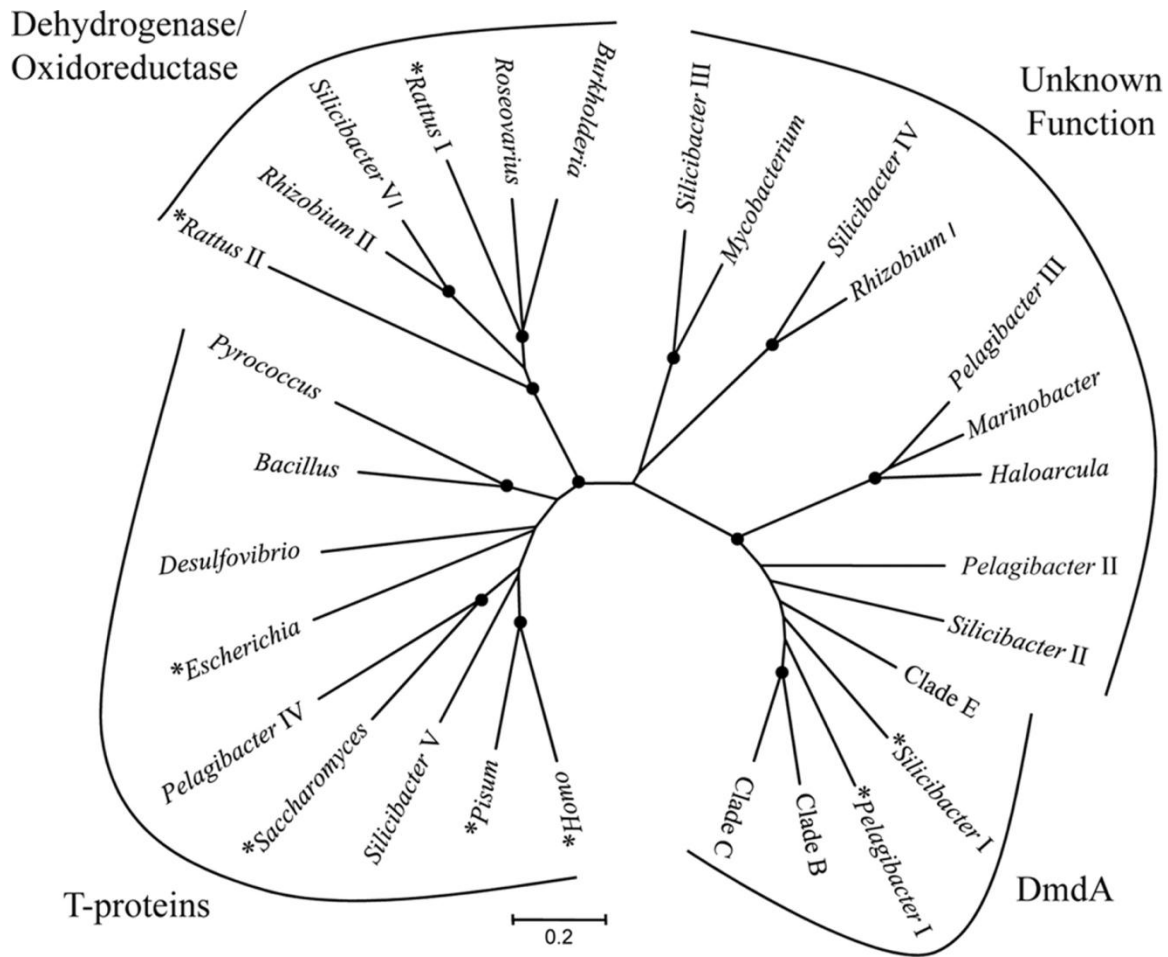
Fig 2-3. Phylogenetic tree of homologs to T-proteins and DmdA. The tree was constructed using the minimum evolution method with MEGA4 software. Enzymes with confirmed activity are indicated by *. Five DmdA sequences were used, representative of the five known phylogenetic clades, including clades A and D, from *Silicibacter pomeroyi* and *Pelagibacter ubique*, respectively(16), and clades B, C, and E from uncultured marine bacterioplankton. Closed circles at the branch points indicate ≥90% replication with 1000 bootstraps. The scale bar represents 0.2 amino acid substitutions per site. GenBank accession numbers of protein sequences are listed in materials and methods.
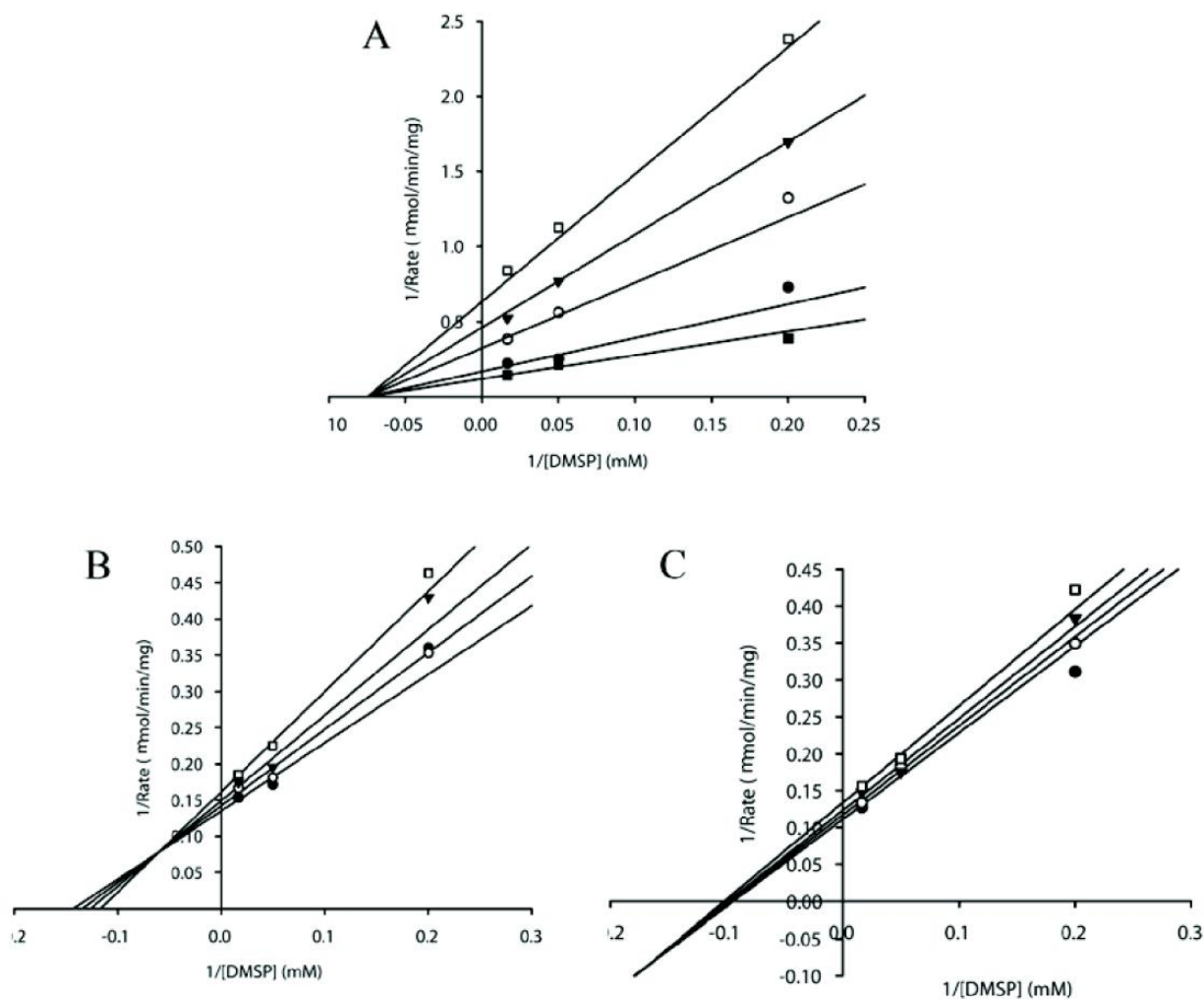
Figure 2-4. Lineweaver-Burke plots of inhibition of *P. ubique* DmdA by MMPA (A), dimethylsulfoniopentanoate (B), and dimethylsulfoniobutanoate (C). Lines are fit to the global data set using the non-competitive partial equation for MMPA and the mixed-partial equation for dimethylsulfoniopentanoate and dimethylsulfoniobutanation. Each plot represents a different inhibitor concentration, as follows; 20 mM (□), 10 mM (■), 5 mM (○), 1 mM (●), and 0 mM (▼).

CHAPTER 4

NOVEL PATHWAY FOR ASSIMILATION OF DIMETHYLSULFONIOPROPIONATE

WIDESPREAD IN MARINE BACTERIA

Abstract

Dimethylsulfoniopropionate (DMSP) accounts for up to 10% of carbon fixed by marine phytoplankton in ocean surface waters (2, 28), producing an estimated 11.7-103 Tmol S per year[14], most of which is processed by marine bacteria through the demethylation/demethiolation pathway (18). This pathway results in the release of methanethiol (MeSH) instead of the climatically active gas dimethylsulfide (DMS) and enables marine microorganisms to assimilate the reduced sulfur (19, 22, 37). Despite recognition of this critical microbial transformation for over two decades, the biochemical pathway and enzymes responsible have remained unidentified. Here we show that three novel enzymes related to fatty acid β-oxidation constitute the pathway that assimilates methylmercaptopropionate (MMPA), the first product of DMSP demethylation/demethiolation, and that two previously unknown CoA derivatives, 3-methylmercaptopropionyl-CoA (MMPA-CoA) and methylthiolacryolyl-CoA (MTA-CoA), are formed as novel intermediates (Fig. 1). A member of the marine roseobacters, *Ruegeria pomeroyi* DSS-3, was shown experimentally to require the MMPA-CoA pathway for MMPA assimilation and MeSH production. This pathway and the ability to produce MeSH from MMPA are present in diverse bacteria, and the ubiquitous SAR11 clade bacterium *Pelagibacter ubique* possesses enzymes for at least the first two steps. Analysis of marine metagenomic data indicates that the pathway is widespread among bacterioplankton in the ocean surface waters, making it one of the most important known routes for acquisition of reduced carbon and sulfur by surface ocean heterotrophs.

Full Text

The global importance of DMSP lies in its availability as a carbon and sulfur source for marine microorganisms and as a precursor of the gas dimethylsulfide (DMS) (1), the oceanic emission of which leads to the formation of cloud condensation nuclei and promotion of solar radiation backscatter (7). The existence of two competing pathways for the bacterial catabolism of DMSP, one releasing DMS and the other releasing methanethiol (MeSH), has been known for over twenty years. Only recently has there been progress on identifying the specific biochemical pathways and genes responsible for these transformations. To date, four genes have been identified that encode proteins which catalyze the cleavage reaction that releases DMS (8, 32, 33, 35), while one gene (*dmdA*) has been identified that encodes the initial demethylase in the pathway to MeSH (15). Following demethylation, the intermediate MMPA is further catabolized to the highly reactive volatile sulfur gas MeSH (17). This demethiolation pathway has long been hypothesized to be either an elimination or reductive cleavage, producing either acrylate or propionate, respectively (20, 30). An alternative proposal suggested that MMPA is catabolized similarly to β-oxidation of fatty acids (4, 31, 36). In either case, MeSH has not been shown to be a major product of DMSP metabolism as its rapid turnover results in very low concentrations in both culture based (Supplementary table 1) and environmental experiments (17). Thus, this report is the first direct evidence that MeSH is indeed a major degradation product of DMSP in at least some organisms.

To elucidate the pathway of DMSP demethiolation in the marine roseobacter *Ruegeria pomeroyi* DSS-3, coenzyme-A containing intermediates were examined. A *dmdA-* strain, which is incapable of DMSP demethylation, was supplied with DMSP and the wild-type was given MMPA. Upon CoA extraction and HPLC separation, an unknown CoA containing intermediate

was highly abundant in cells fed MMPA, as compared to the mutant strain, which could only utilize the cleavage pathway (Supplementary Fig. 1). Fourier transform ion cyclotron resonance (FT-ICR) mass spectrometry indicated that the mass of this unknown product was 870.137 (Supplementary Fig. 2a), consistent with the theoretical monoisotopic mass of a coenzyme-A-MMPA thioester (MMPA-CoA) of 870.137 $[M+H]^+$. MMPA-CoA was synthesized chemically and shown to have the same molecular weight and chromatographic retention time as the compound isolated from cell extracts. When $[1,2,3-^{13}C]$ DMSP was used as the carbon source for a mutant in this pathway (see below), the mass of MMPA-CoA purified from cell extracts by reverse phase chromatography increased as expected to 873.147 $[M+H]^+$ (Supplementary Fig. 2b), indicating that this compound was in fact a product of DMSP metabolism.

To identify the enzyme catalyzing the production of MMPA-CoA, the native enzyme was purified from *R. pomeroyi* DSS-3 cell extracts. One of four proteins remaining after purification, as judged by silver-stained SDS-PAGE, was identified as a medium chain fatty-acid CoA ligase by MALDI-TOF analysis (Supplementary Table 2). This protein, now designated as 3-methylmercaptopropionyl-CoA ligase (DmdB), was encoded by gene SPO2045. Confirmation that the gene encoded the correct protein was obtained by cloning SPO2045 into the pET101 expression vector and expressing in *E. coli*. The recombinant *E. coli* strain possessed MMPA-CoA ligase activity, while the host strain alone did not. The enzymatic reaction consumed ATP and produced AMP (Supplementary Fig. 3a) and is presumed to have produced pyrophosphate as well.

To elucidate the next step of the pathway, MMPA-CoA-consuming activity in *R. pomeroyi* DSS-3 was examined by incubating crude cell extracts with MMPA-CoA and various redox cofactors. Upon the addition of the artificial electron acceptors phenazine methosulfate or

ferrocenium hexafluorophosphate, MMPA-CoA was consumed and an unknown intermediate was produced (Supplementary Fig. 3b), the molecular mass of which was 868.121 [M+H]$^+$ (Supplementary Fig. 2c), exactly two hydrogen atoms less than MMPA-CoA. This mass was consistent with the theoretical monoisotopic molecular mass of methylthioacrylyl-CoA (MTA-CoA; Fig. 1).

Upon the addition of MTA-CoA to *R. pomeroyi* DSS-3 crude cell extract, MeSH and free CoA were released. The enzyme catalyzing the release of MeSH was purified to electrophoretic homogeneity from cell extracts of MMPA-grown *R. pomeroyi* DSS-3 (Supplementary Fig. 4) and identified as SPO3805, an enoyl-CoA hydratase and a member of the crotonase superfamily (cd06558)(Supplementary Table 3). Immediately upstream in the *R. pomeroyi* genome was a gene annotated as acyl-CoA dehydrogenase. We hypothesized that this gene, SPO3804, encoded the enzyme catalyzing the production of MTA-CoA. SPO3804 and SPO3805 were each cloned into the pET101 expression vector and expressed in *E. coli*. The recombinant *E. coli* strains had activity for MMPA-CoA dehydrogenase (SPO3804) and MTA-CoA hydratase (SPO3805), while the host strain alone did not. Therefore, we designate these genes as *dmdC* and *dmdD*, respectively.

The DmdD catalyzed reaction produced stoichiometric amounts of free CoA and MeSH. Using ^{1}H and ^{13}C NMR spectroscopy it was found that the three carbon moiety was transformed into acetaldehyde (Supplementary figures 5 and 6). The thioester bonded carbon of MTA-CoA was lost completely, presumably as CO_2, in the reaction (Supplementary figure7). Quantification of acetaldehyde produced from MTA-CoA found 90% of the theoretical yield. *R. pomeroyi* DSS-3 is capable of further oxidizing acetaldehyde to acetate, based on enzyme assays quantifying acetaldehyde dehydrogenase activity (Table 1).

There are multiple lines of evidence that confirm the physiological significance of these activities. In extracts of chemostat-grown cells the levels of DmdB, DmdC, and DmdD activities exceeded the minimum level, 57 nmol min^{-1} mg^{-1} of protein, necessary to support growth in the chemostat (Table 1 and supplementary methods). In addition, the amount of transcripts for *dmdB, dmdC,* and *dmdD* increased during growth on MMPA or DMSP, as expected if the pathway was required for MMPA metabolism (Supplementary Fig. 8).

Mutations in each of the MMPA-CoA pathway genes also yielded phenotypes consistent with their participation in the pathway. A *dmdC*⁻ mutant (SPO3804::Tn5) could not grow on MMPA as the sole source of carbon (Supplementary Fig. 9), indicating that this pathway was essential for growth on MMPA. In contrast, the mutant grew similarly to wild-type with DMSP, indicating that the cleavage pathway, initiated by DddQ or DddP (33), remained capable of supporting growth. Following growth with DMSP, the levels of DmdC and DmdD activity were greatly reduced (Table 1). The low level of DmdC activity was consistent with the presence of additional *dmdC* orthologs in *R. pomeroyi* DSS-3 (see below). The low level of DmdD activity suggested that *dmdC* and *dmdD* were cotranscribed. This hypothesis was consistent with the absence of a recognizable promoter preceding *dmdD*, the coregulation of both genes, and the reduced levels of *dmdD* transcript in the *dmdC*⁻ mutant (Supplementary Figure 8). Presumably, read-through of the transcriptional terminator on the kanamycin resistance marker was responsible for the low level of DmdD activity. The growth defect of the *dmdC* mutant was complemented with SPO3804 but not SPO3805 expressed on a plasmid, indicating that the failure of the *dmdC*⁻ mutant to grow on MMPA was not due to a polar affect on *dmdD*.

A *dmdD* (SPO3805::*tet*) mutant also failed to grow with MMPA, and growth on DMSP was severely inhibited (Supplementary Fig. 9d). Following growth on acetate, DmdD activity of

the mutant was <0.5 nmol min^{-1} mg^{-1}, while wild-type had activity of 12.7 nmol min^{-1} mg^{-1}.

Lastly, growth of a *dmdB* mutant (SPO2045::*tet*) was somewhat delayed during growth on

MMPA (Supplementary Fig. 9e). Following growth with DMSP, the DmdB activity was

reduced by only 40% compared to the wild-type (data not shown), which was consistent with the

presence of an additional *dmdB* ortholog in *R. pomeroyi* DSS-3 (see below).

Homologs to the *R. pomeroyi* DSS-3 genes are abundant in the genomic database. The

genomic database contained 36 bacteria that possessed *dmdA*, and all 36 also possessed *dmdB*

and *dmdC*. However, the distribution of *dmdB* and *dmdC* was not limited to those bacteria

possessing *dmdA*, and many β and γ-proteobacteria as well as other bacteria not typically

associated with marine systems possessed homologs with high sequence similarity to *dmdB* and

dmdC. To confirm that these *dmdA*-negative bacteria were capable of producing of MeSH from

MMPA, pure cultures of representative bacteria were grown in the presence of MMPA.

B*urkholderia thailandensis, Pseudomonas aeruginosa, Pseudoalteromonas atlantica,*

Myxococcus xanthus, and *Deinococcus radiodurans* all produced MeSH from MMPA. In

contrast, *Escherichia coli*, which does not possess highly similar homologs, did not produce

MeSH under the same conditions (Supplementary Table 4). While a strain of *Burkholderia* was

previously shown to possess a gene product capable of catalyzing the DMSP cleavage reaction

(35), it is unlikely that many of the organisms possessing the MMPA-CoA pathway naturally

encounter DMSP or MMPA derived from DMSP, and an alternative source of MMPA is likely.

One possibility is that MMPA is derived from methionine, via the "off-pathway" reaction in the

salvage pathway (24). Regardless of the source of MMPA, the presence of the MMPA-CoA

pathway in diverse bacteria further emphasizes its importance.

Both *dmdB* and *dmdC* are members of large gene families that encode enzymes with many different functions. To distinguish *dmdC* from closely related homologs with a different function, a selection of *dmdC* homologs from MeSH-producing bacteria were cloned and expressed in *E. coli.* Genes from *B. thailandensis*, *P. aeruginosa*, and *R. lacuscaerulensis* encoded proteins with DmdC activity. Similarly, all three copies of *dmdC* from *R. pomeroyi* DSS-3 yielded functional proteins when expressed in *E. coli*. Lastly, SAR11_0249, the *dmdC* homolog from the SAR11 clade bacterium *Pelagibacter ubique* HTCC1062, was synthesized, expressed in *E. coli*, and shown to possess DmdC activity. These genes encompassed a well-defined clade within the acyl-CoA dehydrogenases (Fig. 2). Likewise, both copies of *dmdB* from *R. pomeroyi* DSS-3 and SAR11_0248, the *Pelagibacter ubique* HTCC1062 *dmdB* homolog, yielded functional proteins when expressed in *E. coli*. These genes defined a similar DmdB clade of acyl-CoA ligases (Supplementary Fig. 10). Of the 49 sequenced genomes currently available in the JGI genomic database from the family *Rhodobacteraceae*, which contains the marine roseobacters, 47 and 49 possess *dmdB* and *dmdC* genes, respectively. The metabolism of reduced sulfur compounds in the marine roseobacters is complex, with some organisms producing MeSH from MMPA while lacking the ability to demethylate DMSP (11). Thus, some roseobacters possess *dmdB* and *dmdC* even though they lack *dmdA* and are unable to demethylate DMSP. In addition to demonstrating that the DMSP-CoA pathway was widespread among marine bacteria, these experiments demonstrated that homologs are widespread in bacteria from a variety of habitats.

Given the abundance of *Pelagibacter* and the roseobacters in the ocean, both *dmdB* and *dmdC* are likely to be abundant in ocean surface waters. Analysis of the GOS metagenomic database (27) confirmed this hypothesis, as over 6200 homologs to DmdB and DmdC were

found, indicating these genes may be present in up to 61% of surface ocean bacterioplankton (Supplementary Table 5).

In contrast, the *P. ubique* homolog to the *R. pomeroyi* DSS-3 DmdD possessed only low protein identity of 24%. When synthesized and expressed in *E. coli*, it did not possess activity with MTA-CoA as the substrate. The gene SAR11_0247, annotated as an α-β fold hydratase, was also cloned and expressed because it was located in between *dmdA* and *dmdB*. However, this gene product also did not have activity with MTA-CoA as the substrate. These results suggested that *dmdD* homologs were not widely distributed and may have been replaced by non-orthologous isofunctional enzymes in some organisms. To investigate the pathway being used by *dmdD*-negative bacteria, the activity of the enzymes of the MMPA-CoA pathway were assayed in the *dmdD*-negative strain *Ruegeria lacuscaerulensis*. Cell extracts had activity for both DmdB and DmdC, as expected, but also for DmdD (Table 1). Therefore, a non-orthologous isofunctional enzyme may have replaced *dmdD* in this bacterium. Whether an isofunctional enzyme is also catalyzing this step in *P. ubique* is unknown, but it is clear that orthologous proteins are not abundant in ocean surface waters as a BLASTp search against the GOS metagenomic database (27) yielded only 16 homologs with scores corresponding to an e-value of less than e^{-30}.

In conclusion, the novel MMPA-CoA pathway is widespread in marine and other bacteria. In oceans, this pathway leads to the formation of MeSH and acetate from the common osmolyte DMSP and prevents formation of the anti-greenhouse gas DMS. Acetate as a final product for the 3-carbon moiety of DMSP is significant in that possible fates of acetate are numerous in cells. The DMSP cleavage pathway in a strain of *Halomonas* also resulted in the production of acetate as an end product, although the distribution and abundance of this pathway

are unclear (34). The ecological function of the MMPA-CoA pathway outside the ocean is less understood. However, its ubiquity is strong evidence for an important role. Further investigations on the abundance, enzymology, and expression of this pathway will be critical to our understanding of biosequestration and flux of reduced sulfur and carbon in marine and other ecosystems.

Methods Summary

Growth of *R. pomeroyi* DSS-3 was performed as described previously (26) . For full details of growth conditions, protein purifications, enzyme assays, and genetic manipulations, see the Supplementary Methods.

Supplementary Methods.

Preparation of *R. pomeroyi* DSS-3 for intracellular acyl-CoA analysis

To investigate the biochemical pathways used to assimilate DMSP and MMPA in *R. pomeroyi* DSS-3, a targeted extraction of CoA-containing intermediates, such as those in the methylmalonyl-CoA or ethylmalonyl-CoA pathways, was performed. These experiments used a rich medium to grow the cells to a high density in order to obtain high amounts of CoA containing intermediates which could be detected by UV absorbance at 260 nm after HPLC separation. Wild- type *R. pomeroyi* DSS-3, *dmdA*⁻ (SPO1913::Tn5), or *dmdC*⁻ (SPO3804::Tn5) was grown overnight in half strength YTSS medium(10). Cells were harvested, washed once, and resuspended in marine basal medium (MBM) (26) with 5 mM MMPA (wild-type) or DMSP (*dmdA*⁻ and *dmdC*⁻) After overnight incubation, cells were again harvested and resuspended in 3 mL of MBM with 5 mM DMSP or MMPA. Cells were incubated for 1 hour, and then coenzyme-A containing intermediates were extracted.

Coenzyme-A extraction and analysis

Cells were quenched by the addition of trichloroacetic acid to 5%. Cell debris was removed by centrifugation at 10,000 x g for 10 min. The supernatant was then passed through an oligo purification cartridge (OPC, Applied Biosystems), which had been pre-washed with 70% acetonitrile/30% 10 mM KH_2PO_4 and then pre-equilibrated with 10 mM KH_2PO_4(9). The OPC was then washed with 3 mL of 10 mM KH_2PO_4 and flushed with 1 mL of air. Products retained on the cartridge were eluted with 0.5 mL of 70% acetonitrile/30% 10 mM KH_2PO_4. The eluent was diluted to 1.5 mL with dH_2O, frozen, and lyophilized.

Products retained by the OPC were resolved by reverse phase chromatography using a 4.6 x 250 mm, 5 μm particle size, Aquasil column (Thermo Fisher). The column was developed at a flow rate of 1 mL min^{-1} with a gradient of 2-20% acetonitrile in 50 mM ammonium acetate (pH 6.0) over 40 minutes. Products were detected by absorbance at 260 nm. Identification of acyl-CoA's was based on the elution time of known standards. Additionally, some products observed on the UV trace did not contain coenzyme-A and were not further identified.

Preparation of *R. pomeroyi* DSS-3 cell extracts

A 9 L culture of *R. pomeroyi* DSS-3 was grown in a 15 L fermentor with MBM and 3 mM MMPA as the sole source of carbon. The air flow was set to 10 L min^{-1}. Cells were harvested after 2 days of growth at an OD_{600} of 0.2 by centrifugation at 10,000 x *g* for 10 min and washed once with ice cold 50 mM Tris-HCl (pH 7.5). The pellet was resuspended in 5 mL of 50 mM Tris- HCl (pH 7.5). Cells were then lysed by passage through a French Pressure Cell at 100,000 KPa three times and centrifuged at 15,000 x g for 10 minutes. The supernatant was then centrifuged at 100,000 x g for 1 h at 4°C. The supernatant at this stage was used for enzyme purifications.

In vivo production of MeSH

Burkholderia thailandensis E264, *Psudoalteromonas atlantica* T6C, and *Ruegeria*

lacuscaerulensis were grown in MBM with 4 mM acetate with and without 1 mM MMPA.

Pseudomonas aeruginosa PAO1 and *Escherichia coli* BL21(DE3) were grown in M9 minimal

medium with 4 mM acetate or 4 mM acetate supplemented with 1 mM MMPA. *Deinococcus*

radiodurans (38) and *Myxococcus xanthus* (5) were grown in defined medium as described

previously, with and without 1 mM MMPA. All experiments were performed with 5 mL of

medium in 28 mL Balch tubes sealed with a Teflon coated stopper.

SPO3805 (DmdD) purification

Q-Sepharose HP chromatography. The cell extract was applied to a Q-Sepharose HP (GE

Healthcare) anion exchange column (1.6 x 10 cm) equilibrated with 50 mM Tris-HCl (pH 8.0) at

a flow rate of 2 mL/min. Protein was eluted with a gradient from 0-1 M NaCl over 8 column

volumes. Activity eluted over 20 mL between 19-30 mS/cm.

Phenyl-superose chromatography. Active fractions from Q-Sepharose chromatography were

pooled and made 1.7 M $(NH_4)_2SO_4$ by addition of solid $(NH_4)_2SO_4$. The solution was applied to

a phenyl-superose HR (GE Healthcare) hydrophobic interaction column (1 x 10 cm) at a flow

rate of 1 mL min^{-1}, and the column was washed with 1 column volume of 1.7 M $(NH_4)_2SO_4$ in 50

mM Tris-HCl (pH 7.5). Protein was eluted with a gradient of 1.7-0 M $(NH_4)_2SO_4$ in 50 mM

Tris-HCl (pH 7.5). Activity eluted at 110-96 mS cm^{-1}. Active fractions were pooled and

concentrated with an Amicon Ultra centrifugal filter (10 kD). The final concentrate was

suspended in 50 mM potassium phosphate buffer (pH 7.5).

HiTrap Blue chromatography. The concentrated protein solution was then applied to a HiTrap

Blue column (6 mL, GE Healthcare) that was equilibrated with 50 mM potassium phosphate (pH

7.5). The column was washed with 4 column volumes of buffer, and protein was eluted with a 0-2 M gradient of KCl in buffer over 6 column volumes. Activity eluted after start of the gradient. The 4 mL fraction containing the highest activity was concentrated using an Amicon Ultra centrifugal filter (10 kD).

Sephacryl S200 chromatography. The protein concentrate was applied to a Sephacryl S200 (GE Healthcare) gel filtration column (1.6 x 25 cm) that was pre-equilibrated with 50 mM Tris-HCl (pH 7.5) and 150 mM NaCl. The protein was eluted with buffer at a flow rate of 1 mL min^{-1}. Fractions with activity were analyzed on an SDS-PAGE gel and stained with Gel-Code Blue. The single protein band was excised with a razor blade and analyzed by in-gel trypsin digestion and MALDI-TOF mass spectrometry at the UGA PAMS facility.

Native SPO2045 (DmdB) purification

Q-Sepharose HP chromatography. The cell extract was applied and eluted from the column as described above. Activity eluted over 20 mL between 33-42 mS/cm.

Phenyl-superose chromatography. Active fractions from Q-Sepharose chromatography were pooled, made 1.7 M $(NH_4)_2SO_4$, and chromatographed as described above. Activity eluted between 39-22 mS/cm. Active fractions were pooled and concentrated with an Amicon Ultra centrifugal filter (10 kD). Final concentrate was suspended in 2 mL of 50 mM potassium phosphate (pH 7.5).

HiTrap Blue chromatography. The concentrated protein solution was then applied to a HiTrap Blue column and eluted as described above. Activity eluted after the start of the gradient. The 4 mL fraction containing the highest activity was concentrated using an Amicon Ultra centrifugal filter (10 kD).

Sephacryl S200 chromatography. The protein concentrate was applied to a Sephacryl S200 gel filtration column and chromatographed as described above. Active fractions were analyzed in duplicate on two SDS-PAGE gels. One gel was stained with silver stain and the second with GelCode Blue. Protein bands from the GelCode Blue stained gel were excised with a razor blade and analyzed by in-gel trypsin digestion and MALDI-TOF mass spectrometry at the UGA PAMS facility.

Preparation of recombinant *E. coli*

Genes were amplified from *R. pomeroyi* DSS-3, *R. lacuscaerulensis*, *Burkholderia thailandensis* E264, and *Pseudomonas aeruginosa* PA01genomic DNA or from pUC57 plasmids containing the synthesized *P. ubique* genes by PCR. PCR product was cloned into the pET101 expression vector using the methods recommended by Invitrogen, constructing the plasmids summarized in Supplementary table 6. All constructs were made using TOP10 *E. coli* and then introduced into BL21(DE3) or Rosetta (DE3) cells for protein expression. Cells for protein expression were grown overnight in LB broth. The culture was used to inoculate a flask containing 250-1000 mL of LB broth, which was incubated at 37° C until reaching an OD of 0.5-0.6. IPTG was then added to a concentration of 0.2 mM, and the culture was incubated overnight at room temperature. The culture was then harvested by centrifugation at 10,000 x g for 10 minutes, washed with 50 mM Tris-HCl (pH 7.5) and again centrifuged. The pellet was resuspended in 4 mL of buffer and lysed by passing twice through a French Pressure cell at 100,000 KPa. Cell debris was removed by centrifugation at 15000 x g for 10 minutes. The soluble fraction was subsequently used for protein purification or enzyme assays.

MALDI-FTICR

Mass spectra were collected on a 7 tesla BioApex Fourier-transform ion cyclotron resonance (FT-ICR) mass spectrometer (Bruker Daltonics, Billerica MA) equipped with an intermediate pressure Scout100 MALDI source. Samples were overlain with a matrix consisting of saturated 2,5-dihydroxybenzoic acid.

Enzyme assays

HPLC analysis. Analysis of DmdB, DmdC, and DmdD, reactions were performed using a 4.6 x 150 mm, 3 μm particle size, Hypersil Gold column (Thermo-Fisher) developed with a linear gradient of 2-20% acetonitrile in 50 mM ammonium acetate (pH 6) over 10 min.

Acetaldehyde dehydrogenase. Acetaldehyde dehydrogenase activity was determined by measuring the increase in absorbance at 340 nm following the reduction of NAD to NADH using an extinction coefficient of 6,220 $M^{-1}cm^{-1}$. Enzyme assay mixture contained 50 mM HEPES (pH 7.5), 25 mM 2-mercaptoethanol, 1 mM NAD, 5 mM acetaldehyde, and 0.02-0.04 mg of cell extract. Reactions were initiated by the addition of acetaldehyde or cell extract.

Gas chromatography

Methanethiol was measured by headspace gas chromatography on an SRI 8610-C gas chromatograph with a Chromosil 330 column (Supelco) with N_2 carrier gas at a flow rate of 60 ml min^{-1}, an oven temperature of 60°C, and a flame photometric detector. A standard curve for MeSH was obtained using a permeation tube (VICI Metronics).

Thiol quantification with DTNB

Free thiols resulting from the reaction of MTA-CoA were measured with 5,5'-dithio-bis(2-nitrobenzoic acid) (DTNB) using an extinction coefficient of 14,150 $M^{-1} cm^{-1}$. DTNB was prepared at a concentration of 10 mM in 50 mM potassium phosphate buffer (pH 7.5). A

reaction mixture containing 50 mM potassium phosphate (pH 7.5), 10 µM MTA-CoA, 0.5 mM DTNB, and 2 µg of purified DmdD were mixed, and the absorbance at 412 nm was taken.

Acetaldehyde quantification

Acetaldehyde was detected and quantified after reaction with semicarbazide to form acetaldehyde semicarbazone and HPLC separation. A reaction containing 0.1 mM MTA-CoA, 10 mM semicarbazide, and 50 mM potassium phosphate (pH 7.5) in 90 µl, was initiated with addition of 2 µg purified recombinant DmdD in 5 µl of buffer and run to completion. Five µl of 1 M formic acid were then added to quench the reaction and convert any acetaldehyde hydrate to acetaldehyde(3). The mixture was incubated at 37° C for two hours and centrifuged at 17,000 x g for 5 min. The supernatant was then analyzed by HPLC using a mobile phase of 2% acetonitrile with 0.5% acetic acid and UV detection at 224 nm (12).

Substrate synthesis

MMPA-CoA was synthesized by the mixed anhydride method(29) or enzymatically using purified recombinant DmdB with the same conditions described above. MMPA-CoA that was synthesized by either method was purified by reverse phase chromatography using an Ultrasphere ODS preparative column (10 x 250 mm). The column was developed with 50 mM ammonium acetate (pH 6) and a gradient of 2-20% acetonitrile. MMPA-CoA was detected at 254 nm. Fractions containing MMPA-CoA were lyophilized, resuspended in dH_2O and again lyophilized.

MTA-CoA was synthesized enzymatically by the dehydrogenation of MMPA-CoA using purified recombinant SAR11_0249 with the same reaction conditions described above. MTA-CoA was then purified by reverse phase chromatography as described for MMPA-CoA.

^{13}C enriched substrates were synthesized enzymatically from ^{13}C enriched DMSP. ^{13}C enriched DMSP was synthesized as described previously(6) using ^{13}C enriched acrylic acid and dimethylsulfide. The ^{13}C enriched DMSP was then demethylated to MMPA using recombinant DmdA and tetrahydrofolate as the methyl acceptor as described previously(26). MTA-CoA was produced enzymatically from MMPA using purified DmdB and DmdC and purified as described above.

Nuclear Magentic Resonance

^{1}H NMR was performed on a Varian Unity Inova 500 MHz spectrometer. A total of 1000 scans were recorded with a relaxation delay of 2 seconds and a pulse angle of 45°. ^{13}C NMR was performed at 125 MHz with a 5 second relaxation delay, 45° pulse angle, and 2000 scans.

Genetic modifications

Transposon mutagenesis was performed on *R. pomeroyi* DSS-3, mutants were screened for deficiency in MeSH production, and location of the transposon insertion was obtained by PCR and sequencing as described previously(14).

Targeted gene replacements were made by introduction of *tetAR* into *dmdB* (SPO2045) and *dmdD* (SPO3805). Up and downstream regions of homology 1000-1500 bp in length and the *tetAR* genes from pRK415 were PCR amplified and cloned into the pCR2.1 vector, which cannot replicate in *R. pomeroyi,* by SLIC cloning (23). Plasmid DNA was methylated by CpG methyltransferase as recommended by New England Biolabs and then introduced into *R. pomeroyi* DSS-3 cells by electroporation(13). Mutants were selected for ability to grow on tetracycline but not kanamycin, and confirmed by PCR.

Plasmids for complementation were made by PCR amplifying genes SPO3804, SPO3805, and both SPO3804 and SPO3805 from *R. pomeroyi* DSS-3 genomic DNA and ligating into the broad host expression vector pRK415(16). The plasmids constructed are summarized in Supplementary Table 6.

Growth curves

Three mL cultures of wild-type *R. pomeroyi* DSS-3 and mutant strains were grown in MBM with 2 mM glucose as the sole source of carbon. After overnight growth, the cultures were used to inoculate fresh 3 mL cultures, and optical density was recorded at 600 nm.

Chemostat cultures

R. pomeroyi DSS-3 was grown at 30°C in a carbon-limited chemostat using 2 mM MMPA in a total volume of 144 ml and a dilution rate of 0.0416 hour^{-1}. *R. lacuscaerulensis* was grown at 33°C with 1 mM MMPA with the same volume and dilution rates as above. A portion, of the culture, 100 mL, was removed and immediately centrifuged at 10,000 x g for 10 min, washed with 1.5 mL of ice cold 50 mM HEPES (pH 7.5). The cell pellet was resuspended in 1 mL of 50 mM HEPES (pH 7.5). Cells were then lysed by bead beating for 2 min. Cell debris was removed by centrifugation at 17,000 for 5 min. To determine the minimum enzyme activity required to sustain growth in the chemostat, the dry weight of the chemostat culture was estimated using the absorbance at 660 nm and the equation $(\mu g\ ml^{-1}) = 364.74A_{660} + 6.7A_{660}$ [21]. Using a substrate concentration of 1 mM for *R. lacuscaerulensis* or 2 mM for *R. pomeroyi* DSS-3 and a flow rate of 0.1 mL min^{-1}, there was a total of 100 or 200 nmol min^{-1} of substrate entering the chemostat. Assuming that 55% of dry weight was protein(25), the minimum enzyme activity required to sustain the observed MMPA consumption in the chemostat was estimated at 57 and 46 nmol min^{-1} mg^{-1} for *R. pomeroyi* DSS-3 and *R. lacuscaerulensis*, respectively.

Volatile organic sulfur consumption

Chemostat cultures of *R. pomeroyi* DSS-3 grown with DMSP were harvested and two mL was immediately placed into a 70 mL vial and sealed with a Teflon coated stopper. Approximately 125 nmol of MeSH was then added to the vials from the MeSH permeation tube, and samples were equilibrated for 10 minutes at 30°C. Headspace samples were then analyzed by gas chromatography at 30 min, 1 hr, and 19 hr.

Quantitative RT-PCR

RNA was extracted from chemostat-grown cell cultures of *R. pomeroyi* DSS-3 with acetate, MMPA, or DMSP as the sole carbon source. Cell culture, 50 mL, was collected into a 5 mL solution of 5% phenol in ethanol and centrifuged at 8000 x g for 10 min. The supernatant was decanted, and pellets stored at -80^0 C. RNA was extracted using the RNeasy mini kit (Qiagen, Valencia CA), and DNA was removed with TURBO DNA-free kit (Ambion, Austin TX). The primer sequences, amplicon sizes, and annealing temperatures are listed in Supplementary Table 7.

Reactions were performed with the Bio-Rad One-Step RT-PCR reaction mix with SYBR Green, 300 nM primer concentrations, and 0.5 µl iScript reverse transcriptase (RT) enzyme. DNA plasmid standards were constructed from a PCR product for each gene using the pCR 2.1-TOPO vector (Invitrogen, Carlsbad, CA). RT-qPCR was carried out on a Bio-Rad iCycler iQ with the following cycling conditions: 50^0 C for 10 min, 95^0 C for 5 min, 40 cycles of 95^0 C for 15 s and 61^0 C for 1.0 min, and a final step of 95^0 C for 1.0 minute and 61^0 C for 1.0 minute, followed by a melt curve analysis. Transcript copies were calculated from standard curves and normalized per ng of RNA.

Phylogenetic analysis

The DmdB (SAR11_0249), DmdC (SAR11_0248), and RecA (SAR11_0641) from *P. ubique* were used as query sequences for a BLASTp search against the genome sequences of: B*urkholderia thailandensis, Pseudomonas aeruginosa, Pseudoalteromonas atlantica, Myxococcus xanthus, Deinococcus radiodurans, P. ubique* HTCC1062, HTCC1002, HTCC7211, HIMB5, HIMB59, marine γ-proteobacteria HTCC2143, *Puniceispirillum marinum* IMCC1322, *R. pomeroyi* DSS-3, *R. lacuscaerulensis* 1157, *Dinoroseobacter shibae* DFL-12, and *Escherichia coli* BL21(DE3). HIMB5 and HIMB59 were not included in the NCBI database at the time of analysis, the peptide sequences of the annotated genomes were obtained from JCVI. All hits with an expect value <e10 were compiled into separate databases for DmdB and DmdC, and then the sequences were aligned using the MUSCLE algorithm in MEGA 5. Sequences with poor alignment and annotated as unrelated proteins were removed. Phylogenetic trees were built using maximum likelihood method in MEGA 5 with 100 bootstraps. Tree topology was confirmed with maximum likelihood method using PHYLIP v3.69.

GOS bioinformatics analysis

A custom reference database was established with DmdB, DmdC, and RecA homologs from the bacteria listed above. Reference sequences were designated as orthologs if they clustered in a phylogenetic tree with authentic DmdBs, DmdCs, or RecAs, or were otherwise considered paralogs. Separately, the DmdB (SAR11_0249), DmdC (SAR11_0248), and RecA (SAR11_0641) sequences from *P. ubique* were used as query sequences in BLASTp analysis against the GOS metagenomic database, and homologs with an expect value $< e^{-20}$ for DmdB and DmdC and <e3 for RecA were retained. The GOS sequences were then blasted against the custom reference databases, and those with top hits to sequences in authentic clusters were

summed while those with top hits to paralagous clusters were discarded. For DmdD, SPO3805

from *R. pomeroyi* DSS-3 was used as the query sequence for BLASTp analysis against the GOS

metagenomic database.

References

1. **Andreae, M. O.** 1990. Ocean-atmosphere interactions in the global biogeochemical sulfur cycle. Mar Chem **30:**1-29.

2. **Archer, S. D., C. E. Widdicombe, G. A. Tarran, A. P. Rees, and P. H. Burkill.** 2001. Production and turnover of particulate dimethylsulphoniopropionate during a coccolithophore bloom in the northern North Sea. Aqua Microb Ecol **24:**225-241.

3. **Bell, R. P., and W. C. E. Higginson.** 1949. The catalyzed dehydration of acetaldehyde hydrate, and the effect of structure on the velocity of protolytic reactions. Proc R Soc Lon Ser-A **197:**141-159.

4. **Bentley, R., and T. G. Chasteen.** 2004. Environmental VOSCs--formation and degradation of dimethyl sulfide, methanethiol and related materials. Chemosphere **55:**291-317.

5. **Bretscher, A. P., and D. Kaiser.** 1978. Nutrition of *Myxococcus xanthus*, a Fruiting Myxobacterium. J Bacteriol. **133:**763-768.

6. **Chambers, S. T., C. M. Kunin, D. Miller, and A. Hamada.** 1987. Dimethylthetin can substitute for glycine betaine as an osmoprotectant molecule for Escherichia coli. J Bacteriol **169:**4845-4847.

7. **Charlson, R. J., J. E. Lovelock, M. O. Andreae, and S. G. Warren.** 1987. Oceanic phytoplankton, atmospheric sulfur, cloud albedo and climate. Nature **326:**655-661.

8. **Curson, A. R. J., R. Rogers, J. D. Todd, C. A. Brearley, and A. W. B. Johnston.** 2008. Molecular genetic analysis of a dimethylsulfoniopropionate lyase that liberates the climate-changing gas dimethylsulfide in several marine alpha-proteobacteria and *Rhodobacter sphaeroides*. Environ Microbiol **10:**1099-1099.

9. **Deutsch, J., E. Grange, S. I. Rapoport, and A. D. Purdon.** 1994. Isolation and quantitation of long-chain acyl-coenzyme-A esters in brain-tissue by solid-phase extraction. Anal. Biochem. **220:**321-323.

10. **Gonzalez, J. M., J. S. Covert, W. B. Whitman, J. R. Henriksen, F. Mayer, B. Scharf, R. Schmitt, A. Buchan, J. A. Fuhrman, R. P. Kiene, and M. A. Moran.** 2003.

Silicibacter pomeroyi sp nov and *Roseovarius nubinhibens* sp nov., dimethylsulfoniopropionate-demethylating bacteria from marine environments. Int. J. Syst. Evol. Micr. **53:**1261-1269.

11.   **Gonzalez, J. M., R. P. Kiene, and M. A. Moran.** 1999. Transformation of sulfur compounds by an abundant lineage of marine bacteria in the alpha-subclass of the class Proteobacteria. Appl Environ Microbiol **65:**3810-3819.

12.   **Gupta, N. K.** 1970. A study of formaldehyde dismutation by liver alcohol dehydrogenase with NAD plus-analogs. Arch. Biochem. Biophys. **141:**632-640.

13.   **Henriksen, J. R.** 2008. Physiology of dimethylsulfoniopropionate metabolism in a model marine Roseobacter, *Silicibacter pomeroyi.* University of Georgia, Athens.

14.   **Howard, E. C., J. R. Henriksen, A. Buchan, C. R. Reisch, H. Burgmann, R. Welsh, W. Ye, J. M. Gonzalez, K. Mace, S. B. Joye, R. P. Kiene, W. B. Whitman, and M. A. Moran.** 2006. Bacterial taxa that limit sulfur flux from the ocean. Science **314:**649-652.

15.   **Howard, E. C., S. L. Sun, E. J. Biers, and M. A. Moran.** 2008. Abundant and diverse bacteria involved in DMSP degradation in marine surface waters. Environ Microbiol **10:**2397-2410.

16.   **Keen, N. T., S. Tamaki, D. Kobayashi, and D. Trollinger.** 1988. Improved broad-host-range plasmids for DNA cloning in Gram-Negative bacteria. Gene **70:**191-197.

17.   **Kiene, R. P.** 1996. Production of methanethiol from dimethylsulfoniopropionate in marine surface waters. Mar Chem **54:**69-83.

18.   **Kiene, R. P., L. J. Linn, and J. A. Bruton.** 2000. New and important roles for DMSP in marine microbial communities. J. Sea. Res **43:**209-224.

19.   **Kiene, R. P., L. J. Linn, J. Gonzalez, M. A. Moran, and J. A. Bruton.** 1999. Dimethylsulfoniopropionate and methanethiol are important precursors of methionine and protein-sulfur in marine bacterioplankton. Appl Environ Microbiol **65:**4549-4558.

20.   **Kiene, R. P., and B. F. Taylor.** 1988. Demethylation of dimethylsulfoniopropionate and production of thiols in anoxic marine sediments. Appl Environ Microbiol **54:**2208-2212.

21.   **Koch, A. L.** 1994. Growth measurement, p. 248-277. *In* R. G. E. M. P. Gerhardt, W. A. Wood, and N. R. Krieg (ed.), Methods for general and molecular bacteriology. American Society for Microbiology, Washington, D.C.

22.   **Ledyard, K. M., and J. W. H. Dacey.** 1996. Microbial cycling of DMSP and DMS in coastal and oligotrophic seawater. Limnol. Oceanogr. **41:**33-40.

23. **Li, M. Z., and S. J. Elledge.** 2007. Harnessing homologous recombination in vitro to generate recombinant DNA via SLIC. Nat. Methods **4:**251-256.

24. **Myers, R. W., J. W. Wray, S. Fish, and R. H. Abeles.** 1993. Purification and characterization of an enzyme involved in oxidative carbon-carbon bond-cleavage reactions in the methionine salvage pathway of *Klebsiella pneumoniae*. J. Biol. Chem. **268:**24785-24791.

25. **Neidhardt, F. C., J. L. Ingraham, and M. Schaechter.** 1990. Physiology of the bacterial cell : a molecular approach. Sinauer Associates, Sunderland, Mass.

26. **Reisch, C. R., M. A. Moran, and W. B. Whitman.** 2008. Dimethylsulfoniopropionate-dependent demethylase (DmdA) from *Pelagibacter ubique* and *Silicibacter pomeroyi*. J Bacteriol **190:**8018-8024.

27. **Rusch, D. B., A. L. Halpern, G. Sutton, K. B. Heidelberg, S. Williamson, S. Yooseph, D. Y. Wu, J. A. Eisen, J. M. Hoffman, K. Remington, K. Beeson, B. Tran, H. Smith, H. Baden-Tillson, C. Stewart, J. Thorpe, J. Freeman, C. Andrews-Pfannkoch, J. E. Venter, K. Li, S. Kravitz, J. F. Heidelberg, T. Utterback, Y. H. Rogers, L. I. Falcon, V. Souza, G. Bonilla-Rosso, L. E. Eguiarte, D. M. Karl, S. Sathyendranath, T. Platt, E. Bermingham, V. Gallardo, G. Tamayo-Castillo, M. R. Ferrari, R. L. Strausberg, K. Nealson, R. Friedman, M. Frazier, and J. C. Venter.** 2007. The Sorcerer II Global Ocean Sampling expedition: Northwest Atlantic through Eastern Tropical Pacific. Plos Biol **5:**398-431.

28. **Simo, R., S. D. Archer, C. Pedros-Alio, L. Gilpin, and C. E. Stelfox-Widdicombe.** 2002. Coupled dynamics of dimethylsulfoniopropionate and dimethylsulfide cycling and the microbial food web in surface waters of the North Atlantic. Limnol. Oceanogr. **47:**53-61.

29. **Stadtman, E. R.** 1957. Preparation and assay of acyl coenzyme-A and other thiol esters - use of hydroxylamine. Method. Enzymol. **3:**931-941.

30. **Taylor, B. F., and D. C. Gilchrist.** 1991. New routes for aerobic biodegradation of dimethylsulfoniopropionate. Appl Environ Microbiol **57:**3581-3584.

31. **Taylor, B. F., and P. T. Visscher.** 1996. Metabolic pathways involved in DMSP degradation, p. 265-276. *In* R. P. Kiene, P. T. Visscher, M. D. Keller, and G. O. Kirst (ed.), Biological and Environmental Chemistry of DMSP and Related Sulfonium Compounds. Plenum Press, New York.

32. **Todd, J. D., A. R. Curson, C. L. Dupont, P. Nicholson, and A. W. Johnston.** 2009. The *dddP* gene, encoding a novel enzyme that converts dimethylsulfoniopropionate into dimethyl sulfide, is widespread in ocean metagenomes and marine bacteria and also occurs in some *Ascomycete* fungi. Environ Microbiol **11:**1376-1385.

33. **Todd, J. D., A. R. Curson, M. Kirkwood, M. J. Sullivan, R. T. Green, and A. W. Johnston.** 2010. DddQ, a novel, cupin-containing, dimethylsulfoniopropionate lyase in marine roseobacters and in uncultured marine bacteria. Environ Microbiol.

34. **Todd, J. D., A. R. Curson, N. Nikolaidou-Katsaraidou, C. A. Brearley, N. J. Watmough, Y. Chan, P. C. Page, L. Sun, and A. W. Johnston.** 2009. Molecular dissection of bacterial acrylate catabolism - unexpected links with dimethylsulfoniopropionate catabolism and dimethyl sulfide production. Environ Microbiol.

35. **Todd, J. D., R. Rogers, Y. G. Li, M. Wexler, P. L. Bond, L. Sun, A. R. J. Curson, G. Malin, M. Steinke, and A. W. B. Johnston.** 2007. Structural and regulatory genes required to make the gas dimethyl sulfide in bacteria. Science **315:**666-669.

36. **Tripp, H. J., J. B. Kitner, M. S. Schwalbach, J. W. H. Dacey, L. J. Wilhelm, and S. J. Giovannoni.** 2008. SAR11 marine bacteria require exogenous reduced sulphur for growth. Nature **452:**741-744.

37. **van Duyl, F. C., W. W. C. Gieskes, A. J. Kop, and W. E. Lewis.** 1998. Biological control of short-term variations in the concentration of DMSP and DMS during a *Phaeocystis* spring bloom. J Sea Res **40:**221-231.

38. **Venkateswaran, A., S. C. McFarlan, D. Ghosal, K. W. Minton, A. Vasilenko, K. Makarova, L. P. Wackett, and M. J. Daly.** 2000. Physiologic determinants of radiation resistance in Deinococcus radiodurans. Appl Environ Microbiol **66:**2620-2626.

Contributions

C.R.R. performed growth experiments, enzyme assays, protein purifications, substrate synthesis, phylogenetic analysis, and all reaction analysis except MALDI-FTICR. M.J.S. and I.J.A. performed MALDI-FTICR analysis. C.R.R. and V.A.V. performed genetic modifications of *R. pomeroyi* DSS-3. V.A.V. performed RT-qPCR. C.R.R. and M.A.M. conducted bioinformatic analyses. C.R.R., M.A.M., and W.B.W. designed the experiments and wrote the paper. All authors reviewed the manuscript before submission.

Acknowledgements
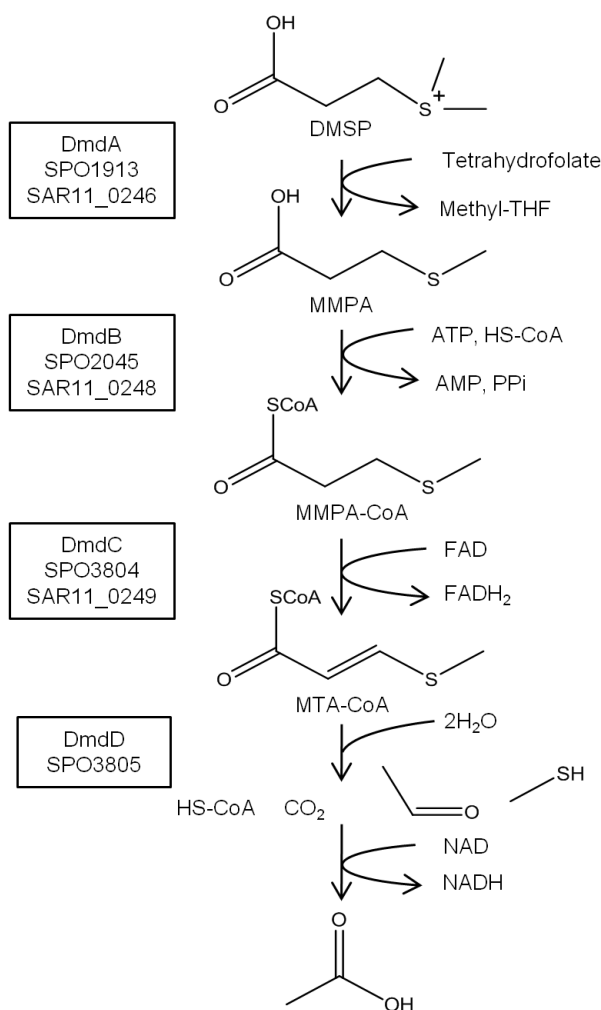
Fig. 3-1. Pathway of DMSP demethylation as identified in *R. pomeroyi* DSS-3. The genes identified thus far in both *R. pomeroyi* DSS-3 and *P. ubique* are indicated at each step. DMSP is first demethylated to MMPA in a tetrahydrofolate-dependent reaction catalyzed by DmdA as described previously[25] . A MMPA-CoA thioester is then formed in a reaction that consumes ATP and produces AMP. MMPA-CoA is then dehydrogenated forming an enoyl-CoA intermediate, MTA-CoA. In *R. pomeroyi* DSS-3, MTA-CoA is then hydrated by MTA-CoA hydratase in a reaction that releases the volatile sulfur product MeSH as well as free CoA, CO_2 and acetaldehyde. Acetaldehyde is then oxidized to acetic acid by acetaldehyde dehydrogenase.
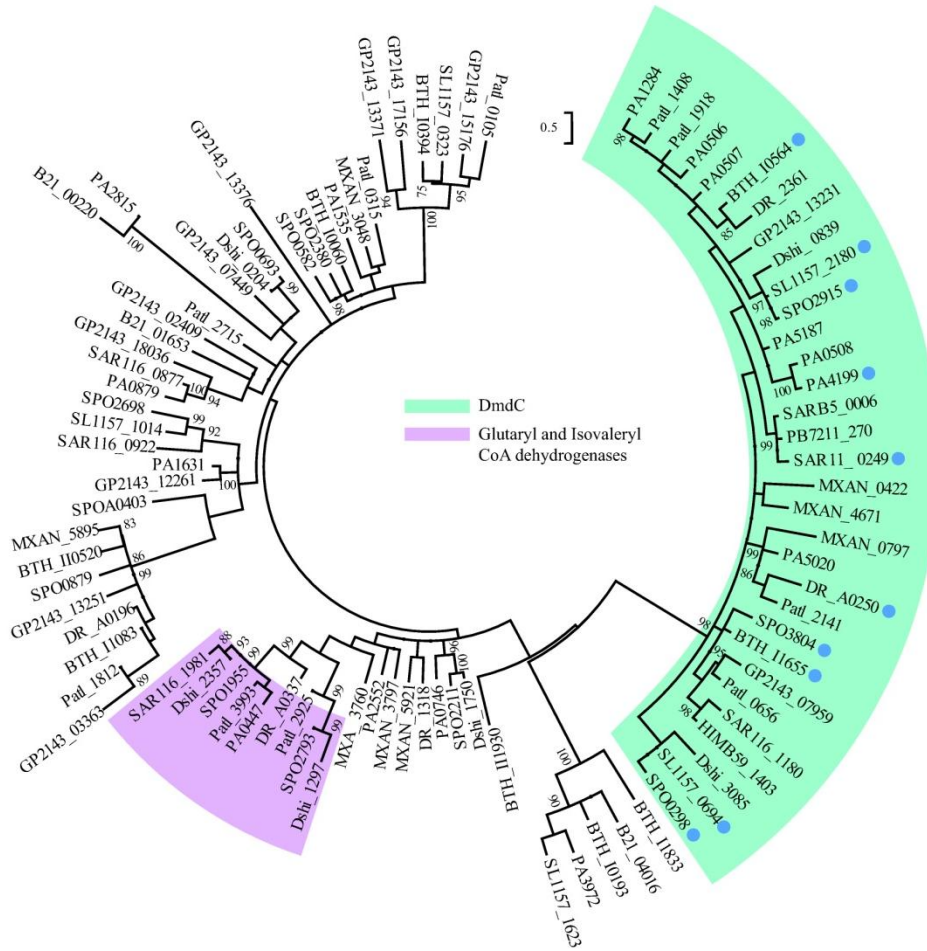
Fig. 3-2. Phylogenetic tree of DmdC from representative bacteria. Proteins from representative bacteria from marine surface waters as well as bacteria shown to produce MeSH from MMPA were included in the phylogenetic analysis. Proteins whose function was verified by recombinant expression in *E. coli* are indicated (●). Methods for selecting homologous sequences are described in the supplementary methods. The original alignment contained 194 sequences, but for clarity, 101 out-group sequences were removed. Clusters with an identified or annotated function are labeled, while the remaining sequences possess conserved domains in the acyl-CoA dehydrogenase superfamily (cl09966). Locus tags correspond to organisms as follows: *Escherichia coli* BL21(DE3) (B21), *Burkholderia thailandensis* (BTH), *Deinococcus radiodurans* (DR), *Dinoroseobacter shibae* (Dshi), marine γ-proteobacteria HTCC2143 (GP2143), SAR11 HIMB59 (HIMB59), *Myxococcus xanthus* (MXAN), *Pseudomonas aeruginosa* (PA), *Pseudoalteromonas atlantica* (Patl), *P. ubique* HTCC7211 (PB7211), *P. ubique* HTCC1062 (SAR11), *Puniceispirillum marinum* IMCC1322 (SAR116), SAR11 HIMB5 (SARB5), *R. lacuscaerulensis* (SL1157), *R. pomeroyi* (SPO).

97

Table 3-1. **MMPA-CoA pathway enzyme activities in cell extracts**.

Strain	Growth Conditions	Enzyme Assay[a]			
		MMPA-CoA Ligase (DmdB)	MMPA-CoA Dehydrogenase (DmdC)	MTA-CoA Hydratase (DmdD)	Acetaldehyde Dehydrogenase
R. pomeroyi DSS-3	2 mM MMPA (Chemostat)	118 ± 17	1226 ± 213	759 ± 36	132 ± 11
R. pomeroyi DSS-3	2 mM DMSP (Batch)[b]	11 ± 1	281 ± 15	186 ± 18	34 ± 6
R. pomeroyi DmdC⁻ (SPO_3804::Tn5)	2 mM DMSP (Batch)[b]	27 ± 2	43 ± 5	12 ± 1	26 ± 3
R. lacuscaerulensis	1 mM MMPA (Chemostat)	198 ± 30	39 ± 5	44 ± 13	n.d.

[a]Activities are reported as nmol min^{-1} mg of protein^{-1} and are the result of triplicate experiments, ±SD.

[b] The mutant and control wild-type strains were grown in batch culture to avoid selection for revertants in the chemostat.

n.d., Not detected
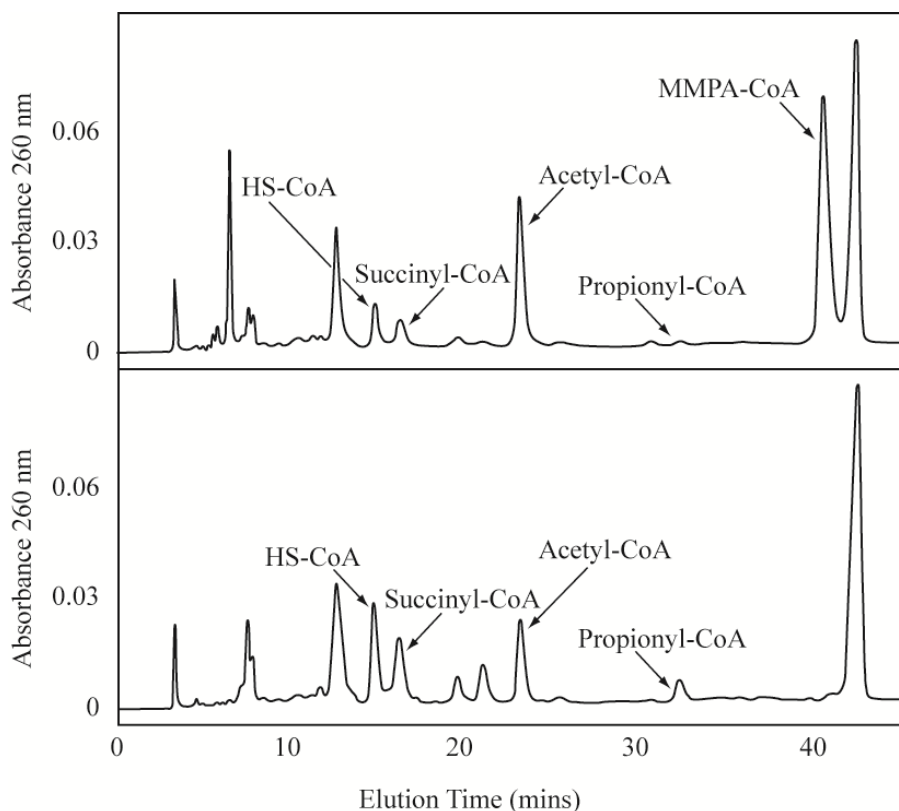
Fig. 3-3. HPLC analysis of intracellular acyl-CoA's.
Identification of coenzyme-A containing intermediates in extracts of wild-type *R. pomeroyi*
DSS-3 incubated with MMPA (top) or the *dmdA*⁻ (SPO1913::Tn5) mutant incubated with DMSP
(bottom). The transposon insertion in this mutant rendered it incapable of forming MMPA from
DMSP. Thus, the intermediates displayed on the top figure are only attributed to the
demethylation pathway, while the intermediates in the bottom figure are only attributed to
cleavage. The shared intermediates were from downstream central metabolic pathways. After
incubation, reaction products were concentrated and purified by binding an oligo purification
cartridge (OPC) as described in the methods. The identities of the coenzyme-A containing
thioesters based on co-elution with standards are indicated. Other major peaks that eluted at 4, 8,
and 42 minutes were not CoA-thioesters based upon their 232/260 nm absorbance ratio and
failure to yield HS-CoA upon alkaline hydrolysis.

99
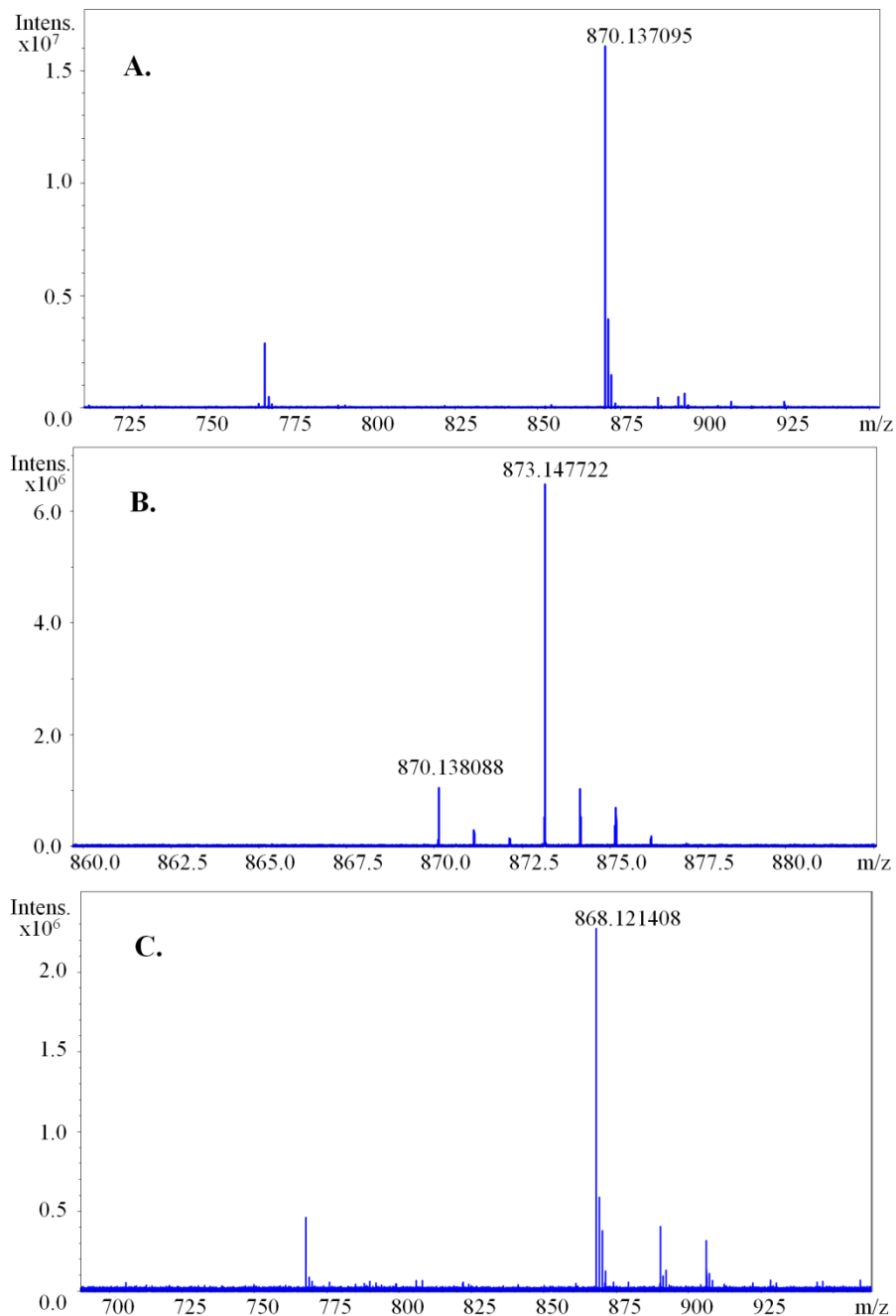
Fig. 3-4. MALDI-FTICR analysis of MMPA-CoA pathway intermediates.
Positive ion mode MALDI-FTICR spectra of (**A**) MMPA-CoA extracted from whole cells after incubation with MMPA, (**B**) MMPA-CoA extracted after incubation of whole cells with [1,2,3-^{13}C] DMSP, and (C) MTA-CoA formed after the incubation of cell-free extracts with MMPA-CoA and ferrocenium hexafluorophosphate. The signal at 768 m/z was attributed to HS-CoA, which was present in all acyl-CoA samples analyzed by MALDI-FTICR due to spontaneous hydrolysis of the thioester bond. In (B), the *dmdC*⁻ mutant was grown in rich medium and then resuspended in minimal medium with unenriched DMSP and incubated for 4 hours. Cells were

then washed to remove the unlabeled DMSP and then incubated for 60 minutes with [1,2,3-^{13}C] DMSP. After extraction with 5% trichloroacetic acid and purification as described in the methods, the masses were determined. The labeled molecules have masses of 873.1477 or an increase in mass of 3 AMUs from the unlabeled molecules, with masses of 870.1380. The unenriched MMPA-CoA is attributed to carry over from the initial incubation.

Explanation of Fig. 3-4.

To identify the unknown intermediate shown in Fig. 3-3, the compound was collected after

HPLC separation and analyzed by MALDI-FTICR. As shown in Fig. 3-4a, the compound had a

molecular weight of 870.138, consistent with the formula for MMPA-CoA. This conclusion was

confirmed by synthesis of MMPA-CoA and demonstrating coelution with the intermediate under

the liquid chromatography conditions used in Fig.3-3. To confirm that the MMPA-CoA was in

fact derived from DMSP, the *dmdC*⁻ strain was grown in rich medium, washed, and resuspended

in minimal medium with [1,2,3-^{13}C] DMSP. CoA containing intermediates were then extracted

and separated by HPLC, and the MMPA-CoA peak was collected. The MALDI-FTICR analysis

shown in Fig. 3-4b shows that the mass of MMPA-CoA increased by 3 AMU's, confirming that

the MMPA-CoA was derived from DMSP. Fig. 3-4c shows the MALDI-FTICR spectrum of the

product of DmdC after incubation with MMPA-CoA and the artificial electron acceptor

ferrocenium hexafluorophosphate. The molecular weight of 868.121 is consistent with that of

MTA-CoA.
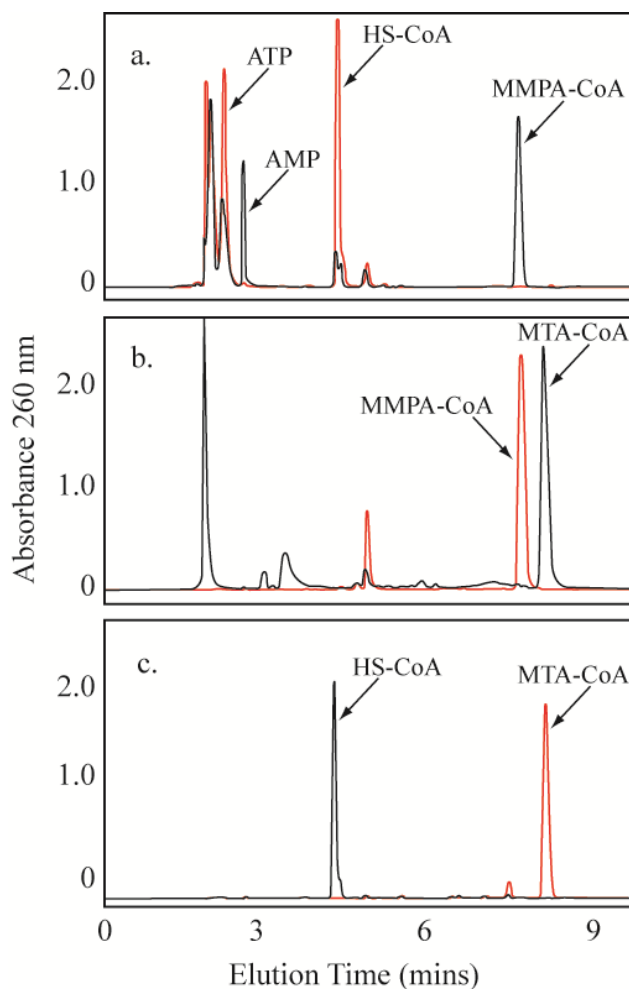
Fig. 3-5. Analysis of MMPA-CoA pathway reactions. Red trace is the HPLC chromatograph before reaction while the black trace is after the reaction. Reactions were performed using purified recombinant enzymes. **a**)MMPA-CoA ligase; reaction mixture contained 50 mM Tris/HCl (pH 7.5), 2 mM MMPA, 0.5 mM CoA, 2 mM ATP, 8 mM MgCl, and (black) 2 µg of purified recombinant DmdB incubated for 5 minutes. **b**) MMPA-CoA dehydrogenase; reaction mixture contained 50 mM Tris/HCl (pH 7.5), 0.5 mM MMPA-CoA, 2 mM ferrocenium hexafluorophosphate, and (black) 4 µg of purified recombinant DmdC after 5 minutes. **c**) MTA-CoA hydratase; reaction mixture contained 50 mM Tris/HCl (pH 7.5), 0.5 mM MTA-CoA and (black) 0.5 µg of purified recombinant DmdD incubated for 5 minutes.
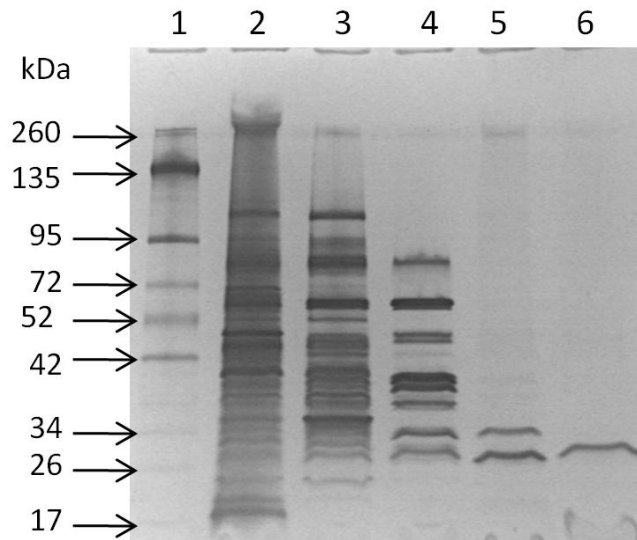
Fig. 3-6. SDS-PAGE of SPO3805 purification from cell extracts of *R. pomeroyi* DSS-3. Gel was a 4-15% mini protean Tris-glycine (BioRad) visualized by silver staining. Lane 1. Prestained Spectra Broad Range Protein Marker; Lane 2. Crude cell extract (10 µg); Lane 3 Q-Sepharose pool (3 µg); Lane 4. Phenyl-Superose pool (1.5 µg); Lane 5. HiTrap Blue pool (0.15 µg); Lane 6. Sephacryl S-200 pool (0.1 µg).
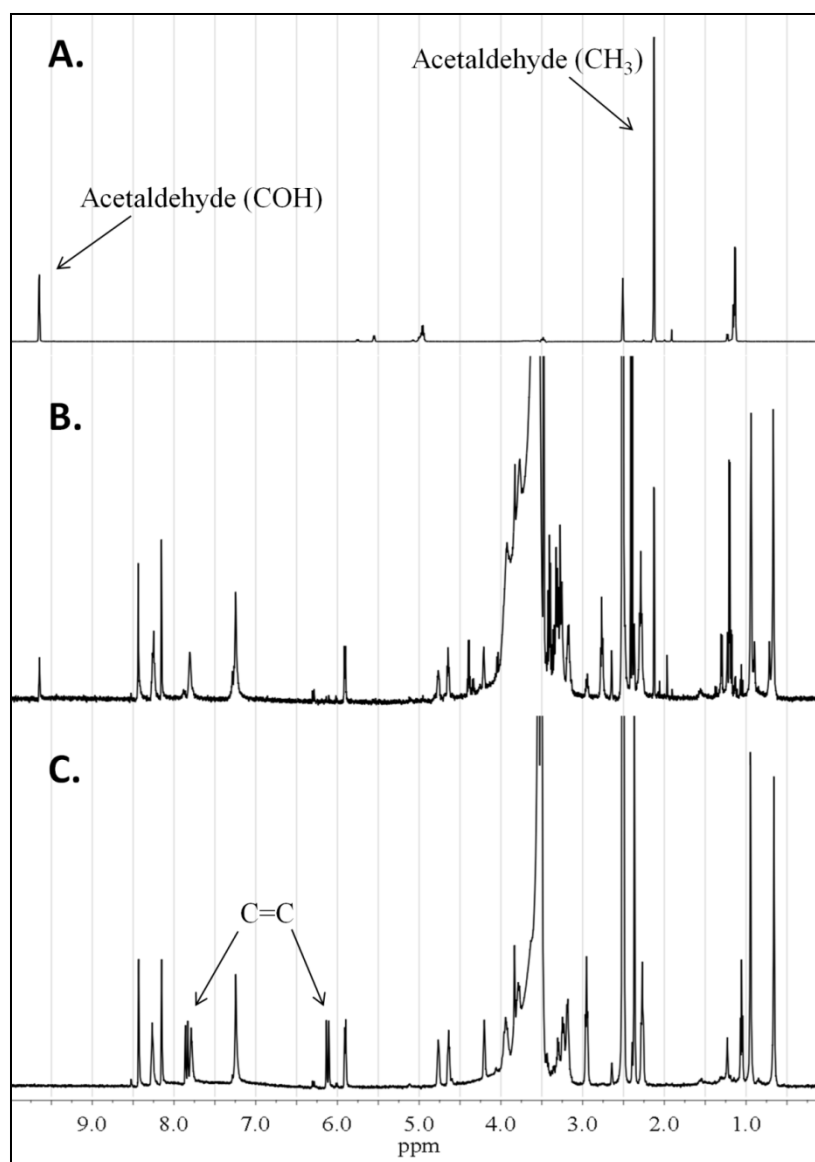
Fig. 3-7. **^{1}H NMR of MTA-CoA hydratase reaction products**. The DmdD catalyzed reaction was performed in 20 μl of 10 mM (pH 7) potassium phosphate buffer for 20 minutes, at which time 450 uL of 99.9% DMSO-d6 was added, and the ^{1}H NMR spectrum was recorded. The signal at 3.5-4 ppm is from H_2O in DMSO-d6, while the signal at 2.5 ppm is from DMSO contaminating the DMSO-d6. The intense H_2O signal is due to the addition of DmdD in buffer containing H_2O. Due to the volatility of acetaldehyde, H_2O was not removed prior to recording the spectrum. **A**. Authentic aqueous acetaldehyde. **B**. MTA-CoA after the addition of purified DmdD. **C**. MTA-CoA before the reaction. The signals indicated as C=C are attributed to the protons of the double-bonded carbons in MTA-CoA. Upon reaction with DmdD, these signals disappeared and the signals for acetaldehyde appeared. The remaining signals were from coenzyme-A and other reaction components.
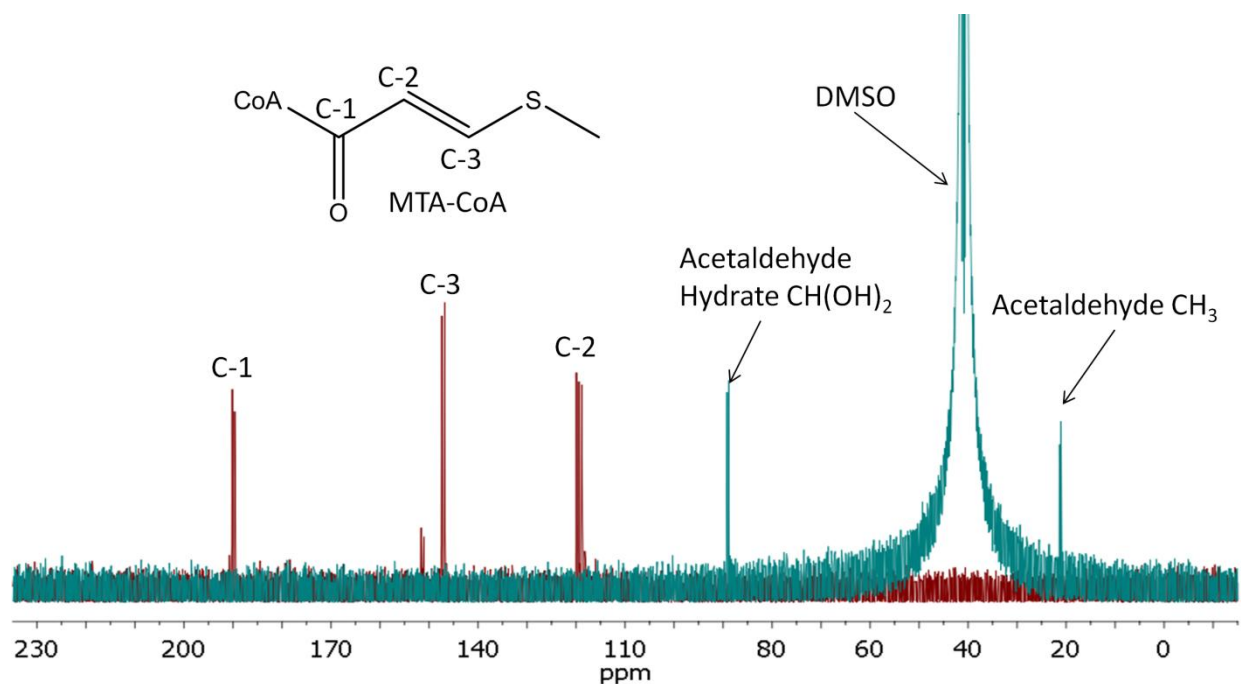
Fig. 3-8. ^{13}C NMR spectrum of ^{13}C enriched MTA-CoA before and after reaction with DmdD. The MTA-CoA was enriched in all three positions of the acrylyl moiety. The red spectrum is before the reaction, while the green spectrum is after 1 hour of incubation with DmdD. The spectrum after the reaction is consistent with ammonium acetaldehyde hydrate. The substrate was prepared as the ammonium salt, and the residual ammonium ion from the substrate complexed with acetaldehyde hydrate, yielding the chemical shift indicated at 90 ppm. The intense signal at 40 ppm is from solvent DMSO added after the reaction.

A.
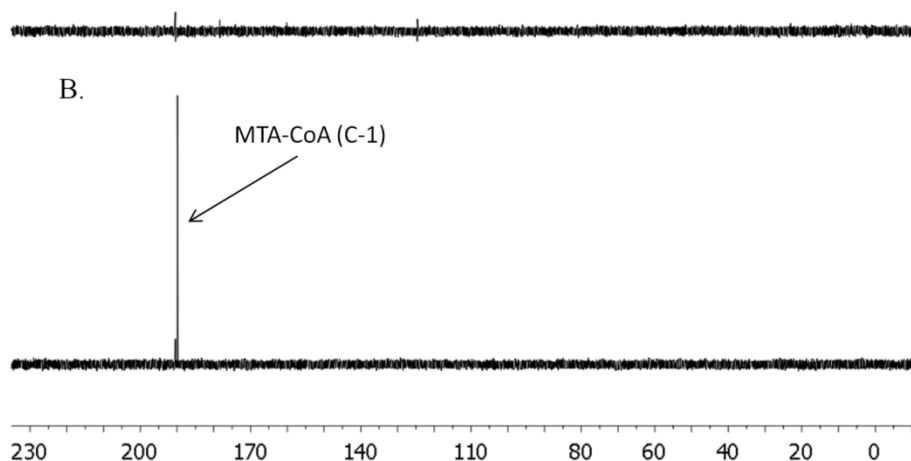
Fig. 3-9. ^{13}C NMR of [1-^{13}C]MTA-CoA before and after the reaction with DmdD. The top panel is one hour after the addition of DmdD, while the bottom panel is before the addition of DmdD. The reaction was performed in D_2O, and the spectrum was recorded without further processing. Both spectra were recorded under identical conditions. Disappearance of the ^{13}C signal indicated a decarboxylation of the C-1 carbon.

Explanation of Fig. (3-7)-(3-9).

^{1}H and ^{13}C NMR were used to identify the product of the DmdD catalyzed reaction of MTA-CoA. Fig. 3-7 shows MTA-CoA before and after reaction with DmdA, as well as authentic acetaldehyde. The ^{1}H NMR spectrum in panel c shows that the indicated proton signals from the C=C bond of methylthioacryl moiety of MTA-CoA disappear upon reaction with DmdD. Panel b shows that after the reaction, there was an appearance of a quartet at 9.6 ppm and a doublet at 2.1 ppm. This spectrum is consistent with that of acetaldehyde, which is displayed in panel a. Further confirmation of acetaldehyde as the reaction product was obtained by ^{13}C NMR of [1,2,3-^{13}C] MTA-CoA. Upon reaction with DmdD, one carbon signal is lost completely while

the remaining two carbon signals were consistent with the formation of acetaldehyde. To investigate which carbon atom was lost during the reaction [^{13}C-1] enriched MTA-CoA was synthesized. Supplementary Fig. 3-9 shows that, upon reaction with DmdD, the enriched ^{13}C is lost completely, indicating a decarboxylation. Whether this decarboxylation was enzyme catalyzed or the result of an unstable chemical formation is not known. Regardless, this reaction is unprecedented as a mechanism of breaking C-S bonds and releasing MeSH.
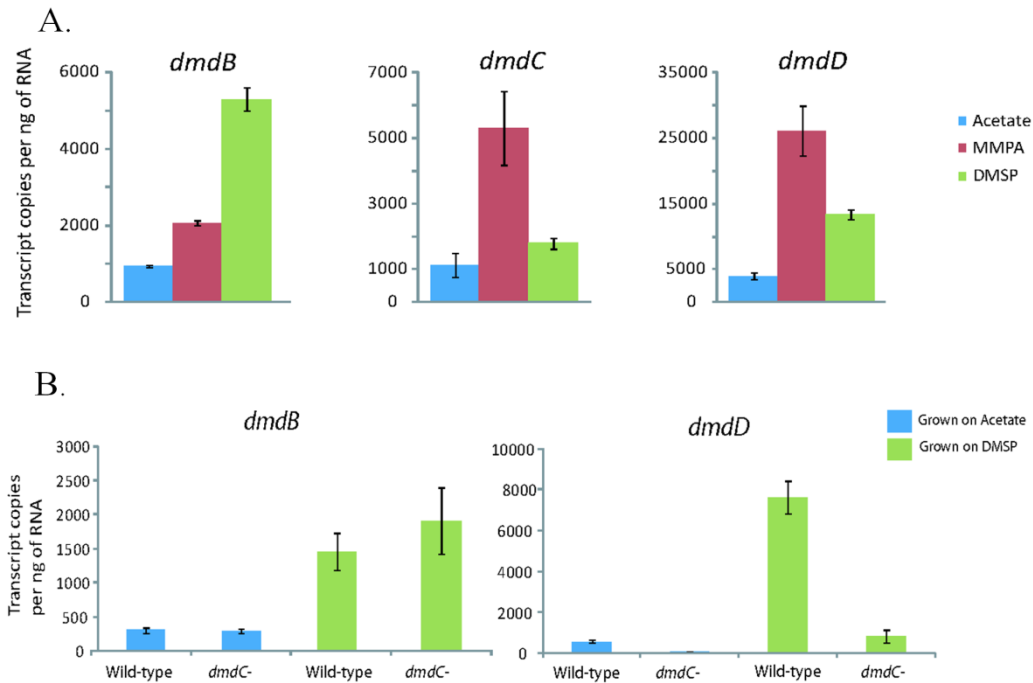
Supplementary Fig. 3-10. Transcript levels for *dmdB*, *dmdC*, and *dmdD* in wild type and the *dmdC⁻* mutant. A. Transcript abundance of *dmdB, dmdC,* and *dmdD* from chemostat-grown wild-type *R. pomeroyi* DSS-3 cells with acetate, MMPA, and DMSP as the sole source of carbon. **B**. Transcript abundance of *dmdB* and *dmdD* from batch-grown wild-type and the *dmdC⁻* mutant cells grown with DMSP or acetate. Error bars are ±SD.

Explanation of Supplementary Fig 3-10.

The data in Supplementary Fig. 3-10A shows the transcriptional response of wild-type cells to acetate, MMPA, and DMSP. As expected, the levels of transcripts increased following growth with MMPA and DMSP. In the microarray experiments of Burgmann et al.[39], changes in expression of these genes were not noted during a time shift from rich medium to minimal medium plus DMSP. Their failure to observe changes in expression probably resulted from differences in the experimental design as well as the low sensitivity of their microarrays. Supplementary Fig. 10B shows that the *dmdC⁻* mutant (SPO3804::Tn5) had similar levels of transcript for *dmdB* as compared to wild-type, which is consistent with levels of enzyme activity displayed in table 3-1. The level of transcripts for dmdD was greatly reduced in the *dmdC⁻*

mutant, indicating that the two genes (*dmdC* or SPO3804 and *dmdD* or SPO3805) may be co-transcribed as part of an operon. However, transcripts are still detected in the mutant, suggesting a low level of read-through from the transcriptional terminator of the kanamcyin marker inserted into *dmdC*. Notably, the transcript level was higher in the *dmdC⁻* mutant when the cells are grown with DMSP compared to acetate. These results were consistent with the data in table 3-1, which showed a decrease but not a complete absence of DmdD activity in cell extracts of the *dmdC⁻* mutant. This low level DmdD activity was likely sufficient to support growth when the *dmdC⁻* mutant strain was complemented with only *dmdC* supplied on a plasmid.
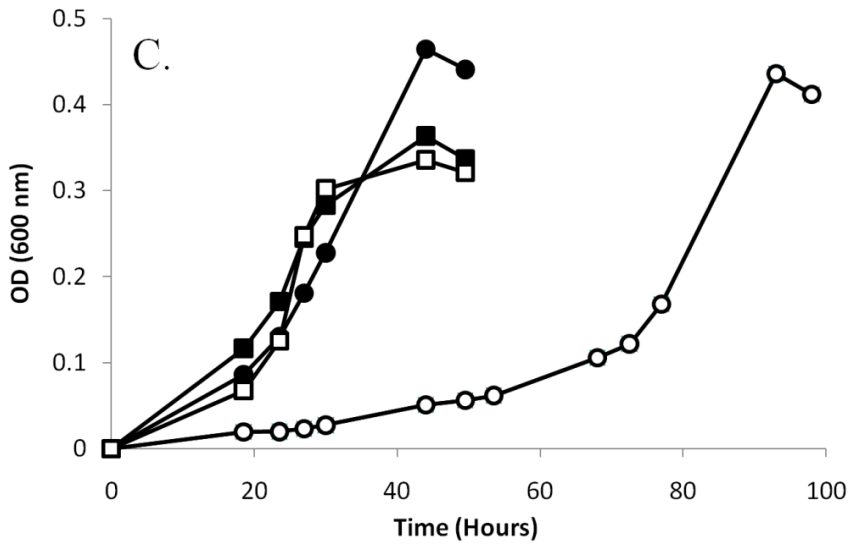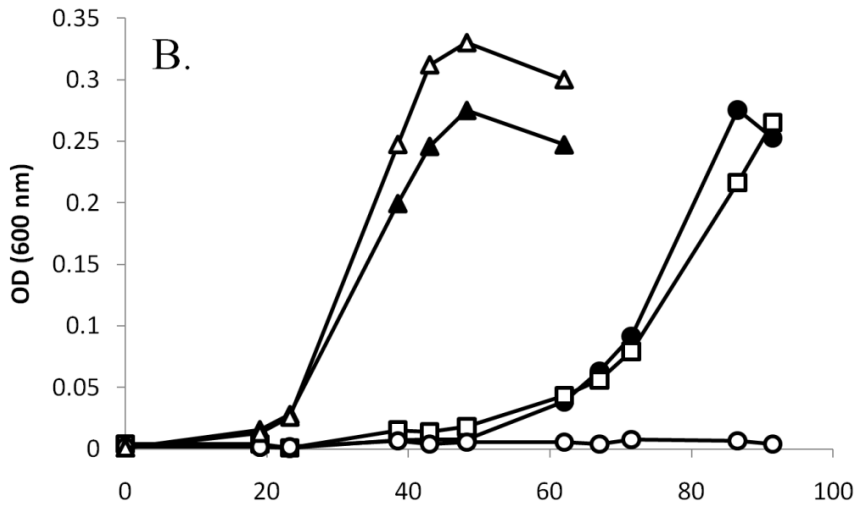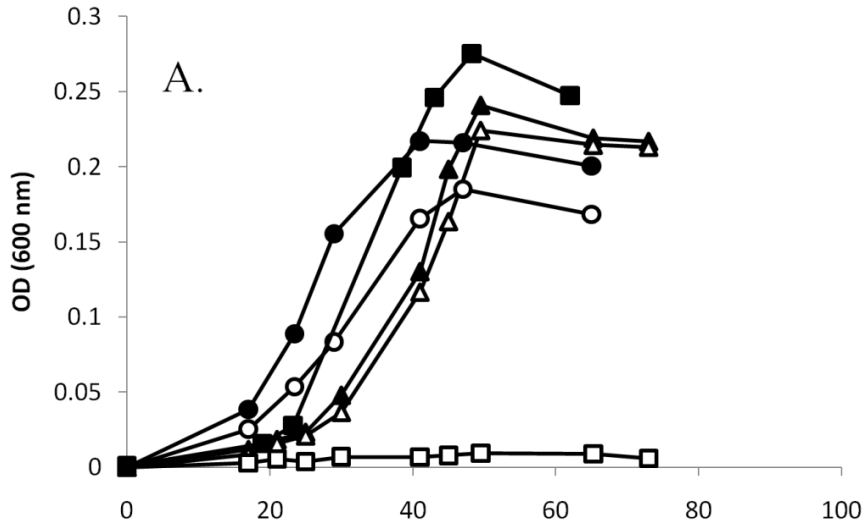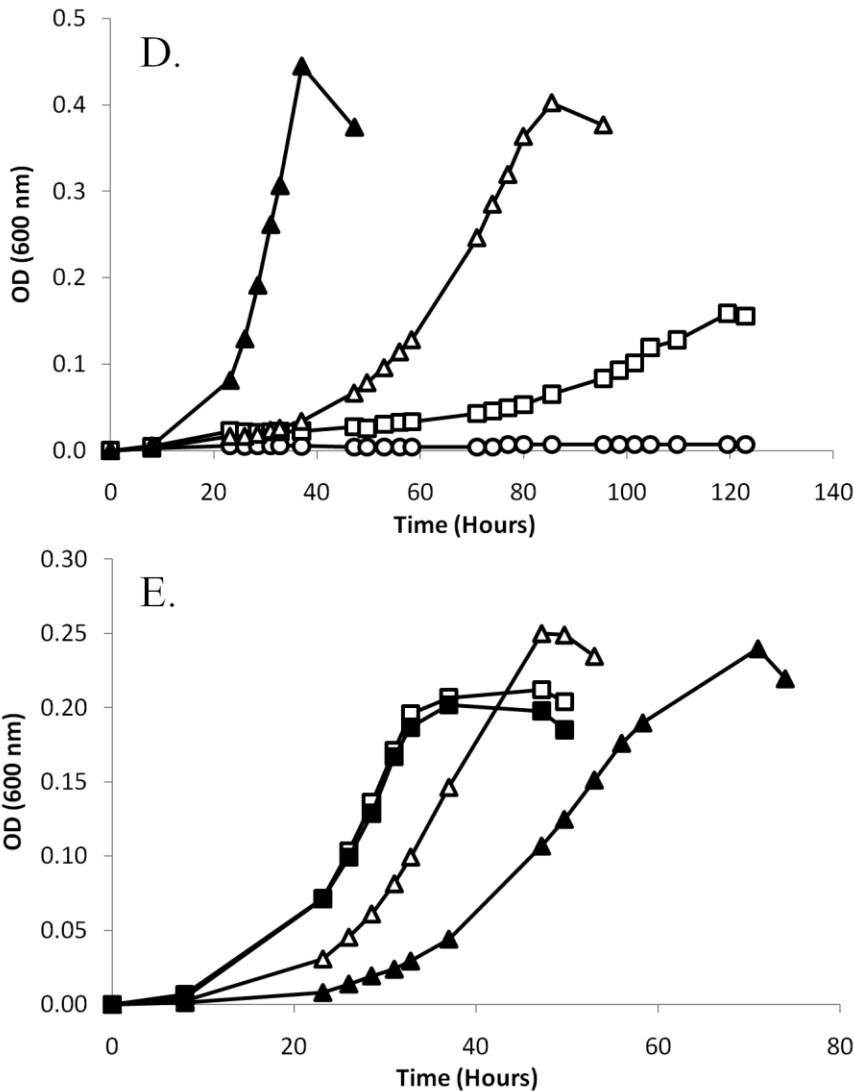
Fig. 3-11. Growth phenotypes of the MMPA-CoA pathway mutants. A. Growth of wild-type
R. pomeroyi DSS-3 and *dmdC⁻* (SPO3804::Tn5). Growth of wild type with 6 mM acetate (▲), 3
mM DMSP (●), and 3 mM MMPA (■). Growth of *dmdC⁻* mutant with 6 mM acetate (Δ), 3 mM
DMSP (○), and 3 mM MMPA (□). **B**. Growth of *dmdC⁻* mutant and complement strains. All
growth experiments contained 3 mM MMPA as the sole source of carbon; wild-type (▲), wild-
type plus the shuttle vector alone (pRK415) (Δ),*dmdC⁻* mutant plus SPO3804 (pCRR301) (●),
dmdC⁻ mutant plus SPO3805 (pCRR302) (○), and *dmdC⁻* mutant plus SPO3804-SPO3805
(pCRR303) (□). **C.** Growth of wild-type and *dmdC⁻* mutant with glucose plus MMPA. Growth
of wild-type with 2 mM glucose (■) and 2 mM glucose plus 1 mM MMPA (●). Growth of the
dmdC⁻ mutant with 2 mM glucose (□) and 2 mM glucose plus 1 mM MMPA (○). **D.** Growth of
wild-type and *dmdD⁻* (SPO3805::*tet*) mutant. Growth of wild-type with 2 mM glucose plus 1
mM MMPA (▲). Growth of *dmdD⁻* mutant with 2 mM glucose plus 1 mM MMPA (Δ), 3 mM
DMSP (□), and 3 mM MMPA (○). **E.** Growth of wild-type and *dmdB⁻* (SPO2045::*tet*) mutant.

Growth of wild-type on 3 mM DMSP (□), and 3 mM MMPA (Δ). Growth of *dmdB*⁻ mutant on 3 mM DMSP (■), and 3 mM MMPA (▲).

Explanation of Fig 3-11.

In addition to the growth experiments described in the main text, several additional growth experiments were performed to verify the mutant phenotypes. Figure 3-11a displays the growth phenotype using DMSP, MMPA, and acetate as the sole source of carbon for the wild-type and the *dmdC*⁻ (SPO3804::Tn5) mutant strain. Only growth on MMPA was inhibited in this mutant, indicating that the mutation was not lethal and that the acetate assimilation pathway was unaffected. Figure 3-11b displays growth of the wild-type and complemented strains of the *dmdC*⁻. Complementation with SPO3804 or SPO3804-SPO3805 restored growth on MMPA, while complementation with SPO3805 only did not. Thus, the growth phenotype was due to a deficiency in DmdC and not DmdD activity. The reason for the long lag upon complementation is not clear but presumably reflects different levels of expression of *dmdC* from the plasmid. *R. pomeroyi* possessed two other *dmdC* genes (see main text). Presumably, the low DmdC activity remaining in the mutant was not sufficient to support growth under these conditions. Figure 3-11c displays growth of the wild-type and mutant with glucose as well as MMPA and glucose. Growth with glucose only was similar for both wild-type and the *dmdC*⁻ mutant, but addition of MMPA with glucose initially inhibited growth of the mutant. This inhibition may have been caused by a buildup of MMPA-CoA and a depletion of free-CoA in the cell. Lack of free-CoA could cause a metabolic collapse that inhibits growth. After several days the growth rate and growth yield became similar to that of wild-type, indicating a restoration of metabolic capability and suggesting that the disrupted *dmdC* had been complemented by one of the two remaining homologs shown to encode functional DmdC proteins.

Fig. 3-11d shows that the *dmdD*⁻ mutant (SPO3805::*tet*) failed to grow on MMPA and grew very slowly on DMSP. In contrast, growth on glucose alone was similar to wild-type (data not shown). When provided glucose and MMPA, the mutant grew after an extended lag. The extended lag during growth with DMSP or glucose plus MMPA may be attributed to metabolic collapse caused by lack of free CoA, as discussed above for the *dmdC*⁻ mutant. The severity of the *dmdD*⁻ mutant phenotype may have been caused by the loss of a side-activity of the DmdD. In the absence of MTA-CoA, DmdD catalyzes the hydrolysis of MMPA-CoA to MMPA and free-CoA (unpublished data). In the *dmdC*⁻ mutant, which has diminished but significant levels of DmdD, this hydrolytic activity may allow for some MMPA-CoA turnover and the release of free CoA. This activity would be absent in the *dmdD*⁻ mutant.

The data in Supplementary Figure 3-11e shows that growth of the *dmdB*⁻ mutant on MMPA was somewhat retarded, while growth on DMSP was similar to wild-type. Upon subsequent transfers in MMPA, growth of the *dmdB*⁻ mutant continued to be delayed. Thus, the restoration of growth late in the culture was not due to selection for a second-site revertant. It is likely that the second copy of *dmdB*, SPO0677, may have complemented this mutation.

Fig. 3-12. Phylogenetic tree of DmdB from representative bacteria. Proteins from bacteria which were shown to produce MeSH from MMPA as well as from representatives from marine surface waters were included in the phylogenetic analysis. Proteins whose function was verified by recombinant expression in *E. coli* are indicated (●). Methods for selecting homologous sequences are described in the supplementary methods. The original tree contained 244 sequences, but for clarity 124 out-group sequences were removed. Clusters with an annotated or identified function are indicated, while the remaining are members of the LuxE superfamily (cl10450) Locus tags correspond to organisms as follows: *Escherichia coli* BL21(DE3) (B21), *Burkholderia thailandensis* (BTH), *Deinococcus radiodurans* (DR), *Dinoroseobacter shibae* (Dshi), marine γ-proteobacteria HTCC2143 (GP2143), SAR11 HIMB59 (HIMB59), α-proteobacteria HIMB114 (HIMB114), *Myxococcus xanthus* (MXAN), *Pseudomonas aeruginosa* (PA), *Pseudoalteromonas atlantica* (Patl), *P. ubique* HTCC7211 (PB7211), *P. ubique* HTCC1062 (SAR11), *Puniceispirillum marinum* IMCC1322 (SAR116), SAR11 HIMB5 (SARB5), *R. lacuscaerulensis* (SL1157), and *R. pomeroyi* (SPO).

114

Table 3-2. Volatile sulfur production from DMSP-grown chemostat cultures of *R. pomeroyi* DSS-3. Values reported are percentages of the DMSP consumed during a typical chemostat culture, where 2 mM DMSP was supplied at a flow rate of 0.1 mL min^{-1}, or 200 nmol of DMSP min^{-1}.

DMS	MeSH	DMSO	DMDS
30-40%	0-2%	<2%	<1%

Explanation of Supplementary Table 3-2.

Only a small fraction of the DMSP sulfur is accounted for in the measured products of a typical chemostat culture. Most of the measured volatile sulfur emitted from the chemostat was in the form of DMS. However, less than half of DMSP-sulfur entering the chemostat was detected as a volatile product. Given the biotic and abiotic reactivity of MeSH, it was likely that most of this missing sulfur was routed through the demethiolation pathway to MeSH. To support this hypothesis, the ability of chemostat-grown cultures of *R. pomeroyi* to consume MeSH and DMS was measured. In short incubations of 1 hour or less, cultures consumed MeSH at a rate of 145 nmol min^{-1} culture^{-1}, which was sufficient to account for the missing sulfur reported in the table 3-2. DMS consumption was not detected in short incubations, but after 19 hours a low level of DMS consumption, 5 nmol min^{-1} culture^{-1}, was observed. This rate would account for only 2.5% of DMSP entering the chemostat. This data supports the hypothesis that most of the MeSH which was formed was consumed in these cultures.

Table 3-3. Peptides identified by MALDI-TOF analysis of MMPA-CoA ligase purification. A search of the Mascot database (www.matrixscience .com) returned SPO2045 as the top hit with a 25% sequence coverage.

Start - End	Mr(expt)	Mr(calc)	Sequence
2 - 17	1795.918	1795.859	M.TQDVTSGYSNLDLDLR.D
2 - 31	3363.676	3363.637	M.TQDVTSGYSNLDLDLRDNGVCVVTLNRPDK.R
33 - 52	2233.154	2233.138	R.NALDVATIEELVTFFSTAHR.K
57 - 78	2394.186	2394.179	R.AVVLTGAGDHFCAGLDLVEHWK.A
82 - 92	1349.611	1349.586	R.SADDFMHVCLR.W
82 - 92	1365.567	1365.581	R.SADDFMHVCLR.W Oxidation (M)
93 - 99	930.3925	930.4348	R.WHEAFNK.M
100 - 112	1388.781	1388.749	K.MEYGGVPIIAALR.G
100 - 112	1404.729	1404.744	K.MEYGGVPIIAALR.G Oxidation (M)
113 - 129	1576.918	1576.869	R.GAVVGGGLELASAAHLR.V
130 - 144	1740.865	1740.814	R.VMDQSTYFALPEGQR.G
130 - 144	1756.831	1756.809	R.VMDQSTYFALPEGQR.G Oxidation (M)
145 - 155	1048.574	1048.567	R.GIFTGGGATIR.V
165 - 173	1064.519	1064.536	R.MIDMILTGR.V Oxidation (M)
174 - 197	2589.221	2589.224	R.VYQGQEAADLGLAQYITEGSSFDK.A
174 - 204	3347.605	3347.587	R.VYQGQEAADLGLAQYITEGSSFDKAMELADK.I
250 - 258	1076.541	1076.561	R.ERLEAFANK.T

Supplementary Table 3-4. Peptides identified by MALDI-TOF analysis of MMPA-CoA hydratase purification. A search of the Mascot database (www.matrixscience .com) returned SPO3804 as the top hit with a 73% sequence coverage.

Start - End	Mr(expt)	Mr(calc)	Sequence
52 - 66	1483.841	1483.8	R.LGSVLTDAGLAPQSR.V
67 - 75	1043.524	1043.551	R.VATLAWNNR.R
67 - 76	1199.649	1199.652	R.VATLAWNNRR.H
194 - 200	830.4038	830.4399	K.GVLYSHR.S
201 - 212	1304.69	1304.647	R.STVLHSFGSNTR.D
213 - 220	924.4201	924.4124	R.DCIGFSAR.D
299 - 315	1775.91	1775.87	R.TVIGGAACPPSMIAEFR.D
299 - 315	1791.858	1791.865	R.TVIGGAACPPSMIAEFR.D Oxidation (M)
355 - 369	1754.901	1754.943	K.LRENQGRPPYGVELK.I
357 - 369	1485.762	1485.758	R.ENQGRPPYGVELK.I
424 - 432	1141.57	1141.519	R.DGYMTIRDR.S Oxidation (M)
459 - 471	1272.693	1272.755	K.LATAAVIGVPHPK.W
472 - 482	1324.78	1324.75	K.WDERPLLVAVK.A
504 - 509	799.403	799.3977	K.WQVPDR.V
510 - 523	1456.766	1456.829	R.VVFVEALPLNATGK.V

Table 3-5. Production of MeSH by pure cultures supplemented with 1 mM MMPA. The limit of detection was 0.5 nmol per culture. Control experiments without the addition of MMPA did not produce detectable levels of MeSH. See the supplementary methods for full description of the experimental procedure.

Strain	MeSH Production (nmol per culture)
Burkholderia. thailandensis E264	302 ±110
Pseudomonas aeruginosa PAO1	79 ±23
Pseuodalteromonas atlantica T6C	88 ±7
Myxococcus xanthus DK1622	13 ±5
Deinococcus radiodurans	10 ±3
Escherichia coli BL21(DE3)	<0.5

Supplementary Table 3-6. Number of homologous protein sequences for DmdB, DmdC, and RecA in the GOS metagenomic database. If each organism harbors only one copy of each gene, we estimate that 61% of cells have an ortholog. This assumption is not the case in most roseobacters, but seems to be true for cultured SAR11 bacteria; of the five cultured and sequenced SAR11-like bacteria, only HIMB59 has two copies of *dmdB*, while none have two copies of *dmdC*.

	Hits	Per RecA
DmdB	6263	61.4%
DmdC	6264	61.4%
RecA	10197	-

Table 3-7. Plasmids used for recombinant expression in this study.

Plasmid	Vector	Geneotype
pCRR201	pET101	SPO3804
pCRR202	pET101	SPO3805
pCRR203	pET101	SPO2045
pCRR204	pET101	SAR11_0247
pCRR205	pET101	SAR11_0248
pCRR206	pET101	SAR11_0249
pCRR207	pET101	SAR11_1260
pCRR420	pET101	BthI0564
pCRR403	pET101	BthI1655
pCRR421	pET101	SL0694
pCRR409	pET101	SL2180
pCRR406	pET101	PAO4199
pCRR407	pET101	PAO5020
pCRR430	pET101	SPO0298
pCRR431	pET101	SPO2915
pCRR301	pRK415	SPO3804
pCRR302	pRK415	SPO3805
pCRR303	pRK415	SPO3804-3805

Supplementary Table 3-8. Primer sequences, amplicon size, and annealing temperatures used

for RT-qPCR anaylysis.

Gene	Primer name and sequences (5`-3`)	Amplicon size (bp)	Annealing temperature (^{0} C)
dmdB	dmdB_F536 cttcgagcctgtgctatacct dmdB_R704 caggcgttgacatggaacat	169	61
dmdC	dmdC_F238 gcctatgaccagttcgtcgatat dmdC_R376 ggcagaggccaaagctcata	139	61
dmdD	dmdD_F508 ctgaccggtcgtgtctatca dmdD_R652 aacagatggcgaagttggtc	145	61

Reference

39. **Burgmann, H., E. C. Howard, W. Ye, F. Sun, S. Sun, S. Napierala, and M. A. Moran.** 2007. Transcriptional response of *Silicibacter pomeroyi* DSS-3 to dimethylsulfoniopropionate (DMSP). Environ Microbiol **9:**2742-2755.

CHAPTER 5

ASSIMILATION OF DIMETHYLSULFONIOPROPIONATE IN *RUEGERIA POMEROYI.*

Abstract

Assimilation of dimethylsulfoniopropionate is common in marine bacteria, but the biochemical pathways used to assimilate carbon from DMSP are still poorly understood. In this study, *Ruegeria pomeroyi* DSS-3 was shown to possess a pathway which transforms the DMSP cleavage product acrylate into propionyl-CoA. First, acrylate is transformed into its CoA thioester, acryloyl-CoA. Acryloyl-CoA is then hydrated to form 3-hydroxypropionyl-CoA, which is then reduced to propionyl-CoA. In chemostat-grown cultures, the enzymatic specific activity for all three reactions was greater than the minimum level required to consume all of the substrate entering the chemostat. The enzyme catalyzing the hydration of acryloyl-CoA was identified by purification as an enoyl-CoA hydratase, encoded by SPO0147. The enzyme catalyzing the reduction of 3-hydroxypropionyl-CoA was encoded by SPO1914, a gene annotated as a zinc-dependent oxidoreductase. Consistent with its role in acrylate assimilation, a *R. pomeroyi* mutant with SPO1914 disrupted was unable to grow on acrylate or 3-hydroxypropionate as the sole source of carbon. *R. pomeroyi* cells grown on ^{13}C-enriched DMSP possessed labeling patterns that were consistent with the carbon from the demethylation pathway being assimilated through the ethylmalonyl-CoA pathway and the carbon from the DMSP-cleavage through the acrylate assimilation pathway proposed here. Microarray experiments examining the transcriptional response of *R. pomeroyi* to DMSP were also consistent with these proposed pathways. Additionally, investigations on the fate of DMSP methyl carbon found that *R. pomeroyi* possessed limited C1 metabolism, as the ^{13}C labeled methyl groups were only found in a few specific carbons derived from the C-1 carrier tetrahydrofolate.

Introduction

The phytoplankton metabolite dimethylsulfoniopropionate (DMSP) is ubiquitous in marine surface waters, making it one of the most abundant known microbial sources of carbon and reduced sulfur in the marine environment. Marine bacteria consume DMSP through two competing biochemical pathways, resulting in the eventual release of either methanethiol (MeSH) or dimethylsulfide (DMS) (25). Some marine bacteria only have the capacity to carry out either the demethylation or cleavage pathways, while others are capable of both pathways. The model organism *Ruegeria pomeroyi* DSS-3 is capable of catabolizing DMSP through both pathways. Recently, the biochemical pathway and genes responsible for the transformation DMSP catabolism resulting in the release of MeSH were elucidated (35). This pathway starts with the demethylation of DMSP by a tetrahydrofolate (THF)-dependent enzyme, DmdA, producing 5-methyl-THF and methylmercaptopropionate (MMPA) (23, 34). MMPA is then catabolized in a series of three coenzyme-A mediated reactions analogous to fatty acid β-oxidation. The terminal step of the pathway results in the release of MeSH, CO_2, acetaldehyde, and free CoA. Acetaldehyde is further oxidized to acetate by an acetaldehyde dehydrogenase. Thus the carbon from this pathway enters central carbon metabolism as acetate. *R. pomeroyi* is missing isocitrate lyase, the key enzyme in the glyoxylate shunt, but does possess all enzymes identified as part of the ethylmalonyl-CoA pathway (14). Therefore, *R. pomeroyi* was hypothesized to use the ethylmalonyl-CoA pathway to assimilate the DMSP carbon that is routed through the demethylation pathway (35).

The cleavage pathway in *R. pomeroyi* is complicated by the fact that the genome contains four genes; *dddD, dddP, dddQ,* and *dddW,* that encode for proteins known to catalyze the cleavage reaction. However, only three of these genes were shown to have activity under the

conditions tested. Gene mutations in *dddP, dddQ,* and *dddW* decreased DMS production, while a mutation in *dddD* had no effect (42, 43). Evidence suggests that all three of these enzymes catalyze reactions that release acrylate in addition to DMS (28, 42, 43). The assimilation of acrylate in *R. pomeroyi* and other marine bacteria is poorly understood. Acrylate metabolism in a strain of *Halomonas* was extensively investigated by recombinant expression of several genes in *E. coli* (41). This work proposed a scheme in which acrylate is hydrated to 3-hydroxypropionate, which is further oxidized to malonate-semialdehyde. Malonate semialdhyde is then decarboxylated and acetyl-CoA is formed. Whether or not the first three steps are CoA mediated reactions is unknown as these investigations were carried out in whole cells of *E. coli* and not test in situ.

Acrylate, in the form of acryloyl-CoA, is also part of the 3-hydroxypropionate pathway for CO_2 fixation described in the green nonsulfur phototrophic bacterium *Chroroflexus auranticus* and the thermoacidophilic Archaea (1, 2). In this pathway hydroxypropionate is converted to its CoA thioester hydroxypropionyl-CoA and then dehydrated to acryloyl-CoA before reduction to propionyl-CoA. In *C. auranticus,* these reactions were catalyzed by a trifunctional fusion protein. In contrast, members of the thermoacidophilic archaea *Sulfolobales* possessed individual enzymes capable of catalyzing each of the three reactions.

Lastly, *Clostridium* was proposed to possess a pathway capable of metabolizing lactoyl-CoA to acryloyl-CoA (22, 29). Like the pathways described above, acryloyl-CoA can then be directly reduced to propionyl-CoA. None of the enzymes that constitute this pathway were identified, and it remains unknown whether these enzymes are related to the enzymes identified in *Sulfolobales* or *C. auranticus.*

In this report the pathways used to assimilate DMSP in *R. pomeroyi* were investigated. Using ^{13}C isotopic labeling and targeted gene mutagenesis, it was found that the demethylation pathway does in fact assimilate the three carbon moiety as acetate through the ethylmalonyl-CoA pathway. DMSP routed through the cleavage pathway was assimilated through a novel pathway that produces propionyl-CoA. Two of the three enzymes that constitute this pathway were identified by purification from cell extracts and confirmed by recombinant expression. Furthermore, the transcriptional response of *R. pomeroyi* to DMSP was consistent with the pathways proposed to assimilate DMSP carbon. The fate of DMSP methyl groups was also investigated by using a ^{13}C tracer. This label was only incorporated into compounds biosynthesized via tetrahydrofolate-dependent pathways indicating that cells do not have a robust C-1 metabolism when grown on DMSP.

Material and Methods

DMSP synthesis

DMSP was synthesized as described previously (6) using [13C-1] acrylic acid (Sigma-Aldrich, St. Louis, MO) and dimethylsulfide or [13C$_2$] dimethylsulfide (Cambridge Isotopes, Cambridge, MA) and acrylic acid.

Growth of cultures

R. pomeroyi was grown at 30° C in a carbon-limited chemostat with a marine basal medium as described previously (34) using 2 mM DMSP at a flow rate of 0.1 ml min^{-1} and a dilution rate of 0.0416 hour^{-1}. For labeling experiments, after 5 volumetric exchanges the outflow was collected into 100% ethanol, with the final concentration of ethanol being kept above 50%. Outflow was harvested daily by centrifugation at 10000 x g for 10 minutes, and the pellet was stored at -20 C.

For microarray experiments, cells were grown using the same conditions. Cells, 50 mL, were collected on ice into a 5 mL solution of 95% ethanol/5% phenol and immediately centrifuged at 10000 x g for 5 min at -20°C. The supernatant was decanted, and the cell pellet was stored at -80° C until processing.

For growth curves *R. pomeroyi* and mutant strains were grown in batch culture using a marine basal medium as described previously (35).

Cell material used for protein purifications was grown in a 1 L chemostat with a flow rate of 0.7 mL min^{-1} and a dilution rate of 0.042 hr^{-1} with 2 mM DMSP and 3 mM sodium acetate as the source of carbon. Approximately 900 mL of cell material was collected each day, for three days. Collected cell material was harvested by centrifugation at 10000 x g for 10 minutes, washed with ice cold 50 mM Tris-HCl (pH 7.5), and then frozen at -20° C. Cell material from three collections was resuspended in 2 mL buffer and lysed by bead beating for with 0.1 mm zirconia beads for 5 minutes using a vortex genie bead beating adapter (MoBio Laboratories). Cell lysate was centrifuged for 10 min at 10000 x g and then used for protein purifications.

Calculations for the minimum amount of enzymatic activity required to consume carbon entering the chemostat were performed as described previously (35), yielding a value of 57 nmol min^{-1} mg^{-1} for the conditions used in these experiments. Since 40% of DMSP is routed through the cleavage pathway in the DMSP-limited chemostat (35), the minimum activity of enzymes function in the cleavage pathway was 23 nmol min^{-1} mg^{-1}.

Methanethiol and dimethylsulfide measurements

Methanethiol and dimethylsulfide were measured by headspace gas chromatography on an SRI 8610-C gas chromatograph with a Chromosil 330 column with nitrogen carrier gas a flow rate of 60 ml min^{-1}, an oven temperature of 60° C, and a flame photometric detector (8).

^{13}C enrichment of carbon dioxide

Carbon dioxide leaving the chemostat was trapped by bubbling the gaseous outflow through a solution of $Ba(OH)_2$. The barium hydroxide solution was prepared by mixing equal volumes of 100 mM $BaCl_2$ and 200 mM of NaOH. The precipitate that formed upon mixing was removed by centrifugation and the clarified solution was gently pipetted into a 28 mL Balch tube and sealed with a stopper so that no air remained in the tube. The chemostat outflow was then bubbled through the barium hydroxide solution using narrow bore plastic tubing. After about 20 minutes, the white precipitate was collected by centrifuge and the supernatant was decanted. The barium carbonate was then washed with degassed water and dried by lyophilization.

Fractionation of labeled cells

Cell pellets were fractionated using a protocol similar to that described previously (37). First, cells were washed in 50:50 solution of ethanol:diethylether for 40 minutes at 37° C. The mixture was then centrifuged at 15000 x g for 10 minutes, and the supernatant containing lipids was discarded. The pellet was dried under a stream of air, and 2 ml of 4 M NaOH was added. The pellet was vortexed vigorously and incubated at 37° C for 4 hours. The solution was brought to pH 2 with concentrated HCl and then centrifuged at 15000 x g for 10 minutes. The supernatant containing hydrolyzed RNA was brought to pH 8 with sodium bicarbonate and saved. The pellet was then suspended in 5% TCA and placed in a boiling water bath for 30 minutes. The mixture was cooled to room temperature and centrifuged at 15000 x g for 10 minutes. The supernatant containing the hydrolyzed nucleic acids was discarded, and the pellet was resuspended in dH_2O and centrifuged as above. The pellet was again suspended in 1 mL H_2O, transferred to a Balch tube and dried under a stream of air. Then 1 mL of 6 M HCl was added to the tube, and the tube was sealed with a butyl stopper. The tube was flushed with N_2

for 15 minutes and incubated in a 110° C sand bath for 24 hours. The HCl was removed by drying under a stream of air. The residue was resuspended in 1 mL of dH_2O and again dried. The residue was then suspended in 1 ml D_2O and centrifuged for 2 minutes at 17000 x g. The supernatant was used for ^{13}C NMR analysis of the crude amino acid pool.

Amino acid purification

Amino acids from the hydrolyzed proteins were benzoylated with benzoyl chloride as described by Carter and Stevens (4). Briefly, the hydrolyzed proteins were resuspended in 1 mL of 2 M NaOH, and 50 µL benzoyl chloride was added in 10 µL increments with vigorous vortexing. After about 20, minutes the solution was acidified with the addition of 6 M HCl. The precipitate was removed by centrifugation, and the solution was used for amino acid purification. The benzoylated amino acids were purified using an AKTA purifier (GE Healthcare) with a C-18 reverse phase column. Amino acids were eluted with a gradient of 8% -50% methanol in water with 0.2% formic acid and detected by absorption at 254 nm. Fractions containing purified amino acids were dried under a stream of air.

Amino acid analysis

Chemostat-grown *R. pomeroyi* grown on 2 mM DMSP was collected and washed in 0.1% HCl and then submitted for amino analysis (Proteomics Core Facility, UC Davis). The amino acid composition is listed in table 4-1.

Nucleoside Purification

Nucleosides were dephosphorylated with alkaline phosphatase and purified using an AKTA purifier (GE Healthcare) with a C-18 reverse phase column. Nucleosides were eluted isocratically using a mobile phase of 8% methanol and 0.2% formic acid. Purified nucleosides were lyophilized and resuspended in D_2O for NMR analysis.

NMR

^{1}H NMR of nucleosides and amino acids was performed on a Varian Unity Inova500 with a broadband probe. For quantitative ^{13}C NMR, a 45 degree pulse angle and 5 second relaxation delay were used with 500-5000 scans. Quantitation was performed as described previously (11) by comparison of the ^{13}C-NMR integrals from experimentally obtained and standard amino acids. First, amino acid standards were benzoylated and purified as described above. These standard amino acids were analyzed under the same conditions as the experimentally obtained amino acids. The ^{13}C-NMR integrals of the signals from the benzoyl carbons from both the experimental and standard amino acids were set equal to 1, since these signals should contain only natural abundance ^{13}C. The ratio of the ^{13}C-NMR integrals from experimental and standard amino acids was obtained to give the relative abundance of ^{13}C at each carbon position. The absolute abundance was then determined by multiplying the relative abundance by 1.1.

Enzyme Assays

Acrylate-CoA ligase

Acrylate-CoA ligase was assayed in 50 mM HEPES (pH 7.5), 2 mM ATP, 2 mM MgCl$_2$, 0.05 mM CoA, and 2 mM acrylate. Reactions were initiated by the addition of cell extract. After 2-5 min, they were quenched by the addition of 4 µl H$_3$PO$_4$. Assays were centrifuged to remove denatured proteins and analyzed by HPLC. Activity was measured by the consumption of CoA.

Acryloyl-CoA hydratase

Acryloyl-CoA hydratase activity was measured in 50 mM HEPES (pH 7.5), and 0.05 mM acryloyl-CoA. Reactions were initiated by the addition of protein, and processed as described above. Activity was measured as the production of acryloyl-CoA.

3-hydroxypropionyl-CoA reductase

3-hydroxypropionyl-CoA reductase activity was measured in 50 mM HEPES (pH 7.5), 0.05 mM 3-hydroxypropionyl-CoA, 1 mM NADPH, and 1 mM $MgCl_2$. Reactions were initiated with the addition of protein. After 2-5 min they were quenched and analyzed as described above. Activity was measured as the production propionyl-CoA or the disappearance of 3-hydroxypropionyl-CoA.

Propionyl-CoA carboxylase

Propionyl-CoA carboxylase activity was measured in 50 mM HEPES (pH 7.5), 0.05 mM propionyl-CoA, 2 mM ATP, 2 mM $MgCl_2$, 10 mM $NaHCO_3$. Reactions were initiated with the addition of protein. After 2-5 minutes they were quenched and analyzed as described above. Activity was measured by the disappearance of propionyl-CoA.

Genetic Modifications

Gene disruptions of SPO0370 andSPO1914 were made by homologous recombination of suicide plasmids as described previously (35).

Recombinant protein expression

Genes SPO1914, SPO0147, and SPO2934 were PCR amplified from *R. pomeroyi* genomic DNA and cloned into the pTrcHisA (Invitrogen) vector by standard techniques.

128

Substrate Synthesis

Acryloyl-CoA was synthesized with acryloyl-chloride and free coenzyme-A as described previously (29). The acryloyl-CoA was purified by reverse-phase chromatography using an Ultrasphere ODS preparative column (10×250 mm). The column was developed with 20 mM ammonium acetate (pH 6) and a gradient of 2–25% acetonitrile. Acryloyl-CoA was detected by its absorbance at 254 nm. Fractions containing acryloyl-CoA were lyophilized, resuspended in dH_2O, and again lyophilized.

3-hydroxypropionyl-CoA was synthesized enzymatically from acryloyl-CoA and purified SPO0147 as described above. The product was purified by reverse phase chromatography as described above.

Acryloyl-CoA hydratase purification

Q-Sepharose HP chromatography. The cell extract was applied to a Mono-Q HR anion exchange column (GE Healthcare, 1.6 x 10 cm) equilibrated with 50 mM Tris-HCl (pH 8.0) at a flow rate of 2 mL min^{-1}. Protein was eluted with a gradient from 0-1 M NaCl over 8 column volumes. Activity eluted between 18-28 mS/cm.

Phenyl-superose chromatography. Active fractions from Q-Sepharose chromatography were pooled and made 1.7 M $(NH_4)_2SO_4$ by addition of solid $(NH_4)_2SO_4$. The solution was applied to a phenyl-superose HR hydrophobic interaction column (GE Healthcare, 1 x 10 cm) at a flow rate of 1 mL min^{-1}. The column was washed with one column volume of 1.7 M $(NH_4)_2SO_4$ in 50 mM Tris-HCl (pH 7.5). Protein was eluted with a gradient of 1.7-0 M $(NH_4)_2SO_4$ in 50 mM Tris-HCl (pH 7.5) over 7 column volumes. Activity eluted at 62-48 mS cm^{-1}. Active fractions were pooled and concentrated with an Amicon Ultra centrifugal filter (10 kD). The final concentrate was suspended in 5 mM potassium phosphate buffer (pH 7.5).

Hydroxyapatite chromatography. The concentrated protein solution was then applied to a type-II hydroxyapatite column (1mL, BioRad) that was equilibrated with 5 mM potassium phosphate (pH 7.5) containing 1 mM $CaCl_2$. The column was washed with four column volumes of buffer, and protein was eluted with a 5-500 mM gradient of potassium phosphate buffer over six column volumes. Activity eluted just after start of the gradient. The two 1 mL fractions containing the highest activity were concentrated using an Amicon Ultra centrifugal filter (10 kD).

3-Hydroxypropionyl-CoA reductase purification

The 3-hydroxypropioinyl-CoA reductase was purified as described above for the acryloyl-CoA hydratase. Activity co-eluted with acryloyl-CoA hydratase during anion-exchange chromatography. Activity eluted at 75-61 mS cm^{-1} after hydrophobic interaction chromatography. Active fractions were pooled, concentrated, and chromatographed with the 1 mL hydroxyapatite column. Activity eluted after the start of the gradient. The two 1 mL fractions with the highest activity were concentrated as described above.

Transcriptional analysis using microarrays

R. pomeroyi microarray design, processing, and image analysis were performed as described previously (3). A non-competitive hybridization scheme was used in which only one RNA sample was hybridized to the microarray. Slides were then normalized so that the average spot each array possessed the same signal intensity. The normalized intensity values were then used to compare the relative signal intensity between different treatments using the significance analysis of microarrays program (45). Those spots with false-discovery rate (q-value) less than 10 were considered significantly regulated.

Results

Recently, the pathway for DMSP demethylation/demethiolation in *R. pomeroyi* was described as series of coenzyme-A mediated reactions, referred to as the MMPA-CoA pathway (35). This pathway results in the release of methanethiol, acetate, and CO_2 from MMPA. With knowledge of this pathway, assimilation of the three carbon moiety of DMSP was investigated. First, enzyme assays were developed to investigate the reactions that transform acrylate, the proposed product of DMSP cleavage (28, 42, 43), to a central carbon metabolism intermediate. Second, targeted gene mutations and ^{13}C isotope tracing experiments were performed to confirm the proposed pathways and further investigate the cell physiology. Finally, analysis *R. pomeroyi*'s transcriptional response to DMSP was investigated using whole-genome microarrays.

Acrylate-CoA ligase

Assuming that free acrylate is product of DMSP cleavage by DddP, DddQ, or DddW (42), it was hypothesized that acryloyl-CoA may be the next intermediate in the pathway. To test this hypothesis, acrylate-CoA ligase activity was assayed in crude cell extracts of *R. pomeroyi* grown in a chemostat with DMSP as the sole source of carbon. Cell free extracts provided with acrylate, free-CoA, and ATP produced acryloyl-CoA at a rate of 23 nmol min^{-1} mg^{-1} protein (Figure 4-1 and Table 4-4), which was sufficient to consume all of the substrate that entered the chemostat and was routed through the cleavage pathway (see methods section for calculation).

It was hypothesized that the enzyme catalyzing this reaction was encoded by the gene annotated as the propionate-CoA ligase (*prpE,* EC# 6.2.1.17). This enzyme normally functions in the methylmalonyl-CoA pathway of propionate assimilation. Propionate-CoA ligase

characterized from other organisms possessed activity with acrylate as the substrate (33). To

further support this hypothesis, the *prpE* from *R. pomeroyi* (SPO2934) was cloned and expressed

in *E. coli*. Cell-free extracts of the recombinant *E. coli* had activity with both propionate and

acrylate, while the host strain alone did not. In addition, the microarray analysis showed that the

prpE gene was up-regulated when grown on DMSP (Table 4-2).

To further test this hypothesis, the recombinant enzyme will be purified and

characterized. The enzyme is expected to possess similar rates of both propionate-CoA and

acrylate-CoA ligase activity. A mutant strain of *R. pomeroyi* with a tet resistance cassette

inserted into the gene encoding the propionate-CoA ligase will be created. It is expected that this

mutant strain will be incapable of growth on acrylate as the sole source of carbon.

Acryloyl-CoA hydratase

To investigate the fate of acryloyl-CoA, cell extracts of *R. pomeroyi* were provided

acryloyl-CoA. There was a rapid conversion to an unknown-CoA containing intermediate. To

identify this compound, it was collected after HPLC separation and analyzed by Fourier

Transformed Ion Cyclotron Resonance mass spectrometry (FTICR). The molecular mass of this

unknown intermediate was 839.14 Da, which was equal to the exact mass of acryloyl-CoA plus

one water molecule. This datum suggested that acryloyl-CoA was hydrated to either 2- or 3-

hydroxypropionyl-CoA. Since standards for these two compounds were not commercially

available nor easily synthesized, ^{1}H NMR was used to distinguish between the two possible

compounds. Upon ^{1}H NMR analysis, the product of acryloyl-CoA hydration contained doublets

at 2.6 and 3.8 ppm, consistent with 3-hydroxypropionyl-CoA. If the product was 2-

hydroxypropionyl-CoA, a distinctive doublet corresponding to the C-3 methyl group would have

been located at 1.3 ppm. Thus, it was concluded that the product of acryloyl-CoA hydratase was

3-hydroxypropionyl-CoA. The specific activity of 3-hydroxypropionyl-CoA synthesis in cell

extracts of *R. pomeroyi* was greater than 8 μmols min^{-1} mg^{-1}, far exceeding the minimum level of

activity required to consume all of the substrate entering the chemostat. This exceedingly high

rate was consistent with the enzymatic efficiency of enoyl-CoA hydratase enzymes, which have

been reported to be limited only by the rate of substrate diffusion (19).

The enzyme catalyzing the hydration reaction was identified by purification from *R.*

pomeroyi crude cell extracts. A three-step purification consisting of anion exchange, hydrophic

interaction chromatography, and hydoxyapaptite chromatography yielded a protein purified to

electrophoretic homogeneity (Figure 4-2). The protein coding gene was identified by in-gel

trypsin digestion and MALDI-TOF mass fingerprinting as SPO0147, annotated as an enoyl-CoA

hydratase. To confirm that this gene encoded for a protein with correct catalytic function, the

gene was cloned and expressed in *E. coli*. Cell extracts of the recombinant *E. coli* possessed

acryloyl-CoA hydratase activity, while the host strain alone did not.

To assess the physiological significance of this protein, a mutant strain of *R. pomeroyi*

will be made in which gene SPO0147 will be disrupted. It is expected that this mutant will be

unable to grow on acrylate as the sole source of carbon, although there are several enoyl-CoA

hydratase gene homologs in the *R. pomeroyi* genome, which may complement growth on

acrylate in the mutant strain.

3-Hydroxypropionyl-CoA reductase

The fate of 3-hydroxypropionyl-CoA was next investigated. In the absence of exogenous

cofactors, cell free extracts did not consume 3-hydroxypropionyl-CoA. Upon the addition of

NADH or NADPH, there was a quantitative conversion of 3-hydroxypropionyl-CoA to

propionyl-CoA, demonstrating an unprecedented 3-hydroxypropionyl-CoA reductase activity

(Figure 4-1). Chemostat-grown *R. pomeroyi* possessed an NADPH-dependent 3-hydroxypropionyl-CoA reductase activity of 195 ±10 nmol min^{-1} mg^{-1}, which was well above the minimum rate required to consume all of the carbon entering the chemostat. In contrast, cells grown on glucose possessed an activity of only 16 nmol min^{-1} mg^{-1}. Furthermore, DMSP-grown cells possessed propionyl-CoA carboxylase activity of 34 nmol min^{-1} mg^{-1}, while glucose-grown cells possessed lower activities of only 4 nmol min^{-1} mg^{-1}. Propionyl-CoA carboxylase is required for the methylmalonyl-CoA pathway for C3 assimilation in *R. pomeroyi.*

The enzyme catalyzing this reaction was partially purified. One of three enzymes remaining on a SDS-PAGE was identified by peptide mass fingerprinting as a zinc-dependent oxidoreductase encoded by gene SPO1914. The SPO1914 gene was cloned and expressed in *E. coli*. The recombinant *E. coli* had activity for 3-hydroxypropionyl-CoA reductase, while the host strain alone did not.

To confirm the physiological significance of this activity, the gene was disrupted by insertion of a tetracycline resistance marker. The mutant strain was incapable of growth on acrylate or 3-hydroxypropionate (Figure 4-3). In contrast, the strain grew similarly to wild-type when provided with propionate as the sole source of carbon. These results were consistent with the hypothesized role of this enzyme catalyzing the reduction of 3-hydroxypropionate to propionate during acrylate assimilation.   The mutant strain grew poorly on DMSP, with only 30% of inoculations capable of yielding growth similar to wild-type (data not shown). This result was unexpected as growth on DMSP should be possible since the demethylation/demethiolation pathway remained uninterrupted. The reason for this irregular growth phenotype was unclear, but one possibility was that there was a build-up of 3-

hydroxypropionyl-CoA in the cells, which may have caused a metabolic collapse due to shortage

of free CoA, thus preventing growth.

The genomic location of 3-hydroxypropionyl-CoA reductase in *R. pomeroyi* was

interesting because it was next to *dmdA,* which encodes the enzyme that catalyzes the

demethylation of DMSP. These two genes were predicted to be on the same transcriptional unit.

The transcriptional response of gene SPO1914 was consistent it being involved in DMSP

metabolism. As shown in table 4-2, this gene was up-regulated 14-fold after growth on DMSP

as compared to glucose. *Candidatus* Puniceispirillum marinum IMC1322, a member of the

SAR116 clade of *Alphaproteobacteria* , also possessed a 3-hydroxypropionyl-CoA reductase

homolog with a protein identity of 62%. Interestingly, this gene was positioned immediately

upstream of a *dddP* gene homolog, which encodes for a DMSP-cleavage enzyme that produces

acrylate in addition to DMS (32).

Ethylmalonyl-CoA pathway for acetate and MMPA assimilation

The recently described MMPA-CoA pathway is hypothesized to form acetate. *R.*

pomeroyi does not possess an isocitrate lyase ortholog nor do cell-free extracts catalyze the

isocitrate lyase reaction (C.R. Reisch unpublished observation), making this organism incapable

of assimilating acetate through the glyoxylate shunt. However, *R. pomeroyi* possesses all known

genes in the ethylmalonyl-CoA pathway, and it is likely that this pathway is used for acetate

assimilation (14). To confirm that the ethylmalonyl-CoA pathway was required for growth on

acetate and MMPA, a *ccr* mutant was constructed. This gene encodes for the crotonyl-CoA

carboxylase reductase enzyme, which is diagnostic of the ethylmalonyl-CoA pathway (13). The

mutant strain was unable to grow on acetate as the sole source of carbon (Figure 4-4), confirming

that acetate was assimilated through the ethylmalonyl-CoA pathway. When MMPA was

provided as the sole source of carbon, the mutant displayed an extended lag phase and the

growth yield was diminished by two-thirds. This result was unexpected, as growth on MMPA

should have behaved the same as acetate. One possible explanation for this growth was that the

cells were utilizing the MMPA-CoA pathway, thus transforming MMPA to acetate. This

conversion is energetically favorable since it consumes one ATP while producing one NADH,

one $FADH_2$, and releases MeSH. It was possible that the cellular growth was due to the

assimilation of the MeSH. To test this hypothesis, the concentration of MMPA and acetate in the

medium will be measured at different time points during the growth curve. An equimolar

conversion of MMPA to acetate would suggest that the growth was due to the assimilation of

MeSH. In contrast to the poor growth on MMPA, the mutant was able to grow on DMSP as the

sole source of carbon, demonstrating that the DMSP cleavage pathway was still functional

(Figure 4-4). These results also indicate that the product of the cleavage pathway does not enter

central carbon metabolism as acetate, which is consistent with the pathway identified here.

Transcriptional response of *R. pomeroyi* to DMSP

To study the transcriptional response of *R. pomeroyi* during growth on DMSP, whole

genome microarrays were used. Steady-state *R. pomeroyi* grown in a carbon-limited chemostat

was used in this investigation to minimize the possibility of growth related changes in

transcriptional response. Those probes with a false-discovery rate (q-value) of less than 10% and

whose gene annotation was of particular interest to DMSP metabolism are listed in Table 4-2.

Several genes that are involved in acetate and propionate assimilation are up-regulated

with growth on DMSP, which is consistent with the pathways presented here. Three probes that

represent genes involved in only the ethylamalonyl-CoA pathway; acetoacetyl-CoA redutase, β-

ketothiolase, and ethylmalonyl-CoA mutase are all significantly up-regulated during growth on

136

DMSP. Similarly, at least one probe from all four genes that constitute the methylmalonyl-CoA pathway were upregulated.

One of the two gene clusters with the highest expression on DMSP included SPOA0268-272. This cluster has genes that encode for a transcriptional regulator, two proteins of unknown function, a methylamine utilization protein (*mauG*), and a glutathione-dependent formaldehyde dehydrogenase. While the roles of these genes in DMSP metabolism are unclear, the increased abundance of the protein encoded by SPOA272 was also observed in proteomic experiments, and it was hypothesized that the proteins may participate in the catabolism of methanethiol or dimethylsulfide (21).

The second gene cluster that was highly up-regulated with growth on DMSP was SPO0989-SPO1001. These genes encode for the Friederich-Kelly pathway of sulfur oxidation, known as the SOX system (15). This pathway functions to completely oxidize inorganic sulfide to sulfate. This pathway is likely used to gain energy from the DMSP sulfur which was either retained in the cell or taken up as MeSH. Conversely, the *cycH* gene that is part of the assimilatory sulfate reduction pathway was down-regulated with DMSP. This data suggests that the cells are assimilating the reduced sulfur from DMSP, which is consistent with hypothesis that DMSP sulfur is assimilated preferentially over sulfate due to the energetic costs associated with sulfate reduction (26).

The most up-regulated gene in the microarray experiments, with an increased expression of over 70-fold on each of two probes, was SPO0453. This gene was recently identified as *dddW,* encoding for a functional DMSP cleavage enzyme in *R. pomeroyi.* However, it was not the only DMSP lyase that was up-regulated in these experiments, as *dddP* had a 5-fold increase in relative expression. The gene that initiates the demethylation pathway, *dmdA*, was also up-

regulated with growth on DMSP, although the increase was much less dramatic than with *dddW*. The genes that constitute the MMPA-CoA pathway were not significantly regulated on these microarrays. However, RT-qPCR performed on RNA extracted from cells grown under similar conditions did find a significant increase in transcript abundance (35). Thus, the lack of a significant response by these probes in the microarray experiments was probably due to issues regarding the sensitivity of microarrays.

Retrobiosynthetic analyses with ^{13}C labeling

An experiment using [[13]C-1] labeled DMSP was performed to test whether the whole cell physiology was consistent with the MMPA-CoA pathway, which results in the production of acetate, and the pathway for acrylate assimilation presented here. In the MMPA-CoA pathway, the DmdD catalyzed decarboxylation of MTA-CoA resulted in the release of the ^{13}C enriched C-1 carbon as [13]CO_2. This decarboxylation caused a significant enrichment of the CO_2 pool within in the chemostat, which was determined to be 28% after trapping as barium carbonate and analysis by combustion mass spectrometry. This enriched CO_2 was then incorporated into cell material via the crotonyl-CoA carboxylase/reductase and propionyl-CoA carboxylase enzymes.

For the assimilation of acetate, it was anticipated that the cells used the ethylmalonyl-CoA pathway, which is a complicated series of reactions that produces propionyl-CoA and glyoxylate. The propionyl-CoA is assimilated through the methylmalonyl-CoA pathway for C3 assimilation, while the glyoxylate is condensed with acetyl-CoA to form malyl-CoA. The pathway for acrylate assimilation proposed here also results in the production of propionyl-CoA. Thus, carbon from both the demethylation and cleavage pathway was expected to be processed through the C3 assimilation pathway. However, the ^{13}C labeling pattern of succinyl-CoA resulting from the acrylate assimilation pathway differs from that of the ethylmalonyl-CoA

pathway (figure 4-5). Conversion of succinyl-CoA to the symmetrical molecule succinate then scrambles these differing enrichments, yielding equal enrichments of the C-1 and C-4 carbon.

As shown in figure 4-5, there were also two sources of malate in the cell, which resulted in different ^{13}C enrichments patterns. The first source of malate was derived from succinate via the TCA cycle and possessed equal enrichments of ^{13}C in both the C-1 and C-4 positions. The second source of malate was derived from the glyoxylate produced in the ethylmalonyl-CoA pathway. Glyoxylate and acetyl-CoA condense to form malyl-CoA, which was then transformed to malate and free CoA. The glyoxylate possessed the CO_2 that was incorporated by the crotonyl-CoA carboxylase/reductase enzyme in the ethylmalonyl-CoA pathway. Thus, the C-1 of glyoxylate, and consequently the C-1 of malate, formed by this route possessed a ^{13}C enrichment of 28%.

The calculation to determine the theoretical ^{13}C enrichment of each TCA cycle intermediate is complicated. The two sources of succinyl-CoA and malate discussed above must be accounted for with precise knowledge of their fluxes. The flux of each source of malate and succinyl-CoA results from the flux of DMSP through either the DMSP cleavage or demethylation pathways as well as the flux of acetyl-CoA produced from the MMPA-CoA pathway. Since 80 nmol min^{-1} of DMSP was routed through the cleavage pathway, the remaining 120 nmol min^{-1} must have been routed through the demethylation pathway, producing acetate. This 120 nmol min^{-1} must be partitioned between the four required inputs of acetyl-CoA shown in figure 4-5, as well as lipid, leucine, and isoleucine biosynthesis. These biosynthetic reactions, which consume 27 nmol min^{-1} of acetate, draw from the pool of acetate before it can be assimilated through the ethylmalonyl-CoA pathway and reach the TCA cycle. The acetyl-CoA inputs that are part of the ethylmalonyl-CoA pathway, must be consumed in stoichiometric

amounts, designated here as variable A. Subtracting the acetyl-CoA used in biosynthesis from the 120 nmol min^{-1} produced in the MMPA-CoA pathway left 93 nmol min^{-1} that were partitioned between the three acetyl-CoA inputs in the ethylmalonyl-CoA pathway. Thus, 3*A was set equal to 93 nmol min^{-1}.

With the exception of α-ketoglutarate, all of the building blocks listed in Table 4-3 were withdrawn for cell material biosynthesis before the acetyl-CoA requiring reaction of citrate synthase. To produce the 7 nmol min^{-1} of α-ketoglutarate required for cell material biosynthesis, stoichiometric amounts of acetyl-CoA must be consumed by citrate synthase. In total, there were 107 nmol min^{-1} of building blocks consumed (table 4-3) of the 142 nmol min^{-1} of substrate available. Thus, the TCA cycle must function to oxidize the remaining 35 nmol min^{-1}. The oxidative TCA cycle consumes one oxaloacetate and one acetyl-CoA, while producing one succinyl-CoA, which necessitates that the 35 nmol min^{-1} must be split between acetyl-CoA and α-ketoglutarate. As shown in figure 4-5, the 17.5 nmol min^{-1} of succinyl-CoA that makes a complete turn of the TCA cycle was completely unenriched with ^{13}C due to the two decarboxylation reactions in the TCA cycle. This unenriched succinyl-CoA then dilutes the enriched succinyl-CoA that came from propionyl-CoA. This 17.5 nmol min^{-1} was additive to the 142 nmol min^{-1} that comes from the DMSP. As shown in table 4-6, after each consecutive turn of the TCA cycle, this value grows at a decreasing rate until equilibrium was reached at 35 nmol min^{-1}. Thus, at equilibrium, the cells must make 35 nmol min^{-1} of acetate through the pyruvate dehydrogenase reaction.

Once the equilibrium was reached, the 35 nmol min^{-1} would dilute the 111 nmol min^{-1} of succinyl-CoA that came from propionyl-CoA, yielding an expected enrichment of 41% in the C-1 and C-4 positions (figure 4-5). Malate from the TCA cycle would have equal enrichments of

41% in the C-1 and C-4 positions, while malate derived from glyoxylate and acetyl-CoA would be enriched at 28% in only the C-1 position. Upon mixing of these two sources of malate an average enrichment of 39% in the C-1 position and 34% in the C-4 position would result. These values are similar to those experimentally measured in aspartate, alanine, and α-ketoglutarate (Table 4-5). This greater enrichment in the C-1 position is mostly observed in the amino acids analyzed, with the exception of threonine, whose biosynthesis is discussed below.

^{13}C Flux Balance

To demonstrate that the measurements of ^{13}C obtained in these experiments were consistent with metabolism of the whole cells, a carbon balance was calculated (Table 4-7). There were 1000 nmol min^{-1} carbon entering the chemostat as DMSP and 70 nmol min^{-1} as carbon dioxide or bicarbonate, of which 201 nmol min^{-1} contained ^{13}C. The amount of carbon in cell material leaving the chemostat was calculated at 300 nmol min^{-1}, while another 160 nmol min^{-1} was evolved as DMS. Thus, the remaining carbon must have been expelled from the chemostat as CO_2. Subtracting the amount of cell material and DMS leaving the chemostat (300 + 160) from the amount of CO_2 and DMSP entering the chemostat (1000 + 70), left 610 nmol min^{-1}. The ^{13}C enrichment of CO_2 leaving the chemostat was measured at 28%, which equals 610 nmol min^{-1} * 28%, or 177 nmol min^{-1}. Calculating the total amount of ^{13}C leaving the chemostat (177 + 27), yields 204 nmol min^{-1} of carbon, which was nearly equal to the 201 nmol min^{-1} of ^{13}C that entered the chemostat. Thus, these measurements which demonstrate that most of the C-1 label was oxidized to CO_2, were consistent with calculations based on the whole cell activities.

[^{13}C-1] DMSP Labeling Pattern

Oxaloacetate

Aspartate is synthesized from the transamination of the TCA cycle intermediate oxaloacetate, which yields a labeling pattern identical to that of oxaloacetate. As shown in figure 4-5, there were essentially two sources of malate in the DMSP grown cells, which yield different enrichments for the C-1 and C-4 carbon. These observed enrichments of 40% and 32% for the C-1 and C-4 positions of aspartate, respectively (Table 4-5). These enrichments were consistent with the theoretical labeling pattern discussed above in Figure 4-5. Threonine was expected to be biosynthesized from aspartic acid. First, the C-4 position of aspartate is reduced to an alcohol, producing L-homoserine. The C-4 should then be reduced to a methyl group, forming threonine. Thus, aspartate and threonine should possess the same labeling pattern. The methyl group on the C-4 position enables the absolute quantification of ^{13}C by ^{13}C coupled satellite signals in the ^{1}H NMR spectra and showed an enrichment of 36%. The quantitative ^{13}C NMR analysis of threonine showed enrichments of 32% and 34% for the C-1 and C-4 atoms, respectively. While not identical, the enrichments obtained by using both the ^{1}H coupled signal and quantitative ^{13}C NMR show similar enrichments. These enrichments were unexpected though, as it was anticipated that the C-1 position would possess a higher enrichment than the C-4 position. The described pathway for threonine biosynthesis starts with homoserine, which is phosphorylated by ThrB in an ATP-dependent reaction. Gene homologs for *thrB* are absent from *R. pomeroyi*, as well as most *Alphaproteobacteria*. Thus, it is possible that threonine biosynthesis in *R. pomeroyi* does not proceed through aspartic acid or homoserine and, which would explain the unexpected labeling pattern observed.

Pyruvate and branched chain amino acids

As shown in figure 4-5, pyruvate was expected to be synthesized from the decarboxylation of malate in a reaction catalyzed by the NAD(P)-dependent malate dehydrogenase (decarboxylating, E.C. 1.1.1.39). This decarboxylation removes one of the two highly enriched carbons from malate. Subsequently, pyruvate may be decarboxylated by the pyruvate dehydrogenase complex, releasing the second highly enriched carbon and leading to the production of acetate.

The labeling pattern for leucine and valine is consistent with the traditional pathway for branched chain amino acid synthesis. This pathway is initiated by acetolactate synthase which requires two molecules of pyruvate to form acetolactate and releases CO_2. The labeling pattern for isoleucine however, was not consistent with it being derived from threonine, as is common in many microorganisms. The ^{13}C NMR spectrum shows no highly enriched carbons, indicating threonine is not a precursor to isoleucine. This observation was consistent with the alternative pathway for isoleucine synthesis in which acetyl-CoA and pyruvate form citramalate (12, 36). Isoleucine synthesized by this pathway would not contain any highly enriched carbons.

α-Ketoglutarate

The labeling pattern of glutamic acid, which was derived from α-ketoglutarate, showed an enrichment of 39.8% ^{13}C in the C-1 position. The C-1 carbon was derived from the two sources of malate discussed previously. The second highly enriched carbon from malate was decarboxylated by isocitrate dehydrogenase. Table 4-5 also shows a slight enrichment of the C-5 carbon, which is derived from the C-2 carbon of acetate. Acetate derived from the decarboxylation reaction catalyzed by DmdD should not possess an enrichment in this position, therefore there must be a second source of cellular acetate. One possible source that would lead

143

to enrichment in the C-2 position is derived from malate. Malyl-CoA could be cleaved by the bifunctional (3*S*)-Malyl-CoA/β-methylmalyl-CoA lyase into glyoxylate and acetyl-CoA (30). This enzyme has two functions in the ethylmalonyl-CoA pathway. First, it cleaves β-methylmalyl-CoA into glyoxylate and propionyl-CoA. Second, the enzyme condenses glyoxylate and acetyl-CoA into malyl-CoA. Thus, it is likely that there is an equilibrium between the condensation and lyase reactions of malyl-CoA, yielding relatively minor amounts of acetyl-CoA enriched in the C-2 position.

^{13}C-methyl labeled DMSP

To investigate the fate of DMSP methyl carbons, *R. pomeroyi* was grown in a carbon-limited chemostat with uniformly labeled ^{13}C methyl groups. While there is little evidence that chemostat-grown *R. pomeroyi* is capable of assimilating carbon from DMS (35), the demethylation pathway contains two potential routes of methyl carbon assimilation. The DmdA catalyzed demethylation of DMSP results in the transfer of a methyl group to 5-methyl-THF (34), a common single carbon carrier. The degradation of MMPA through the MMPA-CoA pathway also releases MeSH, which is a reactive single carbon unit that can be consumed by *R. pomeroyi* and other marine bacteria (16, 26). Thus, it was hypothesized that much of these ^{13}C labeled methyl groups could be incorporated into cellular material and possibly assimilated through the serine cycle.

Initial analysis of the amino acid pool obtained after protein hydrolysis identified significant ^{13}C enrichments in the methyl group of methionine and the C-3 position in serine (Figure 4-6). Purification of methionine and serine as their benzoyl derivatives enabled the ^{1}H NMR quantification of their ^{13}C enrichment. Purified serine showed a ^{13}C enrichment of 30% in the C-3 position, while the methyl group of methionine was enriched at 99%. Protein hydrolysis

144

results in the destruction of cysteine and tryptophan, thus these amino acids were not analyzed. However, the expected pathways for cysteine and tryptophan biosynthesis in *R. pomeroyi* both utilize serine as a three-carbon moiety incorporated into the final amino acid (5). Therefore, although not directly measured, it was expected that the C-3 position of cysteine, and β-position of tryptophan would each be enriched at 30%.

^{1}H NMR of purified guanosine revealed an enrichment of 90% in the C-11. Although it was not possible to quantify the second carbon derived from 5-THF using ^{1}H NMR because there was no hydrogen atom attached to the carbon, an identical enrichment was anticipated. Additionally, although not directly measured, the enrichment of the two carbons derived from 5-THF in adenosine would also have enrichments identical to that of guanosine.

To investigate whether significant amounts of ^{13}C were assimilated but not accounted for in the purified amino acids and nucleosides, the total mass isotope ratio was determined by combustion mass spectrometry. The ^{13}C/^{12}C of the chemostat-grown cells was found to be 8.2%. Subtracting the natural abundance of ^{13}C of 1.1%, the total of 7.1% [13]C would be derived solely from from the enriched methyl groups of DMSP. To determine whether this was consistent with the amount expected based on the specific enrichments described above, the amount of ^{13}C attributed to methionine, serine, cysteine, tryptophan, and the purine nucleosides was calculated (Tables 4-8 and 4-9). The total amount of ^{13}C in these cell components only accounted for one-third of the measured amount of [13]C.

Given that most of the DMSP was routed through the demethylation pathway, but only a small amount of this carbon was assimilated, it was hypothesized that most of the methyl carbons were oxidized. To investigate this hypothesis, CO_2 from the chemostat was trapped as barium carbonate and the ^{13}C enrichment was determined by combustion mass spectrometry. The

enrichment of CO_2 was found to be 16%. This enriched CO_2 was then incorporated into cell material through crotonyl-CoA carboxylase/reductase and propionyl-CoA carboxylase, as described above. Unfortunately, quantitative ^{13}C NMR of purified amino acids was not performed. This data would have allowed for quantification of the amount CO_2 assimilated in the carbon fixing reactions required for C2 and C3 assimilation.

Discussion

Acrylate assimilation

Both the carbon and sulfur in DMSP are assimilated into cellular biomass. However, until the recently identified MMPA-CoA pathway, and preliminary evidence from whole cell experiments in *Marinomonas* sp. MWYL-1, the pathways of DMSP assimilation have remained unknown (35, 41). *R. pomeroyi* possesses two routes of DMSP catabolism. The first route, known as demethylation, is initiated by the enzyme DmdA, which transfers a methyl group from DMSP to THF, producing 5-methyl-THF and methylmercaptopropionate (MMPA). MMPA is then catabolized in a series of coenzyme-A mediated reactions, releasing MeSH, CO_2, and acetate. The second pathway of catabolism is known as DMSP cleavage and results in the production of DMS and a three carbon moiety identified as acrylate or 3-hydroxypropionate. Several gene products have recently been identified that catalyze the cleavage reaction, four of which are possessed by *R. pomeroyi* (40, 42, 44). Mutations in each of these genes showed that *dddP, dddQ,* and *dddW* encoded for functional genes under the conditions tested, as the mutant strains produced less DMS than wild-type, while a mutation in *dddD* had no effect. DddP was purified and characterized *in-vitro*, and shown to product acrylate in addition to DMS, while cell free extracts of *E. coli* expressing DddW also catalyzed the release of DMS and acrylate from DMSP. DddQ has not been characterized in-vitro, but whole cells epxeriments in which *E. coli*

expressed DddQ and was provided with DMSP-produced acrylate, suggesting that acrylate was in fact the product of DddQ. The purpose of the investigations here was to establish the pathway for DMSP and acrylate assimilation in *R. pomeroyi*.

R. pomeroyi possesses three enzymes; pyruvate carboxylase, phosphoenolpyruvate carboxylase, and propionyl-CoA carboxylase, which carboxylate a C3 substrate to form a C4 moiety that enters the TCA cycle. Of these genes, only propionyl-CoA carboxylase was up-regulated in the microarray experiments during growth on DMSP. Furthermore, the other enzymes in the methylmalonyl-CoA pathway for C3 assimilation were up-regulated with growth on DMSP. The methylmalonyl-CoA pathway is composed of four enzymatic steps that transform propionate into propionyl-CoA, which is then carboxylated to methylmalonyl-CoA. Two enzyme-catalyzed rearrangements then transform methylmalonyl-CoA into succinyl-CoA. These microarray results were consistent with previous experiments which found that DMSP caused a significant response of propionate assimilation genes (3, 46).

Transcriptional response studies and bioinformatics analysis are complicated by the fact that a number of metabolic pathways share common intermediates and enzymes. For example, as discussed above, the ethylmalonyl-CoA pathway for C2 assimilation uses the methylmalonyl-CoA pathway to assimilate the propionyl-CoA that is produced in the pathway. Thus, observations of increased expression of C3 metabolic genes may be a physiological response to C2 compounds. Given the recent identification of the MMPA-CoA pathway, which results in acetate production, propionate assimilation gene expression is expected regardless of whether the DMSP demethylation or cleavage pathway is being utilized. However, the propionate-CoA ligase gene, which is proposed to physiologically function as an acrylate-CoA ligase as well, is

not part of the ethylmalonyl-CoA pathway. Thus, the fact that the gene is up-regulated during growth with DMSP is strong evidence for its participation in acrylate assimilation.

To determine the pathway for assimilation of carbon routed through the cleavage pathway, enzyme assays were used to reconstruct the metabolic pathway. Enzyme assays revealed that cell extracts were capable of catalyzing the production of an acryloyl-CoA, hydrating acryloyl-CoA to 3-hydroxypropionyl-CoA, and then reducing 3-hydroxypropionyl-CoA to propionyl-CoA (Figure 4-1). This series of reactions was unprecedented as a means of assimilating acrylate. Acryloyl-CoA consuming enzymes and pathways described to date involve its direct reduction to propionyl-CoA (1, 29, 39) or hydration to 3-hydroxypropionate, followed by further oxidation (9, 41). Elucidation of these redundant pathways is of interest due to the increasingly popular field of synthetic biology, where enzymes that do not occur naturally in the same organism can be introduced into the same pathway for increased simplicity.

The recently described ethylmalonyl-CoA pathway is used for acetate assimilation in many isocitrate lyase-negative bacteria. The diagnostic gene in this pathway, *ccr*, encodes for the crotonyl-CoA carboxylase/reductase, which carboxylates crotonyl-CoA to ethymalonyl-CoA (13). In the isocitrate lyase negative bacteria *Methylobacter extorquens* and *Streptomyces coelicor,* a mutation in *ccr* yielded strains incapable of growth on acetate (7, 20). Accordingly, a strain of *R. pomeroyi* with a disruption of the *ccr* gene, was also incapable of growth on acetate and had a serious defect with growth on MMPA. These results confirm that the ethylmalonyl-CoA pathway is used for acetate assimilation in *R. pomeroyi* and support the hypothesis that MMPA is assimilated as acetate. While the mutant strain was able to grow on MMPA after an extended lag phase, the growth yield was greatly reduced compared to wild-type. The reason for this leaky phenotype is currently under investigation.

[^{13}C-methyl] DMSP assimilation

R. pomeroyi grown in a chemostat with [^{13}C-methyl] DMSP resulted in cell material with

^{13}C enrichments limited to a few specific locations and enriched to a high percentage. Each of

these high enrichments can be attributed to methyl group donations from THF single carbon

carriers. One of the two amino acids identified to have a high enrichment was serine, which had

enrichment in the C-3 position. Labeling in this position was consistent with the transfer an

enriched methylene group from methylene-THF to glycine, in a reaction catalyzed by serine

hydroxymethyltransferase, the first step in the serine cycle. Enrichment in the C-3 position was

quantified at 30% by ^{13}C coupled satellite signals in the ^{1}H NMR spectrum. The remaining 70%

of serine must be synthesized from the traditional pathway of serine biosynthesis, which starts

with a molecule of 3-phosphoglycerate from glycolysis. The microarray data in Table 4-2 shows

that there was a significant transcriptional response of the serine hydroxymethyltransferase gene,

as the two probes for this gene had an increase of 4.8 and 5.7-fold. This upregulation suggests

that the serine hydroxymethyltransferase only function to produce serine in the presence of

single carbon units provided by DMSP.

There were two possible sources for the enriched C1 unit that was transferred to glycine.

First, 5-methyl-THF produced by DmdA during the initial demethylation of DMSP may be

oxidized to 5-methylene-THF, which may then be directly utilized by serine

hydroxymethyltransferase. The genome sequence of *R. pomeroyi* contains a *metF* homolog,

which reduces methylene-THF to 5-methyl-THF. This reaction is reversible, so it is possible that

the physiological reaction under these conditions was to oxidize 5-methyl-THF to methylene-

THF. Alternatively, the cells may assimilate or take-up methanethiol. The methyl group may be

oxidized to formaldehyde, which spontaneously reacts with THF to form methylene-THF.

Several enzymes that catalyze the oxidation of methanethiol to formaldehyde, hydrogen sulfide, and hydrogen peroxide have been purified and characterized (17, 27, 38). However, the genes encoding these enzymes have not been identified, thus it is unknown whether *R. pomeroyi* has this ability. At this time it is unclear why the enrichments were limited to 30%.

Upon purification and ^{1}H NMR analysis, the methyl group of methionine was found to be 99% ^{13}C. There are two possible explanations for this high enrichment. Previous experiments have shown that ^{35}S sulfur from DMSP ends up in cellular amino acids (26). It was hypothesized that a direct incorporation of methanthiol into homoserine was catalyzed by cystathionine γ-synthase and may be responsible for this production of methionine (24). The enzyme methionine γ-lyase, which catalyzes the release of methanethiol from methionine, is possessed by *R. pomeroyi*. Growth of *R. pomeroyi* on methionine results in the production of methanethiol (C.R. Reisch unpublished observation), indicating that the methionine γ-lyase was functional in the forward direction. It is possible that this enzyme works in the reverse direction to catalyze the direct incorporation of methanethiol. The second possible source of highly enriched methyl groups is from 5-methyl-THF. The last step of the traditional pathway of methionine synthesis transfers a methyl group from 5-methyl-THF to homocysteine. Since the initial demethylation of DMSP produces 5-methyl-tetrahydrofolate, it would be expected that cells have an abundance of fully enriched 5-methyl-THF available for synthesis of methionine.

The biosynthesis of purine nucleosides is the third reaction for which a THF derivative provides a single carbon unit. Of the five carbons present in purine nucleosides, two are derived glycine and formyl-THF, while one is derived from carbon dioxide. Upon purification of these purine nucleosides, a ^{13}C enrichment of 90% was found in those carbons derived from formyl-THF. Formyl-THF may be derived from two different sources. The first possible pathway of

formyl-THF production is by the oxidation of 5-10-methylene-THF to 5-10-methenyl-THF and

the subsequent conversion to formyl-THF. Two enzymes that catalyze the first reaction have

been identified in other members of the Alphaproteobacteria, although *R. pomeroyi* does not

possess homologs to these methylene tetrahydromethanopterin dehydrogenase genes (MtdA or

MtdB) (18, 47). *R. pomeroyi* does have two FolD homologs which are annotated as

methylenetetrahydrofolate dehydrogenase/ methenyltetrahydrofolate cyclohydrase (DHCH)

proteins. Functional DHCH proteins oxidize 5-10-methylene-THF to 5-10-methenyl-THF and

hydrolyze the latter to form 10-formyl-THF (10). The second possible reaction for the synthesis

of formyl-THF is catalyzed by formate-THF ligase. This enzyme catalyzes the ATP dependent

reversible reaction of formate and THF to form 10-formyl-THF. The genome sequence of *R.

pomeroyi* contains two formate-THF ligase homologs with identical protein sequences. The 90%

enrichment in carbons derived from formyl-THF suggests that both pathways of formyl-THF

synthesis may be active. If all of the formyl-THF was derived directly from methylene-THF, an

enrichment of 99% would be expected, consistent with the enrichment of methionine. However,

the data suggests that there is a source of formate that is not derived from the methyl groups of

DMSP and therefore must dilute the enriched pool to 90%. *R. pomeroyi* possesses several genes

annotated as formate dehydrogenases which may provide the unenriched carbon.

References
1.   **Alber, B. E., and G. Fuchs.** 2002. Propionyl-coenzyme A synthase from *Chloroflexus aurantiacus*, a key enzyme of the 3-hydroxypropionate cycle for autotrophic CO_2 fixation. J Biol Chem **277:**12137-12143.

2.   **Berg, I. A., D. Kockelkorn, W. Buckel, and G. Fuchs.** 2007. A 3-hydroxypropionate/4-hydroxybutyrate autotrophic carbon dioxide assimilation pathway in archaea. Science **318:**1782-1786.

3.   **Burgmann, H., E. C. Howard, W. Ye, F. Sun, S. Sun, S. Napierala, and M. A. Moran.** 2007. Transcriptional response of *Silicibacter pomeroyi* DSS-3 to dimethylsulfoniopropionate (DMSP). Environ Microbiol **9:**2742-2755.

4.   **Carter, H. E., and C. M. Stevens.** 1941. Benzoylation of amino acids. J Biol Chem **138:**627-629.

5.   **Caspi, R., T. Altman, J. M. Dale, K. Dreher, C. A. Fulcher, F. Gilham, P. Kaipa, A. S. Karthikeyan, A. Kothari, M. Krummenacker, M. Latendresse, L. A. Mueller, S. Paley, L. Popescu, A. Pujar, A. G. Shearer, P. Zhang, and P. D. Karp.** 2010. The MetaCyc database of metabolic pathways and enzymes and the BioCyc collection of pathway/genome databases. Nucleic Acids Res **38:**D473-479.

6.   **Chambers, S. T., C. M. Kunin, D. Miller, and A. Hamada.** 1987. Dimethylthetin can substitute for glycine betaine as an osmoprotectant molecule for Escherichia coli. J Bacteriol **169:**4845-4847.

7.   **Chistoserdova, L. V., and M. E. Lidstrom.** 1996. Molecular characterization of a chromosomal region involved in the oxidation of acetyl-CoA to glyoxylate in the isocitrate-lyase-negative methylotroph *Methylobacterium extorquens* AM1. Microbiol-Uk **142:**1459-1468.

8.   **de Souza, M. P., and D. C. Yoch.** 1995. Purification and characterization of dimethylsulfoniopropionate lyase from an *Alcaligenes*-like dimethyl sulfide-producing marine isolate. Appl Environ Microbiol **61:**21-26.

9.   **Den, H., W. G. Robinson, and M. J. Coon.** 1959. Enzymatic Conversion of Beta-Hydroxypropionate to Malonic Semialdehyde. J. Biol. Chem. **234:**1666-1671.

10.   **Dev, I. K., and R. J. Harvey.** 1978. A complex of N5,N10-methylenetetrahydrofolate dehydrogenase and N5,N10-methenyltetrahydrofolate cyclohydrolase in *Escherichia coli*. Purification, subunit structure, and allosteric inhibition by N10-formyltetrahydrofolate. J Biol Chem **253:**4245-4253.

11.   **Eisenreich, W., G. Strauss, U. Werz, G. Fuchs, and A. Bacher.** 1993. Retrobiosynthetic analysis of carbon fixation in the phototrophic eubacterium *Chloroflexus aurantiacus*. Eur J Biochem **215:**619-632.

12.   **Ekiel, I., I. C. Smith, and G. D. Sprott.** 1983. Biosynthetic pathways in *Methanospirillum hungatei* as determined by ^{13}C nuclear magnetic resonance. J Bacteriol **156:**316-326.

13.   **Erb, T. J., I. A. Berg, V. Brecht, M. Muller, G. Fuchs, and B. E. Alber.** 2007. Synthesis Of C-5-dicarboxylic acids from C-2-units involving crotonyl-CoA carboxylase/reductase: The ethylmalonyl-CoA pathway. P Natl Acad Sci USA **104:**10631-10636.

14. **Erb, T. J., G. Fuchs, and B. E. Alber.** 2009. (2S)-Methylsuccinyl-CoA dehydrogenase closes the ethylmalonyl-CoA pathway for acetyl-CoA assimilation. Mol Microbiol **73:**992-1008.

15. **Friedrich, C. G., D. Rother, F. Bardischewsky, A. Quentmeier, and J. Fischer.** 2001. Oxidation of reduced inorganic sulfur compounds by bacteria: Emergence of a common mechanism? Appl Environ Microbiol **67:**2873-2882.

16. **Gonzalez, J. M., R. P. Kiene, and M. A. Moran.** 1999. Transformation of sulfur compounds by an abundant lineage of marine bacteria in the alpha-subclass of the class Proteobacteria. Appl Environ Microbiol **65:**3810-3819.

17. **Gould, W. D., and T. Kanagawa.** 1992. Purification and properties of methyl mercaptan oxidase from *Thiobacillus thioparus* TK-m. J Gen Microbiol **138:**217-221.

18. **Hagemeier, C. H., L. Chistoserdova, M. E. Lidstrom, R. K. Thauer, and J. A. Vorholt.** 2000. Characterization of a second methylene tetrahydromethanopterin dehydrogenase from *Methylobacterium extorquens* AM1. Eur J Biochem **267:**3762-3769.

19. **Hamed, R. B., E. T. Batchelar, I. J. Clifton, and C. J. Schofield.** 2008. Mechanisms and structures of crotonase superfamily enzymes - How nature controls enolate and oxyanion reactivity. Cell Mol Life Sci **65:**2507-2527.

20. **Han, L., and K. A. Reynolds.** 1997. A novel alternate anaplerotic pathway to the glyoxylate cycle in streptomycetes. J Bacteriol **179:**5157-5164.

21. **Henriksen, J. R.** 2008. Physiology of dimethylsulfoniopropionate metabolism in a model marine Roseobacter, *Silicibacter pomeroyi*. University of Georgia, Athens.

22. **Hetzel, M., M. Brock, T. Selmer, A. J. Pierik, B. T. Golding, and W. Buckel.** 2003. Acryloyl-CoA reductase from *Clostridium propionicum*. An enzyme complex of propionyl-CoA dehydrogenase and electron-transferring flavoprotein. Eur J Biochem **270:**902-910.

23. **Howard, E. C., J. R. Henriksen, A. Buchan, C. R. Reisch, H. Buergmann, R. Welsh, W. Y. Ye, J. M. Gonzalez, K. Mace, S. B. Joye, R. P. Kiene, W. B. Whitman, and M. A. Moran.** 2006. Bacterial taxa that limit sulfur flux from the ocean. Science **314:**649-652.

24. **Kanzaki, H., M. Kobayashi, T. Nagasawa, and H. Yamada.** 1987. Purification and characterization of cystathionine gamma-synthase type-II from *Bacillus sphaericus*. Eur J Biochem **163:**105-112.

25. **Kiene, R. P., and L. J. Linn.** 2000. The fate of dissolved dimethylsulfoniopropionate (DMSP) in seawater: Tracer studies using S-35-DMSP. Geochim Cosmochim Ac **64:**2797-2810.

26. **Kiene, R. P., L. J. Linn, J. Gonzalez, M. A. Moran, and J. A. Bruton.** 1999. Dimethylsulfoniopropionate and methanethiol are important precursors of methionine and protein-sulfur in marine bacterioplankton. Appl Environ Microbiol **65:**4549-4558.

27. **Kim, S. J., H. J. Shin, Y. C. Kim, D. S. Lee, and J. W. Yang.** 2000. Isolation and purification of methyl mercaptan oxidase from *Rhodococcus rhodochrous* for mercaptan detection. Biotechnol Bioloproc E **5:**465-468.

28. **Kirkwood, M., N. E. Le Brun, J. D. Todd, and A. W. B. Johnston.** 2010. The dddP gene of *Roseovarius nubinhibens* encodes a novel lyase that cleaves dimethylsulfoniopropionate into acrylate plus dimethyl sulfide. Microbiol-Sgm **156:**1900-1906.

29. **Kuchta, R. D., and R. H. Abeles.** 1985. Lactate reduction in *Clostridium propionicum* - purification and properties of lactyl-Coa dehydratase. J. Biol. Chem. **260:**3181-3189.

30. **Meister, M., S. Saum, B. E. Alber, and G. Fuchs.** 2005. L-malyl-coenzyme A/beta-methylmalyl-coenzyme A lyase is involved in acetate assimilation of the isocitrate lyase-negative bacterium *Rhodobacter capsulatus*. J Bacteriol **187:**1415-1425.

31. **Neidhardt, F. C., J. L. Ingraham, and M. Schaechter.** 1990. Physiology of the bacterial cell : a molecular approach. Sinauer Associates, Sunderland, Mass.

32. **Oh, H. M., K. K. Kwon, I. Kang, S. G. Kang, J. H. Lee, S. J. Kim, and J. C. Cho.** 2010. Complete genome sequence of "Candidatus Puniceispirillum marinum" IMCC1322, a representative of the SAR116 clade in the Alphaproteobacteria. J Bacteriol **192:**3240-3241.

33. **Rajashekhara, E., and K. Watanabe.** 2004. Propionyl-coenzyme A synthetases of *Ralstonia solanacearum* and *Salmonella choleraesuis* display atypical kinetics. Febs Lett **556:**143-147.

34. **Reisch, C. R., M. A. Moran, and W. B. Whitman.** 2008. Dimethylsulfoniopropionate-dependent demethylase (DmdA) from *Pelagibacter ubique* and *Silicibacter pomeroyi*. J Bacteriol **190:**8018-8024.

35. **Reisch, C. R., M. J. Stoudemayer, V. A. Varaljay, I. J. Amster, M. A. Moran, and W. B. Whitman.** 2011. Novel pathway for assimilation of dimethylsulphoniopropionate widespread in marine bacteria. Nature **473:**208-211.

36. **Risso, C., S. J. Van Dien, A. Orloff, D. R. Lovley, and M. V. Coppi.** 2008. Elucidation of an alternate isoleucine biosynthesis pathway in Geobacter sulfurreducens. J Bacteriol **190:**2266-2274.

37. **Roberts, R. B.** 1955. Studies of biosynthesis in *Escherichia coli*. Carnegie Institution of Washington, Washington,.

38. **Suylen, G. M. H., P. J. Large, J. P. Van Dijken, and J. G. Kuenen.** 1987. Methyl mercaptan oxidase, a key enzyme in the metabolism of methylated sulphur compounds by *Hyphomicrobium* EG. J Gen Microbiol **133:**2989-2997.

39. **Teufel, R., J. W. Kung, D. Kockelkorn, B. E. Alber, and G. Fuchs.** 2009. 3-hydroxypropionyl-coenzyme A dehydratase and acryloyl-coenzyme A reductase, enzymes of the autotrophic 3-hydroxypropionate/4-hydroxybutyrate cycle in the Sulfolobales. J Bacteriol **191:**4572-4581.

40. **Todd, J. D., A. R. Curson, C. L. Dupont, P. Nicholson, and A. W. Johnston.** 2009. The *dddP* gene, encoding a novel enzyme that converts dimethylsulfoniopropionate into dimethyl sulfide, is widespread in ocean metagenomes and marine bacteria and also occurs in some *Ascomycete* fungi. Environ Microbiol **11:**1376-1385.

41. **Todd, J. D., A. R. Curson, N. Nikolaidou-Katsaraidou, C. A. Brearley, N. J. Watmough, Y. Chan, P. C. Page, L. Sun, and A. W. Johnston.** 2009. Molecular dissection of bacterial acrylate catabolism - unexpected links with dimethylsulfoniopropionate catabolism and dimethyl sulfide production. Environ Microbiol.

42. **Todd, J. D., A. R. J. Curson, M. Kirkwood, M. J. Sullivan, R. T. Green, and A. W. B. Johnston.** 2011. DddQ, a novel, cupin-containing, dimethylsulfoniopropionate lyase in marine roseobacters and in uncultured marine bacteria. Environ Microbiol **13:**427-438.

43. **Todd, J. D., M. Kirkwood, S. Newton-Payne, and A. W. Johnston.** 2011. DddW, a third DMSP lyase in a model Roseobacter marine bacterium, *Ruegeria pomeroyi* DSS-3. ISME J.

44. **Todd, J. D., R. Rogers, Y. G. Li, M. Wexler, P. L. Bond, L. Sun, A. R. Curson, G. Malin, M. Steinke, and A. W. Johnston.** 2007. Structural and regulatory genes required to make the gas dimethyl sulfide in bacteria. Science **315:**666-669.

45. **Tusher, V. G., R. Tibshirani, and G. Chu.** 2001. Significance analysis of microarrays applied to the ionizing radiation response. P Natl Acad Sci USA **98:**5116-5121.

46. **Vila-Costa, M., J. M. Rinta-Kanto, S. Sun, S. Sharma, R. Poretsky, and M. A. Moran.** 2010. Transcriptomic analysis of a marine bacterial community enriched with dimethylsulfoniopropionate. ISME J **4:**1410-1420.

47. **Vorholt, J. A., L. Chistoserdova, M. E. Lidstrom, and R. K. Thauer.** 1998. The NADP-dependent methylene tetrahydromethanopterin dehydrogenase in *Methylobacterium extorquens* AM1. J Bacteriol **180:**5351-5356.
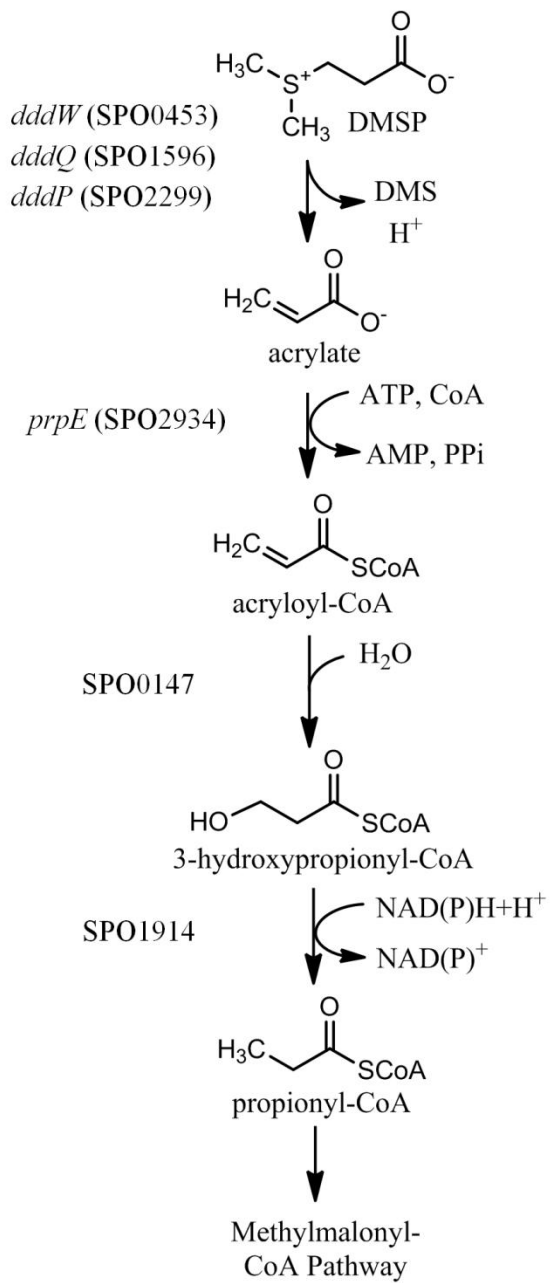
Figure 4-1. DMSP cleavage and acrylate assimilation pathway in *R. pomeroyi*.
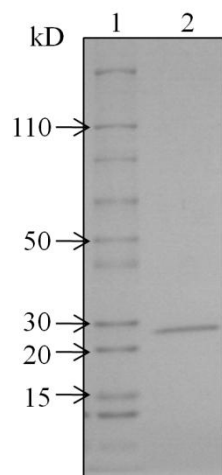
Figure 4-2. SDS-PAGE of purified acryloyl-CoA hydratase. Lane 1. Novex sharp prestained protein marker. Lane 2. Hydroxyapatite chromatography fraction with the highest acryloyl-CoA hydratase activity.
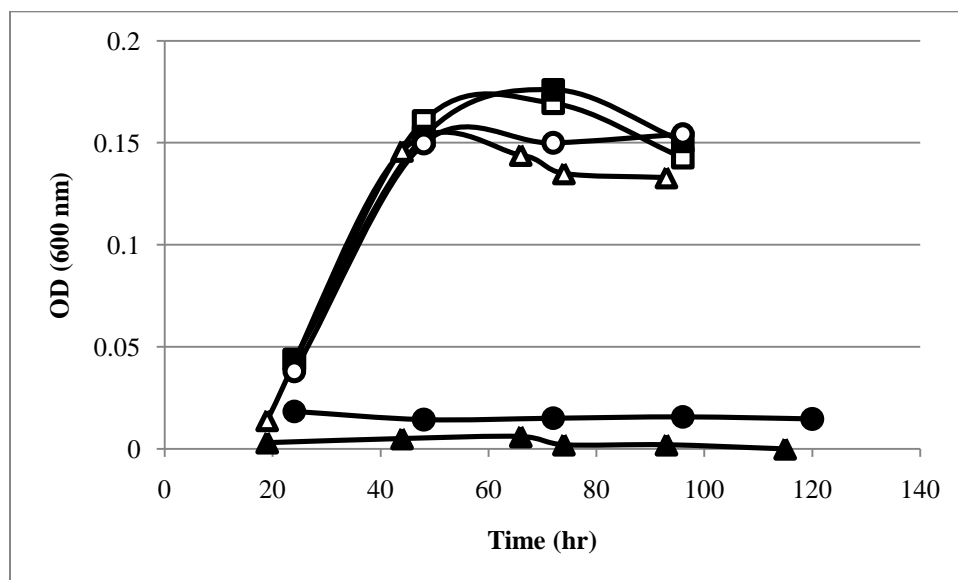
Figure 4-3. Growth curve of wild-type *R. pomeroyi* and SPO1914::*tet*. Wild-type cells grown with 3 mM propionate (□), acrylate (Δ), and 3-hydroxypropionate (○). SPO1914::*tet* grown with 3 mM propionate (■), acrylate (▲), 3-hydroxypropionate (●).
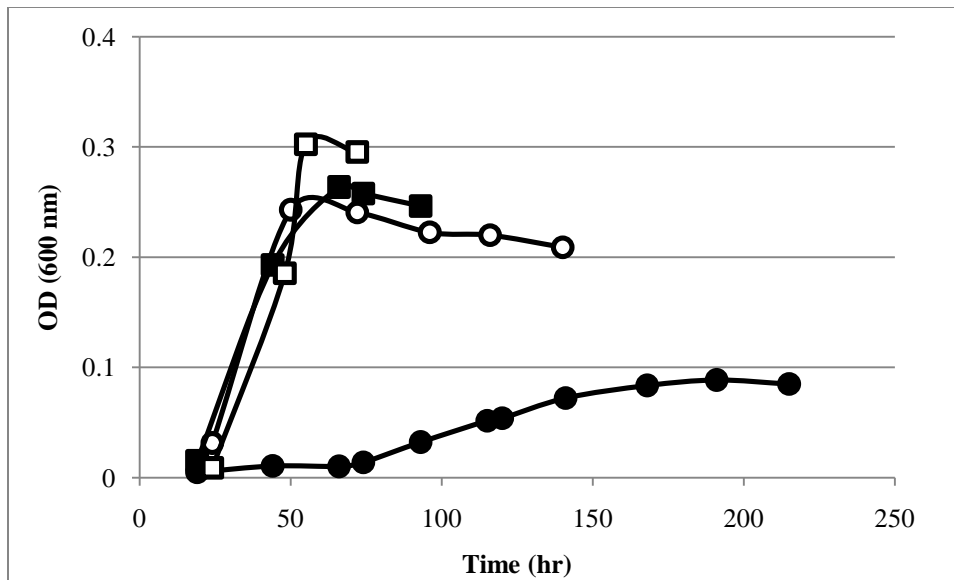
Figure 4-4. Growth curve of wild-type *R. pomeroyi* and *ccr⁻* (SPO0370::*tet*). Growth of wild-type cells grown with 3 mM DMSP (□) and 3 mM MMPA (○). Growth of *ccr⁻* with 3 mM DMSP (■) and MMPA (●)
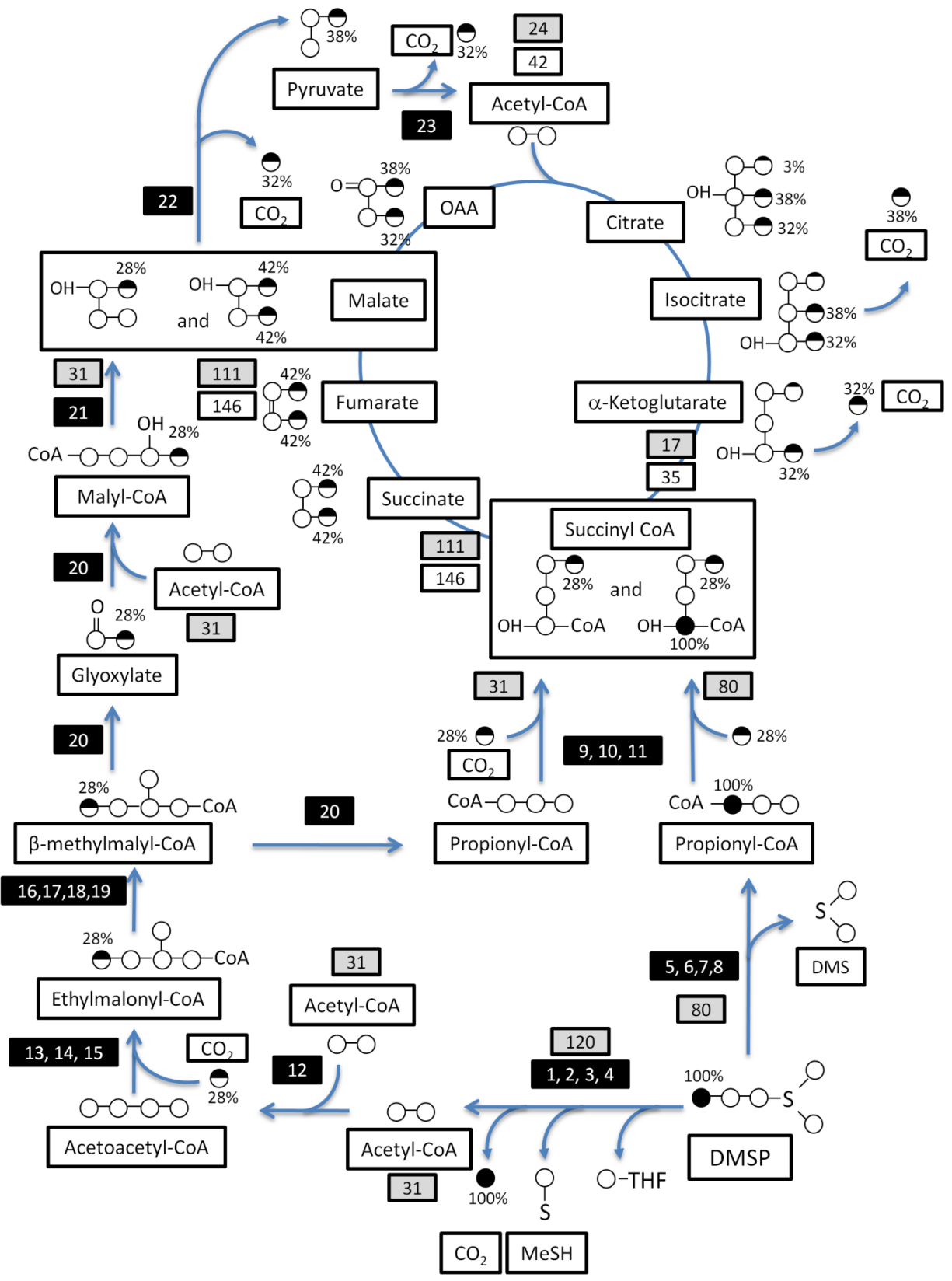
Figure 4-5. Overview of DMSP assimilation pathways in *R. pomeroyi*. The schematic starts with DMSP and displays reactions and labeling patterns of intermediates of central carbon metabolism. The starting point for the TCA cycle is with succinyl-CoA and follows a clockwise direction. Values displayed next to filled or partially filled circles are percentage of ^{13}C enrichment in the corresponding carbon upon first turn of the TCA cycle. Values in gray boxes are the carbon flux in nmol min^{-1} in the first turn of the TCA cycle while the values in white boxes reflect the flux upon reaching equilibrium. Flux values after the first round of the TCA cycle are shown in Table 4. Numbers in the black boxes correspond to enzymes as follows: 1, DMSP dependent demethylase (DmdA); 2, MMPA-CoA ligase (DmdB); 3, MMPA-CoA dehydrogenase (DmdC); 4, MTA-CoA hydratase (DmdD); 5, DMSP cleavage enzyme (DddP , DddQ, or DddW); 6, Acryate-CoA ligase; 7, Acryloyl-CoA hydratase; 8, 3-hydroxypropionyl-CoA reductase; 9, Propionyl-CoA carboxylase; 10, Methylmalonyl-CoA mutase; 11, Methylmalonyl-CoA epimerase; 12, β-ketothiolase; 13, Acetoacetyl-CoA reductase; 14, Crotonase; 15, Crotonyl-Coa carboxylase/reductase; 16, Ethylmalonyl-CoA/methylmalonyl-CoA epimerase; 17, Ethylmalonyl-CoA mutase; 18, Methylsuccinyl-coa dehydrogenase; 19, Mesaconyl-coa hydratase; 20, Malyl-CoA/β-methylmalyl-CoA lyase; 21, Malyl-CoA thioesterase; 22, Malate dehydrogenase; 23, Pyruvate dehydrogenase complex.
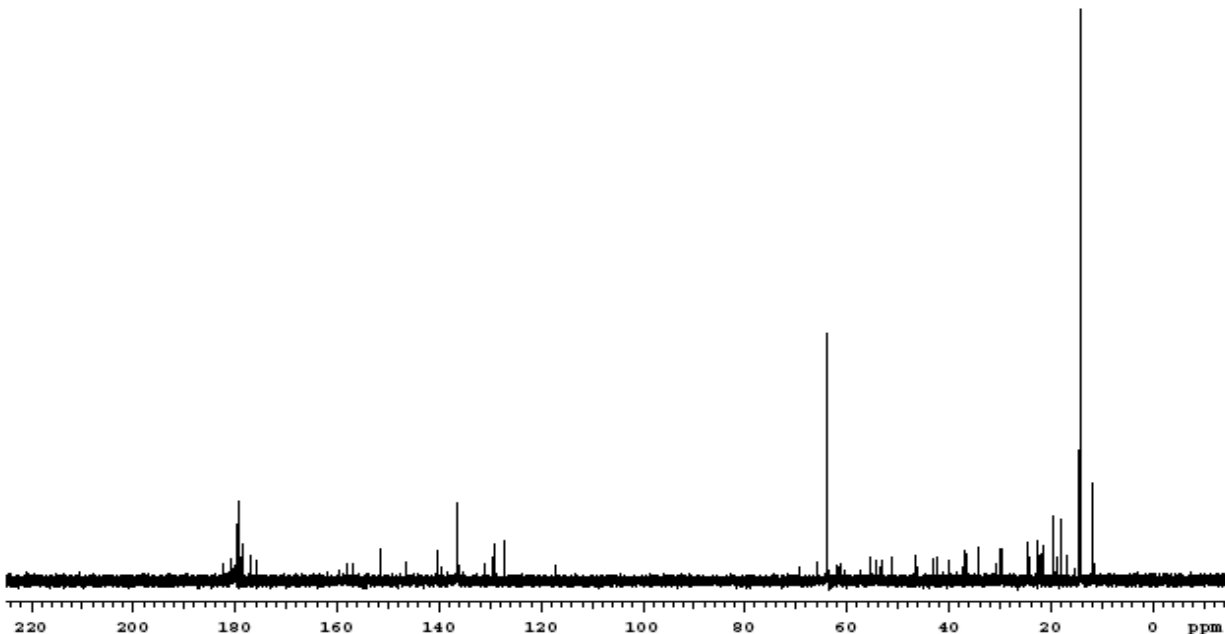
Figure 4-6. ^{13}C NMR analysis of hydrolyzed proteins from chemostat grown *R. pomeroyi* using [^{13}C-methyl] DMSP. Signal intensities are attributed to both amino acid abundance and ^{13}C enrichment. The signal at 17 ppm corresponds to the methyl group of methionine, while the signal at 64 ppm corresponds to the C-3 carbon of serine.

Table 4-1. Amino acids per gram dry weight of DMSP grown *R. pomeroyi*.

Amino Acid	µmol g^{-1} dry cells
alanine	536
arginine	238
aspartate and asparagine	448
cysteine	45
glutamate and glutamine	396
glycine	454
histidine	88
isoleucine	212
leucine	346
lysine	197
methionine	138
phenylalanine	177
proline	187
serine	227
threonine	231
tryptophan	39
tyrosine	123
valine	304

Table 4-2. Gene probes of interest to DMSP metabolism that were significantly regulated

during growth on DMSP compared to glucose.

Gene Annotation	SPO #[a]	Fold change	q-value
β-ketothiolase	SPO0142	4	3.6
Acetoacetyl-CoA reductase	SPO0325	3.5	1.6
Methylmalonyl-CoA mutase	SPO0368	3.3	4.5
dddW (DMSP lyase)	SPO0453	79.0	0.0
dddW (DMSP lyase)	SPO0453	73.9	0.0
Methylmalonyl-CoA epimerase	SPO0932	7.8	0.0
Propionyl-CoA carboxylase alpha subunit	SPO1101	3.5	3.6
Propionyl-CoA carboxylase alpha subunit	SPO1101	5.6	0.0
Methylmalonyl-CoA mutase	SPO1105	2.5	0.0
Serine hydroxymethyltransferase	SPO1572	4.8	1.6
Serine hydroxymethyltransferase	SPO1572	6.7	4.5
transcriptional regulator, GntR family	SPO1912	4.4	0.0
dmdA (DMSP demethylase)	SPO1913	7.3	0.0
dmdA (DMSP demethylase)	SPO1913	4.7	0.0
3-Hydroxypropionyl-CoA reductase	SPO1914	13.3	0.0
dddP (DMSP lyase)	SPO2299	5.9	0
cysH (phosphoadenylyl-sulfate reductase)	SPO2635	0.2	3.8
prpE (Propionate--CoA ligase)	SPO2934	7.5	0.0
prpE (Propionate--CoA ligase)	SPO2934	3.0	3.6
Transcriptional regulator, IclR family	SPOA0268	13.0	0.0
Transcriptional regulator, IclR family	SPOA0268	10.4	0.0
Hypothetical protein	SPOA0269	29.8	0.0
Hypothetical protein	SPOA0269	23.6	0.0
Hypothetical protein	SPOA0270	2.2	8.9
mauG-putative	SPOA0271	5.0	0.0
mauG-putative	SPOA0271	3.2	0.0
glutathione-dependent formaldehyde dehydrogenase	SPOA0272	3.0	3.4

[a]Most genes were spotted with two unique probes, with the only exceptions being when a second

probe could not be designed. Instances where each probe showed a significant response are

shown.

Table 4-3. Building blocks required for DMSP grown chemostat cultures of *R. pomeroyi*.

Building Block	nmol min$^{-1\#}$
pyruvate	20
α-ketoglutarate	7
oxaloacetate	11
phosphoglycerate	10
pentose phosphate	10
acetyl-CoA	21
erythrose phosphate	3
phosphoenolpyruvate	5
triosphosphate	3

$^{\#}$Calculations were based on the published values for building block required for 1 gram of *E. coli*, which account for amino acids, nucleic acids, and lipids (31). These values were modified to account for the amino acid content determined in *R. pomeroyi*, and taking into account the alternate pathway for isoleucine biosynthesis.

Table 4-4. Specific activities of the acrylate assimilation pathway enzymes in cell extracts of chemostat-grown *R. pomeroyi*. Values are nmol min^{-1} mg of protein^{-1} and the result of triplicate assays from a single cell extract ±SD.

	Growth Substrate	
Activity	**Glucose**	**DMSP**
Acrylate-CoA ligase	18 ±1	24 ±2
Acryloyl-CoA hydratase	>8000	>8000
3-hydroxypropionyl-CoA reductase	16 ±1	195 ±10
Propionyl-CoA carboxylase	4 ±1	38 ±1

Table 4-5. ^{13}C enrichment of amino acids by quantititative ^{13}C NMR. (#) ^{1}H coupled satellite.

Amino Acid	C-1	C-2	C-3	C-4	C-5
alanine	39%	<2%	<2%	NA	NA
glutamate	40%	<2%	<2%	<2%	3.9%
aspartate	40%	<2%	<2%	32%	NA
threonine	32.0%	<2%	<2%	34% (36%)	NA

Table 4-6. Calculation of TCA cycle carbon flux at equilibrium. Values are given in nmol min^{-1}.

Turn	Carbon entering the TCA cycle at succinyl-CoA	Carbon remaining after one turn of TCA cycle	Unenriched carbon diluting succinyl-CoA
1	142	35	18
2	160	53	26
3	168	61	31
4	173	66	33
5	175	68	34
6	176	69	34
7	176	69	35
8	177	70	35
9	177	70	35

Table 4-7. Carbon balance for [^{13}C-1] DMSP grown chemostat culture. Units are nmol min^{-1}.

	Total C (In)	^{13}C (In)	Total C (Out)	^{13}C (Out)
DMSP	1000	200	0	0
DMS	0	0	160	0
CO$_2$	70	1	610^a	(600*0.28)=177
cell material	0	0	300	(300*0.092)=27
Total	1070	201	1070	204

^{a}calculated

Table 4-8. Amino acid contribution to cellular ^{13}C in *R. pomeroyi* grown with [^{13}C-methyl] DMSP.

Amino Acid	nmol aa	Carbons	nmol C	ng C	Enrichment	ng ^{13}C	mg ^{13}C (550 mg^{-1})$^{\#}$
serine	3.10	3	9.3	111.7	30%	11.2	.81
cysteine	0.61	3	1.8	22.0	30%	2.2	.161
methionine	1.88	5	9.4	113.0	99%	22.6	1.65
tryptophan	0.52	11	5.8	69.7	30%	1.9	.139

$^{\#}$ To extrapolate the ng of ^{13}C to values corresponding to g^{-1}, it was assumed that 55% of the

cell's dry weight was protein.

Table 4-9. Nucleic acid contribution to cellular ^{13}C in *R. pomeroyi* grown with [^{13}C-methyl] DMSP.

Nucleic Acid	µmol (*E. coli*)	Carbons	µmol C	µg C	Enrichment	mg ^{13}C
ATP	165	10	1650	19800	90%	3.56
GTP	203	10	2030	24360	90%	4.38
dATP	24.7	10	247	2964	90%	0.53
dGTP	25.4	10	254	3048	90%	0.54

CHAPTER 6

CONCLUSIONS

In 2006, the first gene directly involved in dimethylsulfoniopropionate (DMSP) catabolism was identified as a DMSP-dependent demethylase, designated *dmdA*. Since then, numerous other genes involved in DMSP metabolism and its downstream metabolic pathways have been identified. These advances have significantly increased understanding of the physiology of bacterial cells that help to drive the global sulfur cycle.

The aforementioned gene *dmdA* was first identified in the model organism *Ruegeria pomeroyi* and was subsequently confirmed to encode for a functional protein in the ubiquitous SAR11 clade bacterium *Candidatus* Pelagibacter ubique. In chapter two of this dissertation, the properties of DmdA from these two representative marine bacteria were investigated. These investigations confirmed that the gene product identified as DmdA was responsible for the tetrahydrofolate (THF)-dependent DMSP demethylation and that the reaction products were methylmercaptopropionate (MMPA) and 5-methyl-THF. The kinetic properties of the enzymes revealed some surprising characteristics. The enzyme's affinity for THF was similar to values reported previously for THF-consuming enzymes, but the K_M for DMSP of 13.2 and 5.4 mM for the *R. pomeroyi and P. ubique* enzymes, respectively, were higher than typically reported for common intracellular metabolites. To possess maximum activity, the intracellular concentration of DMSP must be about an order of magnitude great than the K_M. Thus, the intracellular concentration of DMSP was measured in the chemostat grown *R. pomeroyi*. The chemostat conditions used in this experiment supplied DMSP at 2 mM, but the steady state concentration of

DMSP in the spent medium was only 2 µM. Despite this very low concentration of DMSP in the medium, the cells maintained an intracellular concentration of about 70 mM. This concentration was great enough to be both osmotically significant and enabled near-maximal activity of DmdA.

These studies proved useful in learning more about the conditions under which the DMSP demethylation reaction occurs. However, the biochemical pathway and gene products responsible for the demethiolation of MMPA and the release of methanethiol (MeSH) remained unknown. To gain insight into the downstream metabolic pathways used to assimilate the three carbon moiety of DMSP, from both the DMS and MeSH releasing pathways, investigations analyzing the coenzyme-A containing intermediates were performed. Surprisingly, an MMPA-CoA thioester was identified in these experiments. Using MMPA-CoA as the starting point, enzyme assays were developed to reconstruct the metabolic pathway of MMPA assimilation in vitro. Cell extracts possessed enzymatic activity that catalyzed the production of MMPA-CoA, the dehydrogenation of MMPA-CoA to methylthioacryloyl-CoA (MTA-CoA), the hydrolysis of MTA-CoA to free-CoA, CO_2, MeSH, and acetaldehyde, and the oxidation of acetaldehyde to acetate. The first three genes in this pathway were identified by purification of the native enzyme and analysis of a transposon mutant library. Knowledge of the genes that encoded for these proteins allowed for interrogation of the genomic and metagenomic databases to determine the distribution of this pathway. Surprisingly, genes for the pathway were found in a diverse range of bacteria, and subsequently these bacteria were shown to be capable of producing MeSH when provided with MMPA. In the marine metagenomic database, these genes were also highly abundant. Using the essential single copy gene *recA* as a proxy for genome equivalents, it was

estimated that over 60% of cells in the surface ocean were capable of degrading MMPA, suggesting this process may be a major player in the global sulfur cycle.

Elucidation of the MMPA-CoA pathway was somewhat surprising, since MMPA metabolism was not generally believed to be CoA-mediated. In light of this discovery, it was hypothesized that assimilation of acrylate, the product of DMSP cleavage in *R. pomeroyi*, may also be CoA-mediated. Like the MMPA-CoA pathway, it was found that a series of three coenzyme-A mediated reactions transformed acrylate into propionyl-CoA. First, acrylate was transformed into acryloyl-CoA, which was then hydrated to form 3-hydroxypropionyl-CoA. An NAD(P)H dependent reaction then reduced 3-hyddroxypropionyl-CoA to propionyl-CoA. The assimilation of propionyl-CoA proceeds through the methylmalonyl-CoA pathway, a standard pathway for three carbon assimilation possessed by *R. pomeroyi*. The enzymes catalyzing the hydration of acryloyl-CoA and the reduction 3-hydroxpropionyl-CoA were identified by purification from crude cell extracts. To test the physiological significance of this pathway a mutant strain was constructed in which the gene encoding the 3-hydroxypropionyl-CoA reductase was disrupted. This mutant was unable to grow on acrylate as the sole source of carbon, consistent with the enzymes role in acrylate assimilation.

These investigations have tremendously advanced the understanding of DMSP metabolism in the surface ocean, which was previously a "black box" of microbial transformations. Elucidation of the MMPA-CoA pathway described in chapter 3 and the acrylate assimilation pathway described in chapter 4, identify at least five novel enzymes. Identification of these novel enzymes now allows for detailed studies on their enzymology and regulation of expression, and how these factors affect the cells physiology. The goal is to fully understand and predict why DMSP is routed through the cleavage pathway that releases DMS, or the

demethylation pathway that releases MeSH, since this routing has major impacts on global sulfur flux, and consequently global climate control. The last, mostly unknown, major of piece of the DMSP-related reduced sulfur budget in the surface ocean is the fate of MeSH. Currently there is no direct evidence of the genes and biochemical pathways responsible for the biological consumption of MeSH. In order to achieve the aforementioned goal of DMSP flux predictions, this important step in the marine sulfur cycle must be better understood.